

Replication of DNA Tetrahedron and  
Higher-order Self-assembly of DNA Origami

by

Zhe Li

A Dissertation Presented in Partial Fulfillment  
of the Requirements for the Degree  
Doctor of Philosophy

Approved April 2012 by the  
Graduate Supervisory Committee:

Hao Yan, Co-Chair  
Yan Liu, Co-Chair  
Dong-Kyun Seo  
Rebekka Wachter

ARIZONA STATE UNIVERSITY

May 2012

## ABSTRACT

Deoxyribonucleic acid (DNA) has been treated as excellent building material for nanoscale construction because of its unique structural features. Its ability to self-assemble into predictable and addressable nanostructures distinguishes it from other materials. A large variety of DNA nanostructures have been constructed, providing scaffolds with nanometer precision to organize functional molecules. This dissertation focuses on developing biologically replicating DNA nanostructures to explore their biocompatibility for potential functions in cells, as well as studying the molecular behaviors of DNA origami tiles in higher-order self-assembly for constructing DNA nanostructures with large size and complexity.

Presented here are a series of studies towards this goal. First, a single-stranded DNA tetrahedron was constructed and replicated in vivo with high efficiency and fidelity. This study indicated the compatibility between DNA nanostructures and biological systems, and suggested a feasible low-cost method to scale up the preparation of synthetic DNA. Next, the higher-order self-assembly of DNA origami tiles was systematically studied. It was demonstrated that the dimensional aspect ratio of origami tiles as well as the intertile connection design were essential in determining the assembled superstructures. Finally, the effects of DNA hairpin loops on the conformations of origami tiles as well as the higher-order assembled structures were demonstrated. The results would benefit the design and construction of large complex nanostructures.

## ACKNOWLEDGEMENTS

I would like to thank my research advisor, Dr. Hao Yan, and co-advisor, Dr. Yan Liu. They introduced me this wonderful DNA nanotechnology world, guided me throughout the graduate career, and provided me both professional support and personal advice. Their informative knowledge, extinct passion, hardworking attitude also inspired me to continue my exploration in science. I also thank my supervisory committee members, Dr. Don Seo and Dr. Rebekka Wachter, for their time and guidance. My collaborators, in particular, Dr. Lei Wang, kindly supported my research.

I am also grateful to all the past and present members in Yan lab. They provided a talented and friendly research atmosphere. I would like to acknowledge Dr. Chenxiang Lin and Dr. Jeanette Nangreave, who gave me invaluable advice on not only research but also personal life.

I would like to dedicate this dissertation to my family. The unconditional love and support from my parents are always with me, regardless of the physical distance. They encouraged me to explore my interest and to overcome all the difficulties. I can never thank them enough. I thank my husband Hanyang with my sincere appreciation. I could not have accomplished all that I have without his endless love, trust and dedication in both my daily life and research work. I am also thankful for my angel Fuyao, who brings the greatest happiness to my life.

## TABLE OF CONTENTS

|  | Page |
|--|------|
| LIST OF TABLES .....   | vi   |
| LIST OF FIGURES .....  | vii  |
| CHAPTER  |      |
| 1. INTRODUCTION: STRUCTURAL DNA NANOTECHNOLOGY .....                                       | 1    |
| 1.1. Introduction.....   | 1    |
| 1.2. 2D DNA Nanostructures.....  | 4    |
| 1.2.1. 2D DNA Nanostructures Assembled by Small Branched Tiles .....                       | 4    |
| 1.2.2. 2D DNA Nanostructures Assembled by DNA Origami .....                                | 8    |
| 1.3. 3D DNA Nanostructures.....  | 11   |
| 1.3.1. DNA Polyhedra.....  | 11   |
| 1.3.2. 3D DNA Origami Structures .....   | 14   |
| 1.4. Spatial Arrangement of Biological Molecules by DNA Nanostructures..                   | 17   |
| 1.5. Challenges and Perspectives.....  | 21   |
| 1.6. Projects .....  | 23   |
| 1.7. References.....   | 23   |
| 2. A REPLICABLE TETRAHEDRAL NANOSTRUCTURE SELF-<br>ASSEMBLED FROM A SINGLE DNA STRAND..... | 29   |
| 2.1. Abstract.....   | 29   |
| 2.2. Introduction.....   | 30   |
| 2.3. Materials and Methods .....   | 33   |
| 2.3.1. Material.....   | 33   |

| CHAPTER   | Page      |
|---|-----------|
| 2.3.2. Structural Design and Assembly.....  | 33        |
| 2.3.3. Restriction Enzyme Digestion .....   | 34        |
| 2.3.4. Ferguson Analysis.....   | 34        |
| 2.3.5. AFM Imaging.....   | 35        |
| 2.3.6. In Vivo Cloning .....  | 35        |
| 2.3.7. Rolling-circle Amplification of the Tetrahedron .....  | 35        |
| 2.4. Results and Discussions.....   | 36        |
| 2.5. Conclusion .....   | 49        |
| 2.6. References.....  | 50        |
| <b>3. MOLECULAR BEHAVIOR OF DNA ORIGAMI IN HIGHER-ORDER</b>   |           |
| <b>SELF-ASSEMBLY.....</b>   | <b>53</b> |
| 3.1. Abstract.....  | 53        |
| 3.2. Introduction.....  | 54        |
| 3.3. Materials and Methods .....  | 59        |
| 3.4. Results and Discussions.....   | 59        |
| 3.4.1. Assembly of Starlike 1D Arrays .....   | 59        |
| 3.4.2. Formation of DNA Origami Tubes.....  | 63        |
| 3.4.3. Tailoring the Structural Features of Origami Tubes by Varying the<br>Dimensions and Intertile Connections of the Zigzag Tile Unit .... | 67        |
| 3.5. Conclusion .....   | 74        |
| 3.6. References.....  | 77        |

| CHAPTER   | Page |
|---|------|
| 4. EFFECT OF DNA HAIRPIN LOOPS ON THE TWIST OF PLANAR DNA                     |      |
| ORIGAMI TILES .....   | 81   |
| 4.1. Abstract.....  | 81   |
| 4.2. Introduction.....  | 82   |
| 4.3. Materials and Methods .....  | 87   |
| 4.3.1. Material .....   | 87   |
| 4.3.2. Assembly of DNA Origami .....  | 87   |
| 4.3.3. AFM Imaging.....   | 87   |
| 4.4. Results and Discussions.....   | 88   |
| 4.4.1. Effects of DNA Hairpin Loops .....                                     | 88   |
| 4.4.2. Rational Design of Planar Origami Tiles.....                           | 99   |
| 4.4.3. Heterogeneous Origami for Information Storage and Computation<br>..... | 102  |
| 4.5. Conclusion .....   | 104  |
| 4.6. References.....  | 105  |
| 5. SUMMARY .....  | 110  |
| BIBLIOGRAPHY.....   | 112  |
| APPENDIX  |      |
| A. SUPPLEMENTAL INFORMATION FOR CHAPTER 2 .....                               | 127  |
| B. SUPPLEMENTAL INFORMATION FOR CHAPTER 3 .....                               | 140  |
| C. SUPPLEMENTAL INFORMATION FOR CHAPTER 4 .....                               | 183  |
| D. CO-AUTHOR APPROVAL.....  | 200  |

## LIST OF TABLES

| Table  | Page |
|--|------|
| 2.1 Sequences of the component strands that were used to synthesized the full length (286-nt) ssDNA..... | 34   |
| 2.2 The expected DNA fragment lengths after the tetrahedron was restriction digested .....               | 39   |
| 2.3 Fragment lengths of the replicated DNA digested by the three restriction enzymes, respectively ..... | 46   |

## LIST OF FIGURES

| Figure  | Page |
|---|------|
| 1.1 Self-assembly of branched DNA with sticky ends into 2D lattices.....  | 3    |
| 1.2 Representative 2D DNA nanostructures assembled by small branched tiles ...  | 7    |
| 1.3 2D DNA nanostructures assembled by scaffolded DNA origami .....   | 10   |
| 1.4 3D DNA polyhedra.....   | 13   |
| 1.5 3D DNA origami nanostructures .....   | 16   |
| 1.6 DNA nanostructures based spatial arrangement of biological molecules .....  | 20   |
| 2.1 Design of the ssDNA tetrahedron.....  | 32   |
| 2.2 Characterization of the single-stranded DNA tetrahedron.....  | 40   |
| 2.3 Schematics and direct comparison of AFM images of tetrahedron DNA<br>structures .....   | 43   |
| 2.4 In vivo replication of the single-stranded DNA tetrahedron .....  | 47   |
| 3.1 Design of the zigzag DNA origami .....  | 58   |
| 3.2 Stairlike 1D DNA arrays assembled from the rectangular origami.....   | 61   |
| 3.3 DNA origami tubes.....  | 66   |
| 3.4 The number of linkers impacts the morphology of the resulting structures ...  | 69   |
| 3.5 Formation of 1D chains by 12-helix zigzag origami tiles.....  | 71   |
| 3.6 Formation of zigzag ribbons or double-layered linear ribbons by 40-helix<br>zigzag origami tiles .....  | 73   |
| 3.7 Summary of the impact of varying the dimensional aspect ratio and intertile<br>connection scheme of zigzag origami tile units on the resulting structures.... | 76   |
| 4.1 1D stairlike DNA ribbons assembled from rectangular origami tiles.....  | 85   |



| Figure   | Page |
|--|------|
| 4.2 AFM images of 1D DNA ribbons assembled from rectangular origami tiles<br>with different numbers of dumbbell loops on the top surface .....       | 90   |
| 4.3 AFM images of 1D DNA ribbons assembled from the rectangular origami<br>tiles with different numbers of dumbbell loops on the bottom surface..... | 93   |
| 4.4 Control of the conformation of a DNA origami tile through the addition of<br>topographical features .....  | 95   |
| 4.5 Predicted structural model of the rectangular shaped DNA origami tile.....   | 98   |
| 4.6 A planar rectangular origami tile was achieved by controlling the number and<br>position of dumbbell loops.....                                  | 101  |
| 4.7 Heterogeneous assembly of six different origami tiles.....   | 103  |

## Chapter 1

### Introduction: Structural DNA Nanotechnology

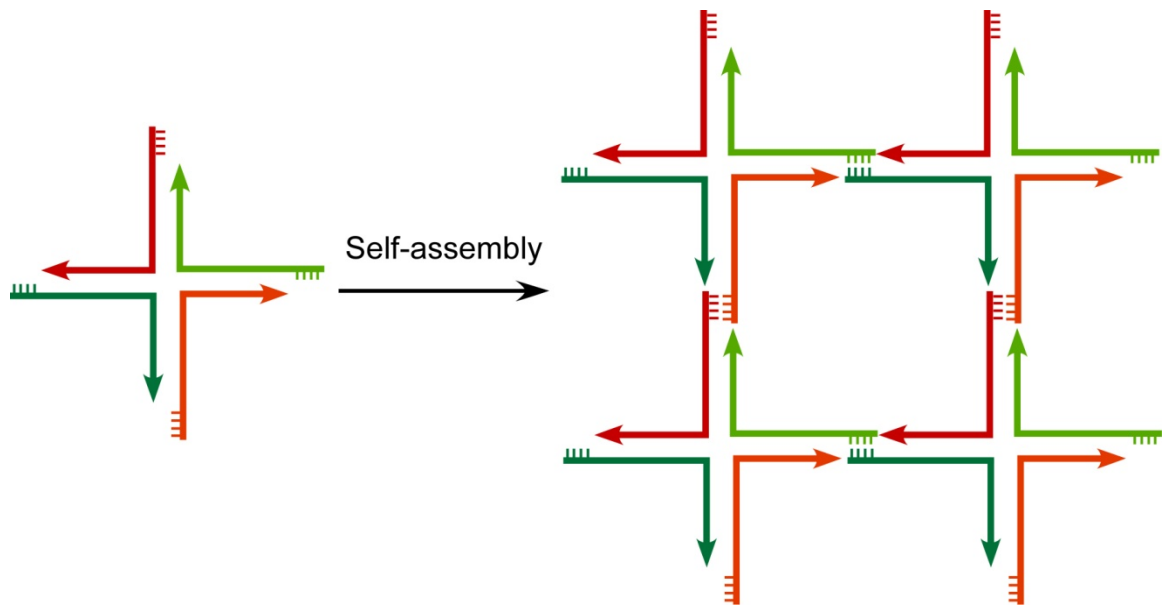
#### 1.1 Introduction

In the past thirty years, structural DNA nanotechnology has shown its great power in rational design and self-assembly of desired structures with nanometer precise. Using DNA molecules as building blocks, structural DNA nanotechnology aims to build well-defined structures with nanometer-scale addressability for a broad range of applications, such as to organize functional materials and to control macromolecular interactions.<sup>1-3</sup>

Carrying genetic information of almost all the living organisms, DNA is one of the most essential macromolecules for life. Aside from its role in biology, DNA is an excellent building material for nanoscale construction. First, the structure of double-helical B type DNA is well-known. As indicated by J. D. Watson and F. C. H. Crick 1953, DNA duplex is consist of 10.5 base pairs (bp) per helical turn spanning 3.4 nm with a diameter of roughly 2 nm, facilitating the modeling and construction of nanoscale materials.<sup>4</sup> Second, the interaction between DNA bases is highly predictable. In the canonical Watson-Crick base pairing model, adenine (A) pairs with thymine (T) via two hydrogen bonds, and guanine (G) pairs with cytosine (C) via three hydrogen bonds. Therefore, multiple DNA molecules can be programmably connected with the use of sticky ends. Third, DNA combines stiffness and flexibility. Double-stranded DNA (dsDNA) behaves like a rigid rod with a persistence length up to 50 nm; while single-stranded DNA (ssDNA) is relatively flexible, which enables the construction of

stable structures with desired angles. Forth, the synthesis and modification of DNA oligonucleotides are well-established, and there are numerous enzymes to manipulate DNA molecules, such as endonuclease, ligase, and polymerase.

Structural DNA nanotechnology relies on the spontaneous self-assembly of DNA strands, which is an essential behavior that can be found widely both in vitro and in vivo. For example, in gene cloning, a recombinant plasmid is formed by inserting DNA molecule of interest with sticky ends at both sides to the vector that contains the complimentary sticky ends. In another case, during the replication process of many living creatures, the Holliday junction is often observed, which plays an important role in genetic recombination. Inspired by this naturally existing four-arm structure, Ned Seeman in 1982 proposed the possibility of self-assembly of branched DNA motifs through sticky ends into two-dimensional (2D) as illustrated in Figure 1.1 and eventually three-dimensional (3D) crystalline arrays, giving birth to the field of structural DNA nanotechnology.<sup>5</sup> Since then, a large variety of 2D and 3D rational designed DNA nanostructures have been constructed, which provide the scaffolds for many advanced applications.



**Figure 1.1.** Self-assembly of branched DNA with sticky ends into 2D lattices.

## 1.2 2D DNA Nanostructures

### 1.2.1 2D DNA Nanostructures Assembled by Small Branched Tiles

Branched DNA junctions that termed as “DNA tiles” are the basic building blocks to construct patterned 2D and 3D nanostructures. In the past three decades, a large number of different DNA tiles with different geometries have been constructed.

The first class of DNA tiles is a group of double crossover (DX) molecules that join two double helices together through two reciprocal exchanges between antiparallel strands.<sup>6</sup> With programmed sticky ends design, these DX tiles were successfully expanded into infinite 2D periodic arrays on the micrometer scale, which were visualized by atomic force microscopy (AFM), as shown in Figure 1.2a.<sup>7</sup> Following the same idea, later on, the use of multiple crossovers between two adjacent helices was commonly applied to build DNA tiles, which include triple-crossover (TX) molecules<sup>8</sup> and 4-, 8-, and 12-helix planar molecules<sup>9, 10</sup>. It was demonstrated that infinite 2D arrays with different periodic patterns can be self-assembled by different varieties of these tiles that carried proper sticky ends.

Other varieties of tiles have also been designed to grow into infinite 2D DNA arrays. These include parallelogram<sup>11</sup> and triangular junctions<sup>12</sup> composed of four or three Holliday junctions, which self-assemble into infinite 2D DNA lattices with tunable diamond-shaped or triangular cavities; three- and six-helix bundles<sup>13, 14</sup>, which are 3D lattices themselves that can self-assemble into infinite 2D arrays; and cross-shaped and three-, and six-point-star motifs<sup>15-18</sup> which use

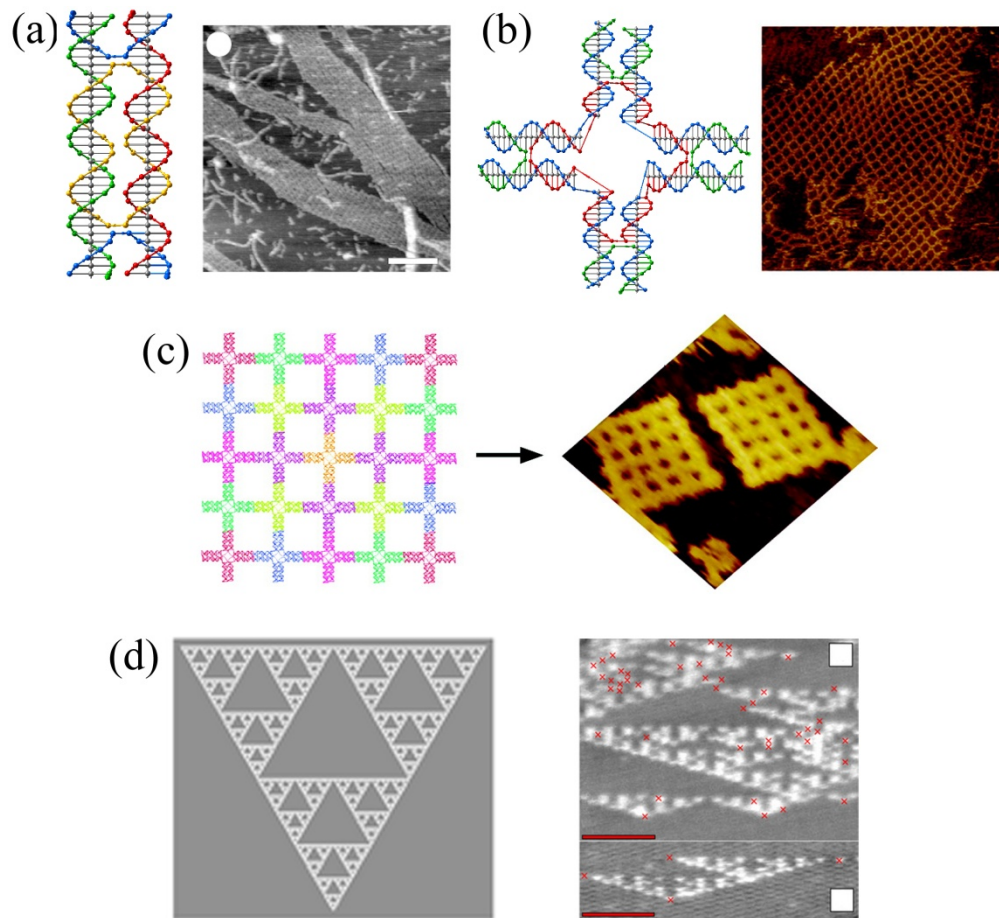
Holliday junction as individual arms connected by a long central strand and can assemble into infinite 2D array with square or hexagonal cavities (Figure 1.2b).

The more advanced generation of structural DNA technology is self-assembly of finite-sized and non-periodic 2D arrays, which have controllable shapes and addressable locations.

Yan's group and LaBean's group reported independently the study of construction of square shaped DNA arrays composed of nine and sixteen cross-shaped tiles, respectively (Figure 1.2c).<sup>19, 20</sup> The uniqueness of sticky ends used in each tile defines its unique position, making the whole array highly addressable. In addition, the outer edge of each tile in the border does not have any sticky end to avoid further assembly of the array into larger structures. Unlike the one-pot assembly of infinite array by the same motif, hierarchical assembly strategy was adopted by first assembling individual tile and subsequently hybridizing them together to form the 2D arrays.

“Algorithmic self-assembly” and “nucleated self-assembly” are also common methods to construct complex aperiodic patterns.<sup>21, 22</sup> In algorithmic self-assembly, DNA tiles are considered as rule units. Following a logic function which is controlled by their sticky ends, tiles can specifically and cooperatively assemble into a complex pattern. Nucleated self-assembly utilizes a scaffold strand as the starting point, upon which other DNA tiles grow into complex patterns. Both ideas have been successfully demonstrated experimentally. For instance, a Sierpinski triangle sheet (a fractal pattern made from smaller and smaller triangles so that at higher magnifications the larger image could be

reproduced) was built by using the combination of the two strategies. The DNA Sierpinski triangle sheet is made by first encoding a set of tiles as nucleating point, from which triangles then follow an XOR truth table to bind to the proper position through the use of DX rule tiles (Figure 1.2d).<sup>21</sup>



**Figure 1.2.** Representative 2D DNA nanostructures assembled by small branched tiles. (a) Double helix tile and corresponding 2D periodic arrays. (b) Cross-shaped tile and corresponding 2D arrays. (c) Finite-sized arrays assembled from 25 cross-shaped tiles. (d) Sierpinski triangle sheets assembled from DX tiles by algorithm and nucleated self-assembly.

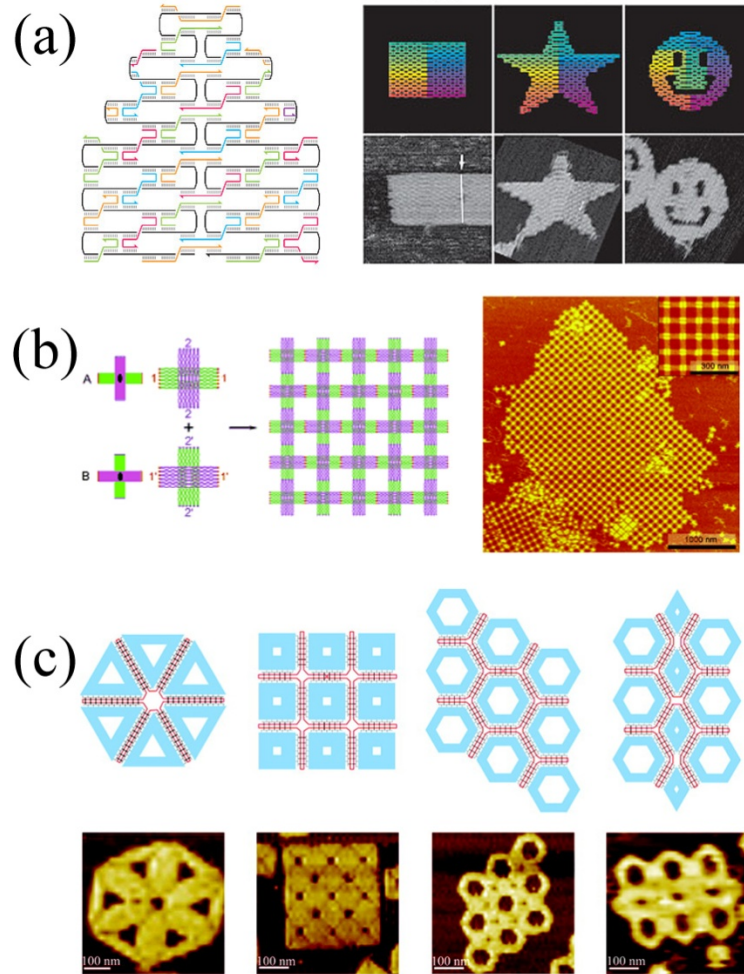


### 1.2.2 2D DNA Nanostructures Assembled by DNA Origami

A revolutionary breakthrough in structural DNA nanotechnology is Paul Rothemund's concept of "DNA origami". In this method, a long, single-stranded DNA (ssDNA) from a virus genome with known sequence is folded into any desired 2D shape using a large number of smaller "staple" strands. Specifically, Rothemund designed the sequence of over 200 staple strands ranging from 30 to 70 nucleotides in length, which are complementary to multiple parts of the 7 kb genome of phage M13m18, so that this long scaffold strand can be folded into various patterns that have relatively large diameter (~100 nm) (Figure 1.3a). Each staple strand occupies a specific position with its unique sequence, so that these structures exhibit fully addressable surfaces. In addition, origami can be programmed to bear complex patterns such as words and images with more than 200 six-nm pixels.<sup>23</sup>

Individual origami can also be considered as a DNA tile, so it can be further assembled into higher-order structures by the connection of extended staples. High yield one-dimensional (1D) arrays were successfully constructed by a few researchers<sup>24, 25</sup>; however, expanding them into 2D arrays seemed to be very unfavorable. To address this issue, Seeman's group designed a double-layered origami tile with the helix axes propagating in perpendicular directions. This origami tile self-assembled into well-ordered 2D arrays with dimensions of 3  $\mu\text{m}$  x 2  $\mu\text{m}$ , large enough to bridge bottom-up patterning methods and top-down approaches (Figure 1.3b).<sup>26</sup>

Yan's group reported another way to scale up the size of DNA origami structures by using DNA tiles as folding staples.<sup>27</sup> In this strategy, the rectangular 8-helix tile rather than traditional staple strands were utilized to fold the single-stranded M13m18 into 2D structures of larger dimensions with high yield. In principle, this method could be applied to create structures with a dimension of 1  $\mu\text{m}$  x 0.5  $\mu\text{m}$ . Following a similar strategy, later on, they used origami tiles as large staples to fold the single-stranded PhiX174 into various "superorigami" structures (Figure 1.3c).<sup>28</sup>



**Figure 1.3.** 2D DNA nanostructures assembled by scaffolded DNA origami. (a) Rectangle, star, and smiley face DNA origami tiles. (b) 2D origami arrays assembled from double-layered origami tiles. (c) “Superorigami” structures formed by using origami tiles as staples.

## 1.3 3D DNA Nanostructures

### 1.3.1 DNA Polyhedra

Since DNA has exhibited its powerful ability to construct complex 2D assemblies, a natural extension focuses on the design of 3D objects, which hold greater promise in advanced applications such as to assist the crystallization of proteins as Seeman proposed, and to mimic natural-existing cellular systems.

The first generation of 3D DNA polyhedra was fabricated by Seeman's group, with the topology of a cube and a truncated octahedron composed of dsDNA at each edge and branched junctions at each vertex. Multiple steps of ligation and purification were adopted to synthesize the closed polyhedra structures, leading to a low yield of the final products.<sup>29, 30</sup>

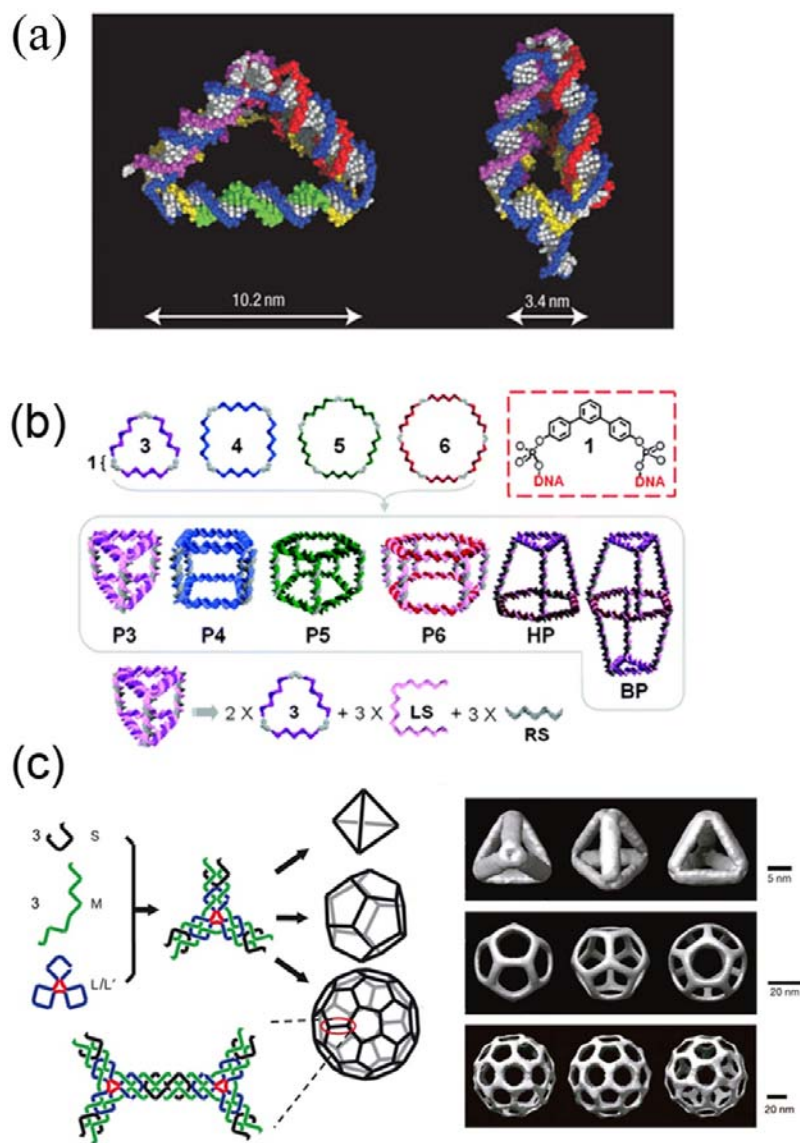
Tuberville's group later created a simple, quick method to generate a family of DNA tetrahedra with the difference of dimensions.<sup>31, 32</sup> These rigid 3D nanostructures are comprised of as few as four strands, and can self-assemble in seconds with the yield of as high as 95%. Later, they demonstrated a dynamic reconfigurable DNA tetrahedron by designing a hairpin loop at one edge. By the addition of a fuel strand or anti-fuel strand through strand displacement reactions, the shapes of the DNA tetrahedron were precisely controlled (Figure 1.4a).<sup>33</sup>

Though great achievements have been made, new methods which could expand the number of 3D DNA assemblies or ease the synthesis process are needed. Sleiman presented the construction of a large number of 3D DNA assemblies using a set of single-stranded and cyclic DNA building blocks which contained rigid organic molecules as vertices. A triangular prism, a cube, a

pentameric and hexameric prisms, a heteroprism and biprism were created (Figure 1.4b); and a structurally dynamic 3D DNA nanostructure, a triangular prism whose length was switched reversibly was also manufactured by this approach.<sup>34</sup>

A great advancement in the construction of 3D polyhedra was reported by Mao's group. Taking advantage of the structural symmetry, they were able to build large 3D nanostructures from many copies of identical units. By controlling the flexibility and concentration of the three-point-star tiles, tetrahedra, dodecahedra, or buckyballs were constructed (Figure 1.4c). They later used the same strategy to assemble an icosahedron from a five-point-star motif.<sup>35, 36</sup>

The minimum number of DNA strands required to construct 3D polyhedra was determined by Yan's group. They constructed a DNA tetrahedron made from merely a 286-nt ssDNA. Using standard molecular cloning techniques, the tetrahedron was successfully replicated *in vivo*, suggesting a promising method to scale up the synthesis of nanomaterials.<sup>37</sup>



**Figure 1.4.** 3D DNA polyhedra. (a) A reconfigurable DNA tetrahedron. (b) Various 3D polyhedra assembled from single-stranded and cyclic DNA building blocks with organic molecules as vertices. (c) Tetrahedron, dodecahedron, and buckyball assembled from three-point-star tiles.

### 1.3.2 3D DNA Origami Structures

In the past few years, the advanced development of DNA origami technique leads to the burst of novel 3D DNA objects with complex geometries and fine details. Joyce first reported the design and synthesis of an octahedron which was folded from a 1.7-kb ssDNA with the help of five short strands, representing an embryonic idea of 3D DNA origami (Figure 1.5a).<sup>38</sup> With double-crossover and paranemic-crossover (PX)<sup>39</sup> at the edges, the octahedron is expected to be highly rigid. In addition, since the sequence of the long ssDNA is not repeated, this structure is fully addressable.

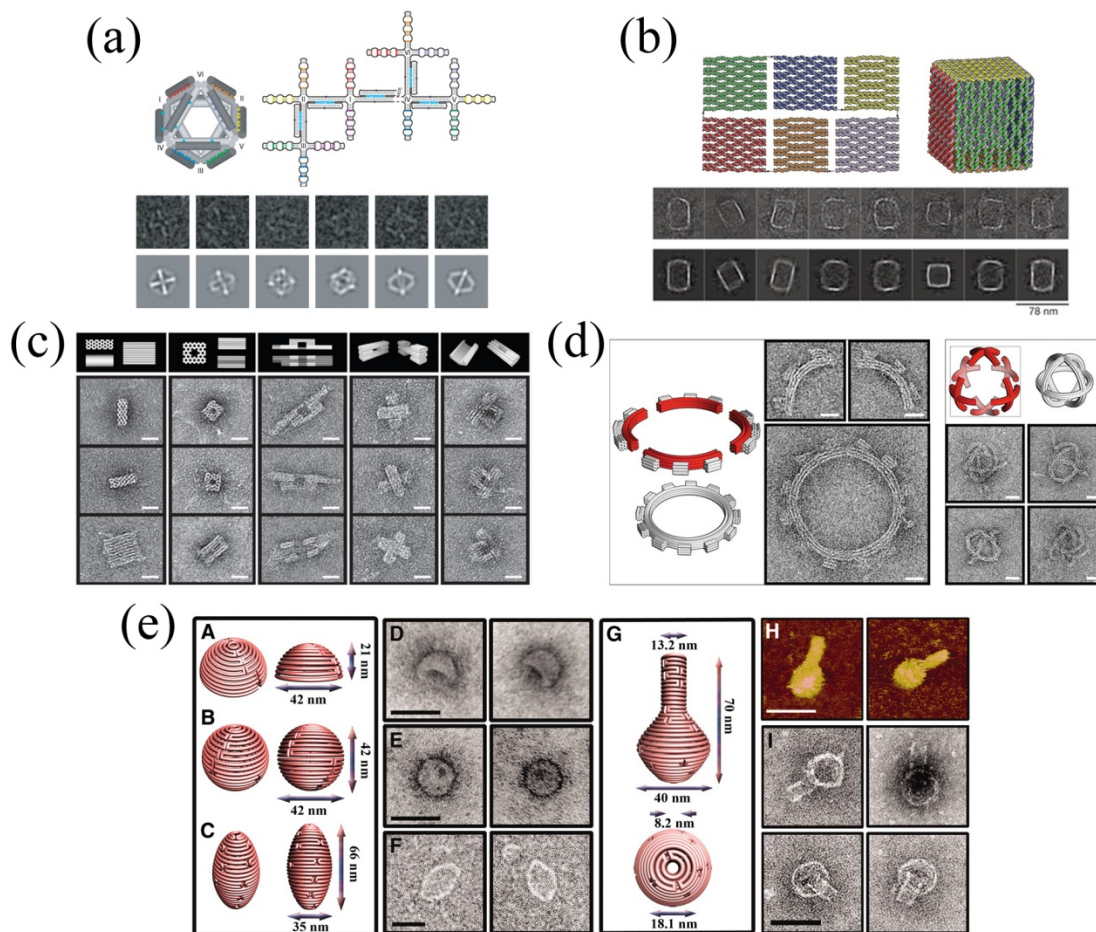
All the 3D polyhedra mentioned above are not completely closed structures because their faces do not contain any DNA duplex or crossovers. DNA origami technique can overcome this limitation.

Very recently, several groups demonstrated the design and assembly of DNA origami containers such as a cube and tetrahedron by bridging multiple faces which are 2D origami patterns themselves (Figure 1.5b).<sup>40, 41</sup> Different from their antecessors, these 3D structures form a completely closed space that the interior compartment is totally isolated from the outside, making them appealing targets to encapsulate functional molecules without worrying about leakage. Space-filling nanostructures including solid cuboids, square nut, railed bridge, genie bottle, stacked and slotted cross were also constructed by packing multiple layers of 2D origami patterns on square or honeycomb lattices (Figure 1.5c).<sup>42, 43</sup> The high helical density makes these sophisticated objects extremely rigid, while long annealing time taking up to a week is required to assemble them. The design

of 3D origami nanostructures was quite elaborative and time-consuming; therefore, computational programs were introduced to aid the structural modeling and conformational prediction. With the help of caDNAno, even one without previous experience can design 3D DNA origami structures after a short tutorial.<sup>44</sup>

To further improve the variety of 3D DNA library, different design principles were necessarily adopted. Shih's group constructed precisely controlled twisted and curved 3D nanostructures, including a wireframe beach ball and square-toothed gears, through targeted insertions and deletions of base pairs (Figure 1.5d).<sup>45</sup> The same group also reported the assembly of tensegrity structures that can resist against high forces by involving stretched ssDNA as springs.<sup>46</sup> Carefully adjusting the position and pattern of crossovers, Yan's group was able to assemble highly intricate DNA nanostructures with subtle curvatures such as a nanoflask, spherical and ellipsoidal shells (Figure 1.5e).<sup>47</sup>





**Figure 1.5.** 3D DNA origami nanostructures. (a) A DNA octahedron formed by folding 1.7-kb ssDNA with five short strands. (b) A DNA cube assembled by bridging multiple 2D origami faces. (c) Solid structures constructed by packing multiple layers of 2D origami patterns on square or honeycomb lattices. (d) Twisted and curved 3D nanostructures. (e) Highly intricate DNA nanostructures with subtle curvatures.

## 1.4 Spatial Arrangement of Biological Molecules by DNA Nanostructures

Precise spatial control is one of the most eye-catching features of self-assembled DNA nanostructures, so that they have been utilized as scaffolds to organize functional components (e.g. metallic nanoparticles<sup>48-59</sup>, quantum dots<sup>60</sup>, carbon nanotubes<sup>61</sup>, nucleic acids<sup>62</sup> and proteins) with well-defined intermolecular distances for a lot of advanced applications. Among all the molecules, proteins draw our attentions most because of their striking biological functions.

A linear array assembled from TX tiles was first selected to template streptavidin. One or two hairpin loops were modified with biotin groups to facilitate their binding to streptavidin, resulting in single-layer or double-layer protein arrays with well-controlled spacing.<sup>51</sup> Similarly, a two-tile system composed of the cross-shaped tiles led to periodic 2D streptavidin arrays (Figure 1.6a).<sup>63</sup>

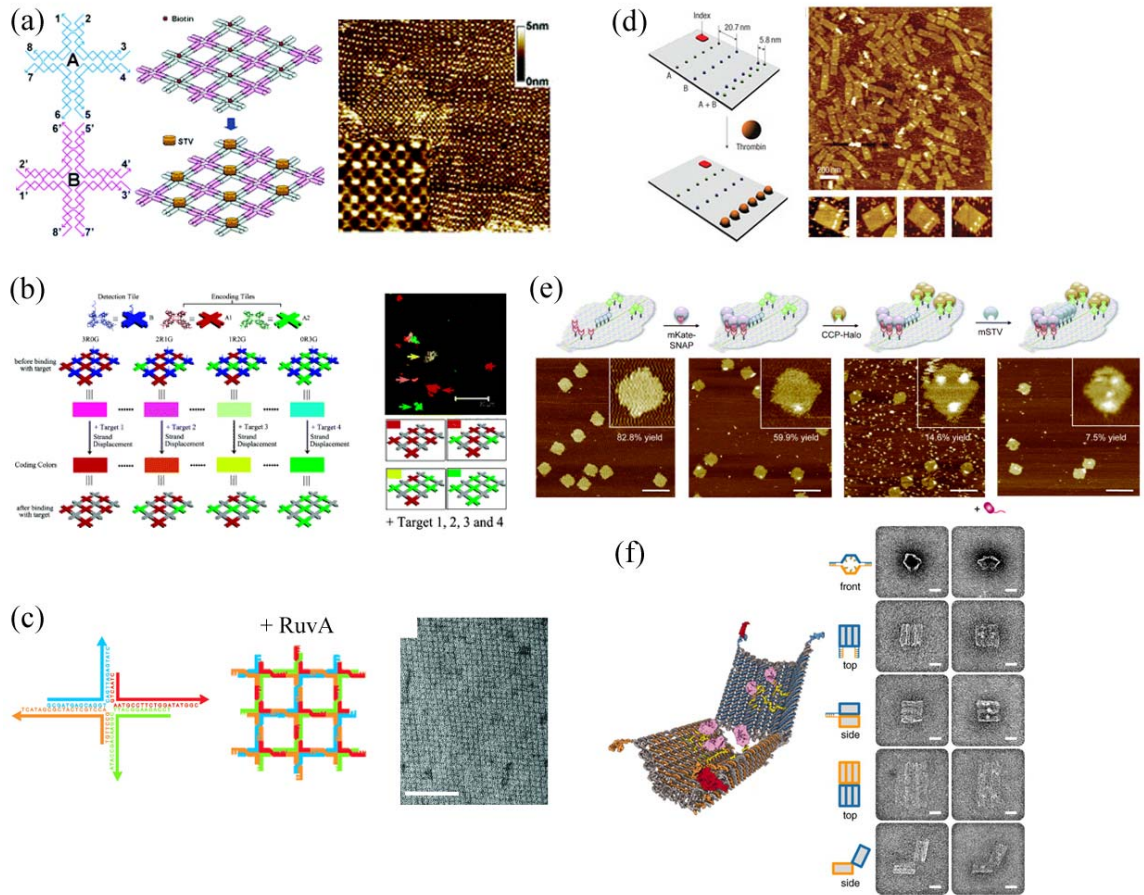
Yan's group then reported a work to organize thrombin by incorporation selective aptamer with high affinity into 1D arrays.<sup>64</sup> In another work, a signaling aptamer was chosen to modify the cross-shaped tiles. Once thrombin was added, a significant increase of fluorescence was observed under confocal microscopy due to the high density of the signaling aptamers displayed on the 2D DNA arrays, allowing for high sensitivity detection of low concentrations of thrombin.<sup>65</sup> The thrombin detection array was further developed by attaching multiple fluorophores to tiles. Different ratios of these encoding tiles were mixed with a detection tile composed of either an aptamer to a target molecule or a complementary strand to a viral DNA, to generate combinatorial colored

detection arrays, which allowed for the detection of multiple different targets at one time (Figure 1.6b).<sup>66</sup>

Besides taking advantage of biotin-streptavidin interactions and aptamers, using DNA-binding proteins and chemical modifications can also organize proteins by DNA nanostructures. An example of the former method was demonstrated by Turberfield's group. They incorporated a Holliday junction binding protein, RuvA, into 2D arrays assembled from Holliday junctions (Figure 1.6c).<sup>67</sup> In the latter method, chemical modified DNA and proteins are covalently conjugated. For example, the same group utilized cross-linking chemicals SPDP and SMCC to conjugate cytochrome *c* protein to amine-modified oligonucleotides, to encapsulate a single protein molecule within a tetrahedral cage.<sup>68</sup> In another case, Willner's group linked Sulfo-EMCS-modified glucose oxidase and horseradish peroxidase with thiolated oligonucleotides. The enzyme cascades were assembled on hexagon-like DNA scaffolds, leading to an activation of their enzymatic activities.<sup>69</sup>

The DNA origami tiles provide fully addressable scaffolds for label-free multi-target detection. A rectangular origami was designed to consist of three rows of detection probes complementary to three genes.<sup>70</sup> The target sequences were simultaneously incubated with the barcoded DNA origami array and all three were successfully detected with height changes under AFM. Later on, the multi-valency of biological systems inspired Yan's group to incorporate multiple-affinity ligands into DNA origami with precise controlled distances (Figure 1.6d). 50-fold stronger binding affinity of bivalence thrombin-specific aptamers was

observed on the nanoarray.<sup>71</sup> As demonstrated by Niemeyer's group, by using coupling systems such as "Snap-tag" and "Halo-tag", multiple different proteins could be site-specifically incorporated into face-shaped DNA origami (Figure 1.6e).<sup>72</sup> 3D DNA origami nanostructures hold great promise as drug delivery carriers. Very recently, an autonomous DNA origami nanorobot loaded with various antibody fragments was constructed. After opened by signals through aptamer-target recognition, the inside cargos can bind to their corresponding cell surfaces (Figure 1.6f).<sup>73</sup>



**Figure 1.6.** DNA nanostructures based spatial arrangement of biological molecules. (a) Streptavidin 2D arrays formed on DNA lattices through biotin-streptavidin interactions. (b) Barcoded DNA arrays for multiplexed detection of biological molecules. (c) The Holliday junction binding protein RuvA was aligned into 2D square lattices. (d) Distance-dependent binding of thrombin to the bivalence thrombin-specific aptamers on rectangular origami tiles. (e) Site-specific multiplex binding of various proteins on face-shaped DNA origami. (f) A DNA nanorobot loaded with antibody fragments.

## 1.5 Challenges and perspectives

The past three decades have witnessed numerous exciting breakthroughs in the fast-growing field of structural DNA nanotechnology. Nowadays, we can construct various 2D and 3D DNA nanostructures with high complexity and precise controlling of many functional molecules. Their distinct characterizations such as programmability, addressability, and self-assembly attract more and more scientist from various backgrounds to involve into the field. However, there are still quite a lot of challenges need to be addressed for its further development.<sup>74</sup>

First, most of the current DNA nanostructures are assembled in vitro. The recent progress in RNA nanotechnology that rationally designed 2D RNA arrays can be constructed in cells<sup>75</sup> makes us wonder if it is possible to assemble DNA nanostructures in vivo. If yes, it will lead to new solutions to many practical biological and medical issues such as in situ diagnostics, engineering of cell signaling pathways, and proteomics analysis. To address this issue, the very first consideration is the interface of DNA nanostructures and biological systems. It has been shown that DNA origami tiles are stable in cell lysate<sup>76</sup>, and simple branched tiles as well as a 3D tetrahedron structure can be amplified by molecular cloning<sup>77,37</sup>, indicating their biocompatibility. So the next step would focus on the ability of in vivo assembly of DNA nanostructures.

Second, the largest fully addressable DNA origami structures are within a few hundreds square nanometers range. In the effort to bridge bottom-up self-assembly to top-down approaches, and to mimic sophisticated biological systems, larger-sized structures are desirable. To design larger and more complex origami

tiles, the availability of longer nonperiodic ss-scaffolds is required, but the species of natural existing long ssDNA is scarce. Synthetic biology might provide possible solutions. Moreover, synthetic DNA is still pricy which not only hinders the construction of larger-sized DNA structures but also prevents the broad application of structural DNA nanotechnology. Reducing such cost will greatly boost the development of this field, but needs the effort of both chemists and biologists.

Third, the mechanisms of DNA self-assembly are not completely understood. It is not always the case that the assembled structures are exactly the same as designed. What kind of geometry and connecting strategy should a tile contain in order to form a specific higher-order assembled superstructure? What are the determining factors of the self-assembly process? What are the optimized conditions (e.g. tile concentration, annealing temperature, and annealing process) to achieve effective and efficient assembly? How to reduce the error rate, especially for complex structures? How is the kinetic process of the self-assembly? Thorough studies are necessary to answer these questions. Ideally, in the near future, we can construct any desired DNA structures, no matter 2D or 3D, exactly as what we design.

## 1.6 Projects

My graduate research work mainly focused on two projects. First, in order to study the biocompatibility of complex DNA nanostructures, and to increase the yield of synthetic DNA through low-cost method, I replicated a geometrically complex 3D DNA tetrahedron using molecular cloning (Chapter 2). Second, in an effort to investigate the higher-order assembly of DNA origami tiles, I did a systematic study of varying the inter-tile connection and the dimensional aspect ratios of tiles. The two factors were discovered to play important roles to determine the higher-order assembled products (Chapter 3). In addition, the effect of DNA hairpin loops on the origami tiles and on their high-order assembled structures was elucidated. The twisted structural model of origami tiles was proposed, consistent with the prediction by simulation software (Chapter 4).

## 1.7 References

- (1) Seeman, N. C. *Nature* **2003**, *421*, 427–431.
- (2) Aldaye, F. A.; Palmer, A.; Sleiman, H. F. *Science* **2008**, *321*, 1795-1799.
- (3) Lin, C.; Liu, Y. and Yan. H. *Biochemistry* **2009**, *48*, 1663-1674.
- (4) Watson, J. D.; Crick, F. H. C. *Nature* **1953**, *171*, 737-738.
- (5) Seeman, N. C. *J. Theor. Biol.* **1982**, *99*, 237–247.
- (6) Fu, T-J.; Seeman, N. C. *Biochemistry* **1993**, *32*, 3211–3220.
- (7) Winfree, E.; Liu, F.; Wenzler, L.A.; Seeman, N. C. *Nature* **1998**, *394*, 539–544.
- (8) LaBean, T.; Yan, H.; Kopatsch, J.; Liu, F.; Winfree, E.; Reif, J. H.; Seeman, N. C. *J. Am. Chem. Soc.* **2000**, *122*, 1848–1860.
- (9) Reishus, D.; Shaw, B.; Brun, Y.; Chelyapov, N.; Adleman, L. *J. Am. Chem.Soc.* **2005**, *127*, 17590–17591.



- (10) Ke, Y.; Liu, Y.; Zhang, J.; Yan, H. *J. Am. Chem. Soc.* **2006**, *128*, 4414–4421.
- (11) Mao, C.; Sun, W.; Seeman, N. C. *J. Am. Chem. Soc.* **1999**, *121*, 5437–5443.
- (12) Liu, D.; Wang, M.; Deng, Z.; Walulu, R.; Mao, C. *J. Am. Chem. Soc.* **2004**, *126*, 2324–2325.
- (13) Park, S. H.; Barish, R.; Li, H. Y.; Reif, J. H.; Finkelstein, G.; Yan, H.; LaBean, T. H. *Nano Lett.* **2005**, *5*, 693–696.
- (14) Mathieu, F.; Liao, S. P.; Kopatscht, J.; Wang, T.; Mao, C. D.; Seeman, N. C. *Nano Lett.* **2005**, *5*, 661–665.
- (15) Yan, H.; Park, S. H.; Ginkelstein, G.; Reif, J. H.; LaBean, T. H. *Science* **2003**, *301*, 1882–1884.
- (16) He, Y.; Tian, Y.; Chen, Y.; Deng, Z. X.; Ribbe, A. E.; Mao, C. D. *Angew. Chem. Int. Ed.* **2005**, *44*, 6694–6696.
- (17) He, Y.; Chen, Y.; Liu, H.; Ribbe, A. E.; Mao, C. *J. Am. Chem. Soc.* **2005**, *127*, 12202–12203.
- (18) He, Y.; Tian, Y.; Ribbe, A. E.; Mao, C. *J. Am. Chem. Soc.* **2006**, *128*, 15978–15979.
- (19) Lund, K.; Liu, Y.; Lindsay, S.; Yan, H. *J. Am. Chem. Soc.* **2005**, *127*, 17606–17607.
- (20) Park, S. H.; Pistol, C.; Ahn, S. J.; Reif, J. H.; Lebeck, A. R.; Dwyer, C.; LaBean, T. H. *Angew. Chem. Int. Ed.* **2006**, *45*, 735–739.
- (21) Rothmund, P. W. K.; Papadakis, N.; Winfree, E. *PLoS Biol.* **2004**, *2*, 2041–2053.
- (22) Yan, H.; LaBean, T. H.; Feng, L. P.; Reif, J. H. *Proc. Natl. Acad. Sci. USA* **2003**, *100*, 8103–8108.
- (23) Rothmund, P. W. K. *Nature* **2006**, *440*, 297–302.
- (24) Endo, M.; Sugita, T.; Katsuda, Y.; Hidaka, K. and Sugiyama, H. *Chem. Eur. J.* **2010**, *16*, 5362–5368.
- (25) Li, Z.; Liu, M.; Wang, L.; Nangreave, J.; Yan, H. and Liu, Y. *J. Am. Chem. Soc.* **2010**, *132*, 13545–13552.
- (26) Liu, W.; Zhong, H.; Wang, R. and Seeman, N.C. *Angew Chem Int Ed* **2011**, *50*, 264–267.

- (27) Zhao, Z.; Yan, H.; Liu, Y. *Angew Chem Int Ed* **2010**, *49*, 1414-1417.
- (28) Zhao, Z.; Yan, H.; Liu, Y. *Nano Lett.* **2011**, *11*, 2997-3002.
- (29) Chen, J.; Seeman, N. C. *Nature* **1991**, *350*, 631-633.
- (30) Zhang, Y.; Seeman, N. C. *J. Am. Chem. Soc.* **1994**, *116*, 1661-1669.
- (31) Goodman, R. P.; Berry, R. M.; Turberfield, A. J. *Chem. Commun.*, **2004**, 1372-1373.
- (32) Goodman, R. P.; Schaap, I. A. T.; Tardin, C. F.; Erben, C. M.; Berry, R. M.; Schmidt, C. F.; Turberfield, A. J. *Science* **2005**, *310*, 1661-1665.
- (33) Goodman, R. P.; Heilemann, M.; Doose, S.; Erben, C. M.; Kapanidis, A. N.; Turberfield, A. J. *Nat. Nanotechnol* **2008**, *3*, 93-96.
- (34) Aldaye, F. A.; Sleiman, H. F. *J. Am. Chem. Soc.* **2007**, *129*, 13376-13377.
- (35) He, Y.; Ye, T.; Su, M.; Zhang, C.; Ribbe, A. E.; Jiang, W.; Mao, C. *Nature* **2008**, *452*, 198-202.
- (36) Zhang, C.; Su, M.; He, Y.; Zhao, X.; Fang, P.; Ribbe, A. E.; Jiang, W.; Mao, C. *Proc. Natl. Acad. Sci. U.S.A.* **2008**, *105*, 10665-10669.
- (37) Li, Z.; Wei, B.; Nangreave, J.; Lin, C.; Liu, Y.; Mi, Y.; Yan, H. *J. Am. Chem. Soc.* **2009**, *131*, 13093-13098.
- (38) Shih, W. M.; Quispe, J. D.; Joyce, G. F. *Nature* **2004**, *427*, 618-621.
- (39) Shen, Z.; Yan, H.; Wang, T.; Seeman, N. C. *J. Am. Chem. Soc.* **2004**, *126*, 1666-1674.
- (40) Andersen, E. S.; Dong, M.; Nielsen, M. M.; Jahn, K.; Subramani, R.; Mamdouh, W.; Golas, M. M.; Sander, B.; Stark, H.; Oliveira, C. L. P.; Pedersen, J. S.; Birkedal, V.; Besenbacher, F.; Gothelf, K. V.; Kjems, J. *Nature* **2009**, *459*, 73-76.
- (41) Ke, Y.; Sharma, J.; Liu, M.; Jahn, K.; Liu, Y.; Yan, H. *Nano Lett.* **2009**, *6*, 2445-2447.
- (42) Ke, Y.; Douglas, S. M.; Liu, M.; Sharma, J.; Cheng, A.; Leung, A.; Liu, Y.; Shih, W. M.; Yan, H. *J. Am. Chem. Soc.* **2009**, *131*, 15903-15908.
- (43) Douglas, S. M.; Dietz, H.; Liedl, T.; Högberg, B.; Graf, F.; Shis, W. M. *Nature* **2009**, *459*, 414-418.

- (44) Douglas, S. M.; Marblestone, A. H.; Teerapittayanon, S.; Vazquez, A.; Church, G. M.; Shis, W. M. *Nucleic Acids Research* **2009**, *37*, 5001-5006.
- (45) Dietz, H.; Douglas, S. M.; Shih, W. M. *Science* **2009**, *325*, 725-730.
- (46) Liedl, T.; Högberg, B.; Tytell, J.; Ingber, D. E. and Shih, W. M. *Nature Nanotechnology* **2010**, *5*, 520-524.
- (47) Han, D.; Pal, S.; Nangreave, J.; Deng, Z.; Liu, Y.; Yan, H. *Science* **2011**, *332*, 342-346.
- (48) Mirkin, C. A.; Letsinger, R. L.; Mucic, R. C.; Storhoff, J. J. *Nature* **1996**, *382*, 607-609.
- (49) Alivisatos, A. P.; Johnsson, K. P.; Peng, X.; Wilson, T. E.; Loweth, C. J.; Bruchez Jr, M. P.; Schultz, P. G. *Nature*, **1996**, *382*, 609-611.
- (50) Le, J. D.; Pinto, Y.; Seeman, N. C.; Musier-Forsyth, K.; Taton, T. A.; Kiehl, R. A. *Nano Letters* **2004**, *4*, 2343-2347.
- (51) Li, H.; Park, S. H.; Reif, J. H.; LaBean, T. H.; Yan, H. *J. Am. Chem. Soc.* **2004**, *126*, 418-419.
- (52) Sharma, J.; Chhabra, R.; Liu, Y.; Ke, Y.; Yan, H. *Angew. Chem., Int. Ed.* **2006**, *45*, 730-735.
- (53) Zheng, J.; Constantinou, P. E.; Micheel, C.; Alivisatos, A. P.; Kiehl, P. A. and Seeman, N. C. *Nano Letters* **2006**, *6*, 1502-1504.
- (54) Sharma, J.; Chhabra, R.; Andersen, C. S.; Gothelf, K. V.; Yan, H.; Liu, Y. *J. Am. Chem. Soc.* **2008**, *130*, 7820-7821.
- (55) Sharma, J.; Chhabra, R.; Cheng, A.; Brownell, J.; Liu, Y. and Yan, H. *Science* **2009**, *323*, 112-116.
- (56) Bhatia, D.; Mehtab, S.; Krishnan, R.; Indi, S. S.; Basu, A.; Krishnan, Y. *Angew. Chem., Int. Ed.* **2009**, *48*, 4134-4137.
- (57) Mastroianni, A. J.; Claridge, S. A.; Alivisatos, P. A. *J. Am. Chem. Soc.* **2009**, *131* (24), 8455-8459.
- (58) Ding, B.; Deng, Z.; Yan, H.; Cabrini, S.; Zuckermann, R. N.; Bokor, J. *J Am Chem Soc* **2010**, *132*, 3248-3249.
- (59) Pal, S.; Deng, Z.; Ding, B.; Yan, H.; Liu, Y. *Angew Chem Int Ed* **2010**, *49*, 2700-2704.

- (60) Sharma, J.; Ke, Y.; Lin, C.; Chhabra, R.; Wang, Q.; Nangreave, J.; Liu, Y.; Yan, H. *Angew Chem Int Ed* **2008**, *47*, 5157-5159.
- (61) Maune, H. T.; Han, S.; Barish, R. D.; Bockrath, M.; Goddard III, W. A.; Rothmund, P. W. K.; and Winfree, E. *Nature Nanotechnology* **2010**, *5*, 61-66.
- (62) Lund, K.; Manzo, A. J.; Dabby, N.; Michelotti, N.; Johnson-Buck, A.; Nangreave, J.; Taylor, S.; Pei, R.; Stojanovic, M. N.; Walter, N. G.; Winfree, E.; Yan, H. *Nature* **2010**, *465*, 206-210.
- (63) Park, S. H.; Yin, P.; Liu, Y.; Reif, J. H.; LaBean, T. H.; Yan, H. *Nano Lett.* **2005**, *5*, 729-733.
- (64) Liu, Y.; Lin, C.; Li, H.; Yan, H. *Angew. Chem. Int. Ed.* **2005**, *44*, 4333-4338.
- (65) Lin, C.; Xie, M.; Chen, J. J.-L.; Liu, Y.; Yan, H. *Angew. Chem. Int. Ed.* **2006**, *45*, 7537-7539.
- (66) Lin, C.; Liu, Y.; Yan, H. *Nano Lett.* **2007**, *7*, 507-512.
- (67) Malo, J.; Mitchell, J. C.; Vénien-Bryan, C.; Harris, J. R.; Wille, H.; Sherratt, D. J.; Turberfield, A. J. *Angew. Chem. Int. Ed.* **2005**, *44*, 3057-3061.
- (68) Erben, C. M.; Goodman, R. P.; Turberfield, A. J. *Angew. Chem. Int. Ed.* **2006**, *45*, 7414-7417.
- (69) Wilner, O. I.; Weizmann, Y.; Gill, R.; Lioubashevski, O.; Freeman, R.; Willner, I. *Nature Nanotechnology* **2009**, *4*, 249-254.
- (70) Ke, Y.; Lindsay, S.; Chang, Y.; Liu, Y.; Yan, H. *Science* **2008**, *319*, 180-183.
- (71) Rinker, S.; Ke, Y.; Liu, Y.; Chhabra, R.; Yan, H. *Nat. Nanotechnol* **2008**, *3*, 418-422.
- (72) Sacca, B.; Meyer, R.; Erkelenz, M.; Kiko, K.; Arndt, A.; Schroeder, H.; Rabe, K. S.; Niemeyer, C. M. *Angew. Chem. Int. Ed.* **2010**, *49*, 9378-9383.
- (73) Douglas, S. M.; Bachelet, I.; Church, G. M. *Science* **2012**, *335*, 831-834.
- (74) Pinheiro, A. V.; Han, D.; Shih, W. M.; Yan, H. *Nat. Nanotechnol* **2011**, *6*, 763-772.
- (75) Delebecque, C. J.; Lindner, A. B.; Silver, P. A.; Aldaye, F. A. *Science* **2011**, *333*, 470-474.

- (76) Mei, Q.; Wei, X.; Su, F.; Liu, Y.; Youngbull, C.; Johnson, R.; Lindsay, S.; Yan, H.; Meldrum, D. *Nano Lett.* **2011**, *11*, 1477–1482.
- (77) Lin, C.; Rinker, S.; Wang, X.; Liu, Y.; Seeman, N. C.; Yan, H. *Proc. Natl. Acad. Sci. U.S.A.* **2008**, *105*, 17626–17631.

## Chapter 2

### **A Replicable Tetrahedral Nanostructure Self-Assembled from a Single DNA Strand**

Adapted with permission from Li, Z.; Wei, B.; Nangreave, J.; Lin, C.; Liu, Y.; Mi, Y.; Yan, H.: A Replicable Tetrahedral Nanostructure Self-Assembled from a Single DNA Strand, *J. Am. Chem. Soc.* **2009**, *131*, 13093-13098. Copyright 2009 American Chemical Society.

#### **2.1. Abstract**

We report the design and construction of a nanometer-sized tetrahedron from a single strand of DNA that is 286 nucleotides long. The formation of the tetrahedron was verified by restriction enzyme digestion, Ferguson analysis and atomic force microscopy (AFM) imaging. We further demonstrate that the synthesis of the tetrahedron can be easily scaled up through in vivo replication using standard molecular cloning techniques. We found that the in vivo replication efficiency of the tetrahedron is significantly higher in comparison to in vitro replication using rolling-circle amplification (RCA). Our results suggest that it is now possible to design and replicate increasingly complex, single-stranded DNA nanostructures in vivo.

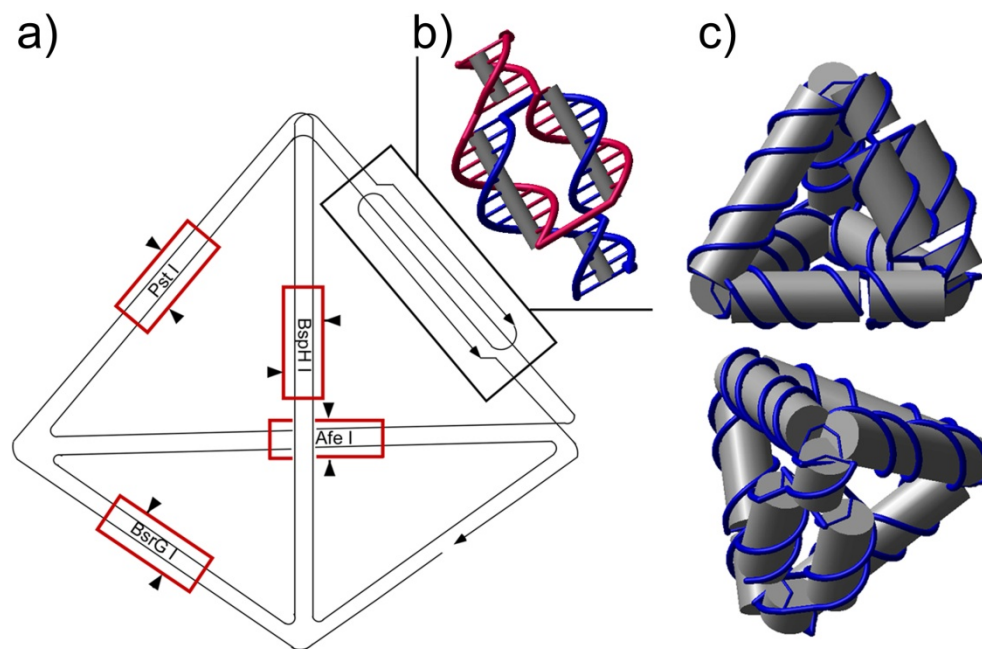
## 2.2. Introduction

With highly specific Watson-Crick base pairing and a well-characterized double helical structure, DNA has been utilized as a programmable building material to construct designer nanoscale architectures for a broad range of applications, such as organizing nanoparticles and proteins and confining the motions of DNA-based nanomotors.<sup>1-10</sup> To date, a large variety of one- and two-dimensional (1D and 2D) DNA nanostructures have been successfully designed and assembled.<sup>11-25</sup> Recently, a series of three-dimensional (3D) polyhedra DNA nanoarchitectures<sup>26-35</sup> were generated through either one-step or hierarchical assembly approaches, further enriching the vast library of artificial DNA constructions. Nevertheless, these DNA polyhedrons were constructed from multiple oligonucleotides with deliberately designed sequences. In one case, Shih et al.<sup>29</sup> synthesized an octahedron by folding a 1.7-kb single-stranded DNA (ssDNA) with the help of five short DNA strands, suggesting the possibility of folding a ssDNA molecule into a well-defined 3D nanostructure. However, the minimum number of DNA strands required to build a complete 3D polyhedron remained to be determined. In addition, recent progress in replicating artificial DNA nanostructures revealed that ssDNA molecules with complicated secondary structures can be amplified efficiently and with high fidelity using biological methods<sup>36</sup>, making the replication of a single-stranded 3D polyhedron an appealing objective to pursue. Here we present the facile preparation and in vivo replication of a DNA tetrahedron folded from one ssDNA molecule that is 286-nucleotides (nt) long. This study demonstrates a reliable method that can be used

for the design and replication of other types of single stranded, 3D DNA nanostructures of considerable complexity.

The folding pathway of the single-stranded tetrahedron is illustrated in Figure 2.1a. Among its six edges, five are composed of 21-base-pair (bp) double helices, while the remaining edge contains a “twin double helical” motif (Figure 2.1b) to accommodate the required reverse polarity of complementary DNA strands. Four cleavable sites specific to the following restriction enzymes: *Pst*I, *Bsr*GI, *Afe*I and *Bsp*HI, were designed in the middle of four edges of the DNA tetrahedron (Figure 2.1a) for restriction digestion characterization of the assembly product. An unpaired thymine base was incorporated at each vertex to allow adequate flexibility for folding. When annealed, the DNA strand self-assembled into the desired tetrahedron (Figure 2.1c) through designated intra-molecular base pairing.





**Figure 2.1.** Design of the ssDNA tetrahedron. (a) Folding pathway of the single-stranded tetrahedron. Five edges are composed of 21-bp double helices, while the remaining edge contains a “twin double helical” component. In the middle of four edges of the DNA tetrahedron, four restriction enzyme sites (*PstI*, *BsrGI*, *AfeI* and *BspHI*) are designed. The restriction digestion sites of the corresponding enzymes are indicated by red boxes and black arrow heads. (b) Structural design of the twin double helical component of the remaining edge. (c) Front and top views of the 3D molecular model the tetrahedron.

## 2.3. Materials and Methods

**2.3.1. Materials.** Detailed information about the materials used in this study can be found in the supporting information.

**2.3.2. Structural Design and Assembly.** The tetrahedron structure was modeled using Nanoengineer-1 ([www.nanorex.com](http://www.nanorex.com)) and the DNA sequence was generated by Uniquimer (Figure S1 in Appendix A).<sup>37</sup> Due to the extremely low yield of the synthesis of DNA oligonucleotides longer than 200 bases, the 286-nt ssDNA was divided into three segments (Table 2.1); they were first synthesized separately and subsequently ligated to yield the complete strand. Equal molar amounts of component strands 1, 2, and 3 were mixed at 0.5  $\mu\text{M}$  in 1 $\times$  TAE/ $\text{Mg}^{2+}$  buffer [Tris-acetic acid 40 mM, pH 8.0, magnesium acetate 12.5 mM, EDTA 1 mM] and annealed in a water bath from 95  $^{\circ}\text{C}$  to room temperature for approximately 48 hours. Ten units of T4 DNA ligase in 1 $\times$  T4 DNA ligase buffer were added to 100 pmol of annealed sample and left at 4  $^{\circ}\text{C}$  overnight, to seal the two nicks. Denaturing polyacrylamide gel electrophoresis (PAGE) purification was utilized to obtain the full-length strand (Figure S2 in Appendix A).

|                     |  |
|---------------------|--|
| Component strand 1  | AGACGTGCGTTAGATATGCTGTACAAGCGCG<br>ATCGTGACGACTGCAGAAAGTGCTTCACGCAT<br>TTCATGATACGAGCTACGCACGTCTACTCTA<br>GGGCGTGGGTGC                                 |
| Component strand 2* | /Phos/GGAGCGCTGGCCGAATTCGCGCTTGTA<br>CAGCATATCTTGCTCGTATCATGAAA  |
| Component strand 3* | /Phos/TGCGTGTGCGACTCTCGTGCCGGCTTG<br>CGTCCGCGTCGCTAGCACTTCTGCAGTCGTC<br>ACGTTTCGGCCAGCGCTCCGCACCCTGCGGC<br>CCGGCACGAGAGCGGACGCAAGGCCGCTCG<br>CCCTAGAGT |

\* The 5' end of the strand is phosphorylated.

**Table 2.1.** Sequences of the component strands that were used to synthesize the full length (286-nt) ssDNA.

**2.3.3. Restriction Enzyme Digestion.** The purified, full-length DNA strand was annealed in a water bath from 95 °C to room temperature for about 48 hours to facilitate the folding of the single strand into the desired tetrahedron, and the annealed DNA sample was then digested by restriction enzymes (*Pst*I or *Bsr*GI or *Afe*I or *Bsp*HI). Two picomoles of DNA were digested by 10 Units of enzyme in 40 µL of 1× NE buffer 1 at 37 °C for 3 hours. The digested products were analyzed by 10% denaturing PAGE.

**2.3.4. Ferguson Analysis.** The pre-annealed, single-stranded DNA tetrahedron, the DNA tetrahedron assembled from four oligonucleotides as described by Goodman et al.<sup>30</sup>, and a 25-bp DNA ladder were loaded into separate lanes of nondenaturing 6%, 8%, 10%, and 12% polyacrylamide gels. The four gels were simultaneously run for 3 hours at a constant voltage of 10 V/cm. After

staining, the mobilities of corresponding bands were measured from the gel images manually, using a millimeter-scale ruler.

**2.3.5. AFM Imaging.** The DNA tetrahedron samples (2  $\mu\text{L}$ , 10 nM) were deposited onto a freshly cleaved mica (Ted Pella, Inc.) and left to adsorb for 3 min. Buffer (1x TAE- $\text{Mg}^{2+}$ , 30  $\mu\text{L}$ ) was added to the liquid cell and the sample was scanned in tapping mode on a Multimode-V AFM (Veeco, Inc) with NP-S tips (Veeco, Inc.).

**2.3.6. In Vivo Cloning.** The single-stranded DNA tetrahedron was extended at both the 5' and 3' ends and hybridized to its Watson-Crick complement to form a double strand with the proper sticky end sequence (*Pst*I and *Sac*I) for insertion into a plasmid. To avoid undesired digestion products, the *Pst*I cleavage site [d(CTGCAG)] on one edge of the tetrahedron was changed to d(CTGTAG). The in vivo cloning procedures were adapted from a protocol previously reported by Lin et al.<sup>36</sup> (see Appendix A for additional details). Restriction enzyme digestion and Ferguson analysis were used to characterize the replicated product, as described above.

**2.3.7. Rolling-circle Amplification of the Tetrahedron.** RCA was initially attempted to amplify this strand (see Appendix A for details).

## 2.4. Results and Discussion

Synthesis of the single-stranded tetrahedron began with ligation of the three component strands (105-nt, 53-nt and 128-nt) to yield the full-length 286-mer oligonucleotide. First, the three component strands were mixed in stoichiometric ratios and annealed to allow intermolecular self-assembly, and T4 DNA ligase was subsequently added to seal the phosphorylated nicks. From the denaturing PAGE assay (Figure S2 in Appendix A), the yield of the ligation reaction was estimated to be ~50%. The relatively high yield of ligation suggested that the self-assembly of the three component strands formed a discrete nanostructure as expected. The full-length 286-nt ssDNA molecule extracted from the gel was then annealed to fold into the desired tetrahedron. Since the self-assembly process involved only a single DNA strand, experimental uncertainties such as pipetting errors that could lead to stoichiometry problems were minimized. It is worth noting that the annealing process was carried out at a relatively low DNA concentration (50 nM), to minimize undesired interstrand associations and achieve optimal assembly yield.

To confirm the correct formation of the tetrahedron after annealing, three experiments were performed: restriction enzyme digestion, Ferguson analysis and AFM imaging.

According to the design illustrated in Figure 2.1a, each of the four restriction enzymes will digest the tetrahedron into three fragments with specific lengths (Table 2.2). Following reference 28, we analyzed the restriction-digested samples by non-denaturing PAGE (Figure 2.2a). After cleavage by each enzyme,

a shift of the mobility of the original band was observed without fragmentation, which suggested that the major structure was assembled from ssDNA rather than from multiple strands. The slightly lower mobility of the digested samples was expected, due to their higher flexibility than the uncut structure. Moreover, a denaturing PAGE assay (Figure 2.2b) revealed that, after restriction cleavage, the major DNA fragments that resulted were in perfect agreement with the expected enzyme digestion patterns, indicating correct folding of the tetrahedron. A few side products were also observed as faint bands in the gel image in Figure 2.2b. These are attributed to the products of star reactions of the enzymes or the cleavage of other DNA nanostructures. For example, although the single-stranded tetrahedron represented the major self-assembly product, dimers, trimers, or even higher order aggregates of the ssDNA molecules could form through intermolecular base-pairing, which may have led to the observed side products upon treatment with the restriction enzymes. This assumption was supported by the non-denaturing PAGE assay (Figure 2.2c), which shows a few minor bands with reduced mobility as compared to the major band of the tetrahedron. These minor bands can be assigned to some multimolecular aggregates. From the gel images, the yield of the correct tetrahedron structure is estimated to be >90%. On the basis of the results above, including one denaturing gel and two non-denaturing gels, we concluded that the assembled structure was formed from ssDNA and folded as designed.

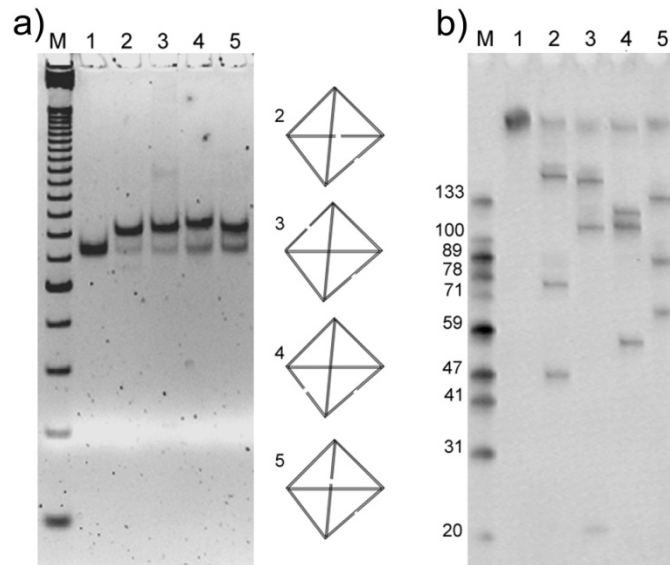
Ferguson analysis (Figure 2.2d) was also utilized to characterize the conformation of the DNA molecules using nondenaturing gel electrophoresis. By

measuring the mobility of the DNA nanostructure at different gel concentrations, the friction constant of the DNA nanostructure is obtained, which is related to its surface area and shape. The single-stranded tetrahedron was run together with a previously reported tetrahedron assembled from four individual strands, as a positive control (Figure 2.2b). The one-stranded tetrahedron has the same geometry as the four-stranded tetrahedron, with a wider edge containing the twin double-helical component and fewer nicks. As expected, it ran slightly slower than the four-stranded tetrahedron because of its higher molecular weight (137-bp versus 120-bp). Most importantly, the two tetrahedral molecules displayed very similar slopes in the Ferguson plot. In contrast, the negative controls, a 125-bp double-stranded DNA (dsDNA) molecule, and the partial structures formed from component strand 1 and 3 respectively, showed significantly different slopes from the two tetrahedron structures. These results strongly suggested that the 286-nt single-stranded DNA folded into the desired tetrahedral nanostructure.

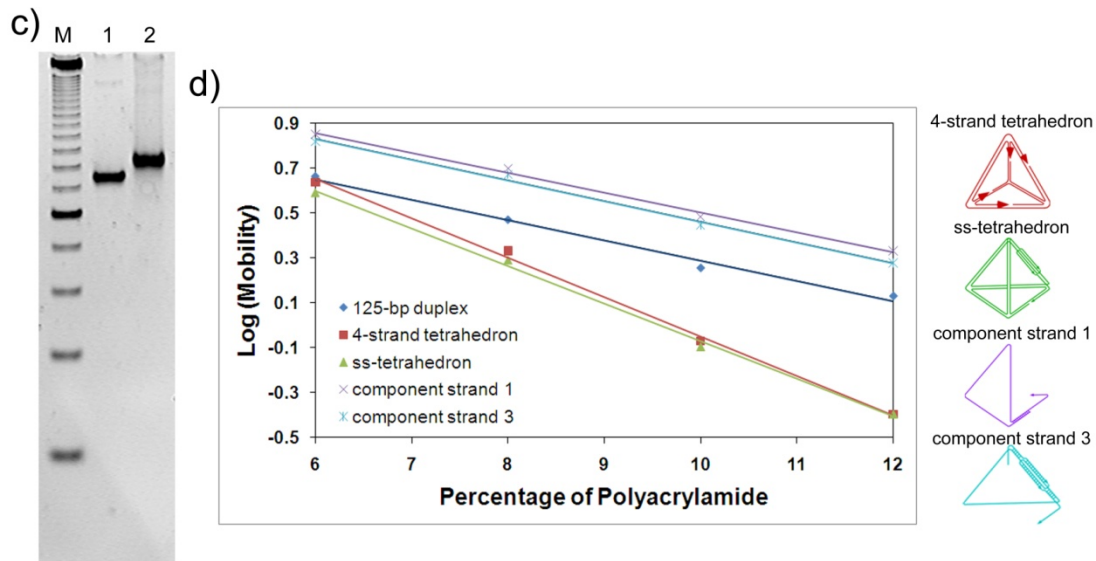
| Restriction Enzyme    | <i>Pst</i> I | <i>Bsr</i> GI | <i>Afe</i> I | <i>Bsp</i> HI |
|-----------------------|--------------|---------------|--------------|---------------|
| Fragment Lengths (nt) | 46, 76, 164  | 20, 109, 157  | 56, 110, 120 | 64, 87, 135   |
| Lane in Figure 2.2a   | 2            | 3             | 4            | 5             |

**Table 2.2.** The expected DNA fragment lengths after the tetrahedron was restriction digested.



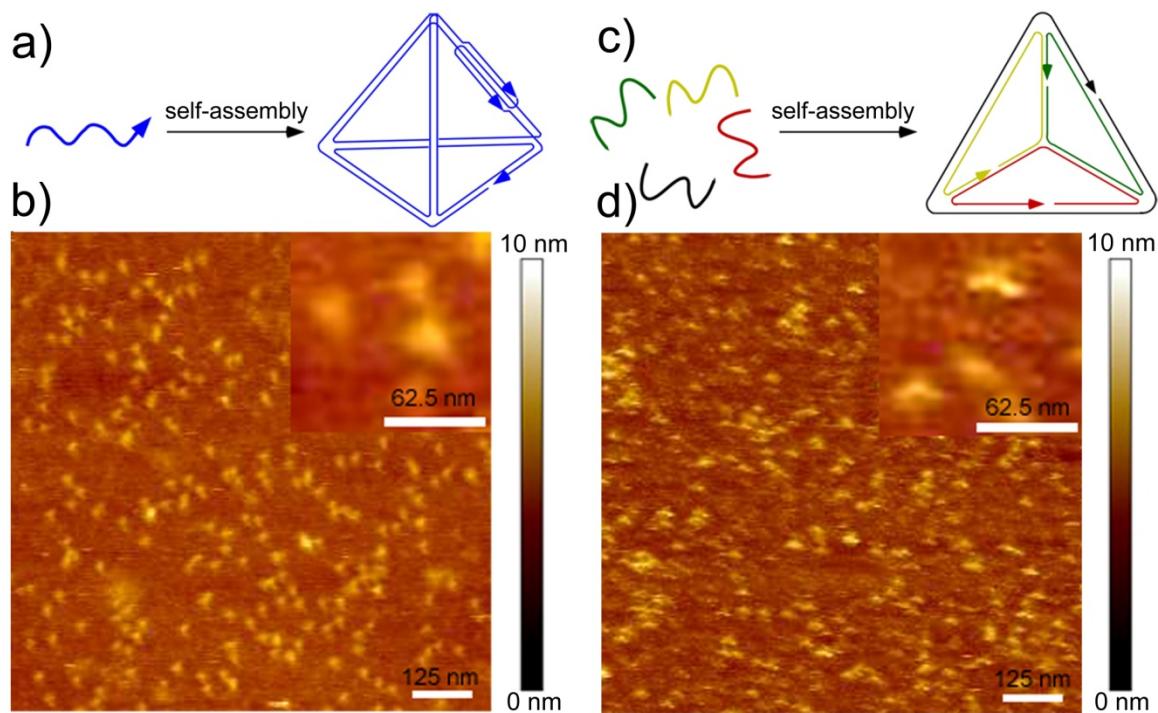


**Figure 2.2.** Characterization of the single-stranded DNA tetrahedron. (a) Result of the restriction enzyme digestion of the ss-tetrahedron on a nondenaturing PAGE (8% polyacrylamide gel). A 125-bp DNA marker was loaded in lane M. *AfeI*, *PstI*, *BsrGI*, and *BspHI* digested samples were loaded in lanes 2, 3, 4, and 5, respectively. The cutting sites are illustrated on the right. (b) Denaturing PAGE showing the result of the restriction enzyme digestion. Single-stranded DNA markers were loaded in lane M with the lengths shown on the left of the corresponding marker band. Lane 1 was loaded with the undigested 286-nt ssDNA. *PstI*, *BsrGI*, *AfeI* and *BspHI* digested samples were loaded in lanes 2, 3, 4, and 5, respectively. Note that the lengths of the corresponding fragments were in perfect agreement with the expected digestion product lengths as listed in Table 2.2.



**Figure 2.2. Continued** (c) Nondenaturing PAGE (8% polyacrylamide gel) comparing the mobility of the four-stranded tetrahedron (lane 1) and single-stranded tetrahedron (lane 2). Lane M contains 25-bp dsDNA marker as a reference. (d) Ferguson analysis of the ss-tetrahedron (137 bp, green), a four-stranded tetrahedron (120 bp, red), a 125-bp dsDNA (black), the structure formed by component strand 1 (purple), and the structure formed by component strand 3 (cyan). The two tetrahedron molecules displayed similar Ferguson slopes; both were significantly different from that of a 125-bp DNA duplex and partially formed structures.

AFM imaging was further used to visualize the assembled structure. We compared our structure assembled by the one-strand strategy with Turberfield's tetrahedron structure<sup>30</sup> formed by the four-strand method. The AFM images shown in Figure 2.3b, d demonstrate that the particles deposited on the mica surface feature similar morphology with a triangular starlike shape. The sample containing the tetrahedron assembled by the one-strand strategy is more monodisperse, both in size and in shape, as compared to the four-strand tetrahedron sample. This is likely because the tetrahedron composed of four strands has more nick points and is thus more prone to deformation by scanning with an AFM tip. Both structures measure about the same height of  $\sim 2$  nm, which is consistent with previous observations of tetrahedral structures by the Mao group.<sup>31</sup> The height is slightly higher than a DNA duplex, which commonly measures about 1.4 nm on a mica surface via AFM. A height of  $\sim 2$  nm corresponds to a tetrahedron that has been flattened on the mica surface and squashed by the AFM tip. The lateral dimension of the individual particles measures  $\sim 20$  nm, larger than the expected  $\sim 7$  nm, due to resolution that is limited laterally by the tip diameter. This enlargement effect has also been observed by Mao's group with their tetrahedral DNA structures.<sup>31</sup> Overall, side-by-side AFM comparison of our one-strand tetrahedron with the four-stranded tetrahedron, combined with the Ferguson analysis, strongly suggests the correct formation of our designed structures.



**Figure 2.3.** Schematics and direct comparison of AFM images of tetrahedron

DNA structures. (a, b) Tetrahedron formed by one-strand strategy. (c, d)

Tetrahedron formed by four-strand strategy. Scale bars are labeled in each image

and zoom-in images.

After confirmation of the successful assembly of the single-stranded tetrahedron, we sought to scale up the synthesis and replicate the nanostructure by a biological approach. RCA was first used to replicate the structure (see Appendix A for experimental details and results). However, the replication efficiency was not satisfactory, most likely a result of the complicated 3D structure of the tetrahedron, preventing efficient strand displacement in the RCA reaction.

Encouraged by recent findings that artificial DNA nanostructures, such as a Holiday junction-like structure and a paranemic DNA crossover (PX) molecule, can be replicated in viruses and bacterium,<sup>36</sup> we exploited the *in vivo* cloning protocol to amplify the single-stranded tetrahedron (see Figure S4 in Appendix A for replication scheme). Briefly, the single-stranded tetrahedron (sense strand, 292-nt including the core structure and terminal sticky-end extensions) was inserted into a phagemid, transformed into XL1-Blue cells, and amplified *in vivo* in the presence of helper phages. The replicated tetrahedrons were recovered by restriction digestion of the single-stranded phagemid extracted from the viral particles. Denaturing PAGE (Figure 2.4a) was used to evaluate the replication efficiency. The results clearly showed that the replication product had the same molecular weight as the 292-nt sense strand (with the sticky ends added). Approximately 50 pmol of tetrahedron was produced (calculated from the OD<sub>260</sub> value of purified DNA) from 250 ml culture medium. It is very important to point out that this amplification is fully scalable. The final yield of nanostructure is proportional to the volume of the culture medium used. The yield could be improved further by optimizing digestion conditions and the purification process.

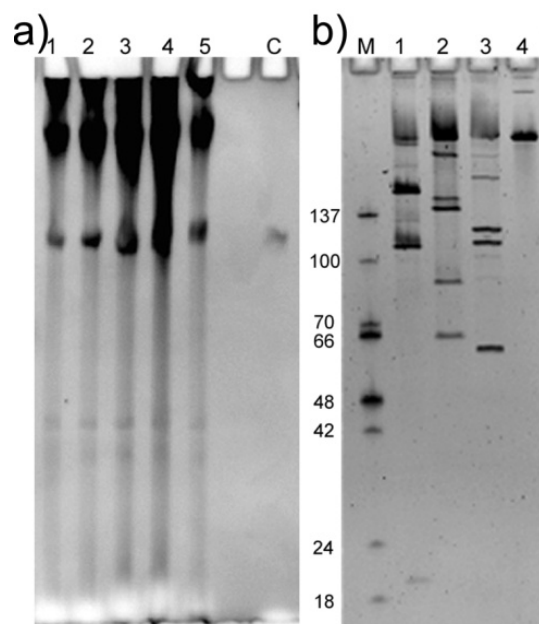
The replicated strand was then subjected to restriction enzyme digestion and Ferguson analysis to verify that it could still fold into the tetrahedron structure as designed. First, the replication product was separately treated with the restriction enzymes, *BsrGI*, *BspHI*, and *AfeI*. It should be noted that the *PstI* site in the original design was removed to avoid conflicts with the sticky end design for ligation with the plasmid. Denaturing PAGE was used to analyze the digestion results (Figure 2.4b). Again, all fragment lengths were consistent with the expected pattern summarized in Table 2.3. Some irregular digestion products were also observed, possibly due to misfolding of the long ssDNA that contained extensive self-complementary sequences and potential for aggregation, similar to the observations in Figure 2.2c. Second, nondenaturing PAGE (Figure 2.4c) showed that the replicated tetrahedron (292 nt) exhibited almost the same migration rate as the original 286-nt tetrahedron molecule. The slight difference is a result of the additional sticky ends at the 5' and 3' ends of the replicated molecule. Ferguson analysis was then used to compare the friction constant of the replicated tetrahedron to that of the original 286-nt tetrahedron (Figure 2.4d). The plot of the two molecules nearly overlapped, while the plot for a 100-bp double-stranded DNA showed a dramatically different slope. This observation strongly suggested that the replicated strand correctly folded into the tetrahedron structure, confirming that the single-stranded tetrahedron was replicated with high fidelity by in vivo cloning.

Compared with in vitro enzymatic amplification (RCA), in vivo replication resulted in significantly higher amplification efficiency, demonstrating

the power of naturally existing cellular machinery. This is consistent with our former finding<sup>36</sup> that in vivo replication yields higher replication efficiency of complicated nanostructures such as a paranemic crossover.

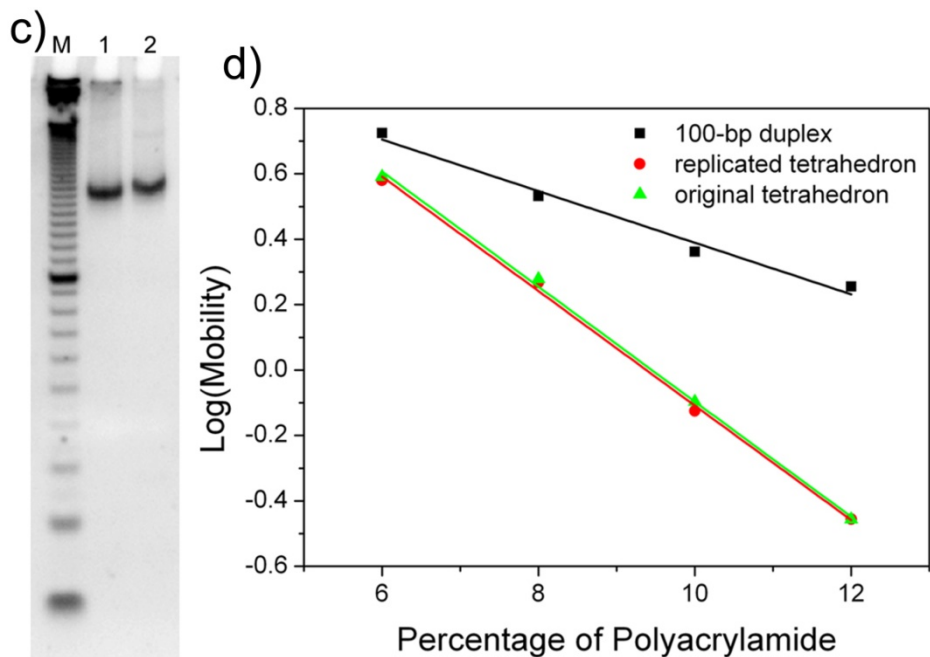
| Restriction Enzyme    | <i>Bsr</i> GI | <i>Bsp</i> HI | <i>Afe</i> I |
|-----------------------|---------------|---------------|--------------|
| Fragment lengths (nt) | 21, 109, 162  | 65, 87, 140   | 61, 111, 120 |
| Lane in Figure 2.4a   | 2             | 3             | 4            |

**Table 2.3.** Fragment lengths of the replicated DNA digested by the three restriction enzymes, respectively.



**Figure 2.4.** In vivo replication of the single-stranded DNA tetrahedron. (a) Denaturing PAGE showing the final replication product. Lane C, 292-nt sense strand; lanes 1-5, replication products. The DNA species at the top of the gel image represent digested and undigested phagemid vectors; the bands that migrate faster than the complete tetrahedron are truncated nanostructures that may result from incomplete replication. (b) Restriction enzyme digestion assay performed on the replicated tetrahedron. Lane M was loaded with ss-markers with the lengths shown on the left of the corresponding marker band. Lane 4 was loaded with the undigested 292-nt tetrahedron strand. Lanes 1, 2, and 3 are *BsrGI*, *BspHI* and *AfeI* digested samples, respectively.





**Figure 2.4. Continued** (c) Nondenaturing PAGE assay showing the mobility of the replicated tetrahedron. Lane M, 10-bp double-stranded DNA ladder; lane 1, annealed original 286-nt tetrahedron; lane 2, annealed replicated tetrahedron (292-nt). (d) Ferguson analysis of the tetrahedron after replication (red circles), the tetrahedron assembled from the original 286-nt strand (green triangles), and a 100-bp dsDNA (black squares).

## 2.5. Conclusion

In summary, we have successfully constructed a DNA tetrahedron folded from one ssDNA molecule. To the best of our knowledge, this is the first example of a discrete single-stranded 3D DNA nanostructure experimentally constructed. We expect that our method is highly adaptable for the construction of other polyhedra nanostructures. Compared to the multistrand system, the single-stranded folding strategy features the following advantages: First, it simplifies the assembly process and eliminates stoichiometric dependence, leading to a better assembly yield. Second, it makes the resulting 3D nanostructures readily amplifiable. This is important for scaling up the preparation of DNA nanostructures. Third, the single-stranded nanostructures can easily be circularized to impart exonuclease-resistance, resulting in longer life-spans in biological systems (e.g., inside living cells). This property is appealing for in vivo applications such as biosensing and drug delivery. Finally, the success in building single-stranded 3D DNA nanostructures prompts us to explore other nucleic acid species, such as RNA, for the construction of 3D molecules. Conceivably, we should be able to synthesize an analogous polyhedron using RNA obtained by transcription.

## 2.6. References

- (1) Seeman, N. C. *Nature* **2003**, *421*, 427-431.
- (2) Mirkin, C. A.; Letsinger, R. L.; Mucic, R. C.; Storhoff, J. J. *Nature* **1996**, *382*, 607-609.
- (3) Alivisatos, A. P.; Johnsson, K. P.; Peng, X.; Wilson, T. E.; Loweth, C. J.; Bruchez Jr, M. P.; Schultz, P. G. *Nature*, **1996**, *382*, 609-611.
- (4) Le, J. D.; Pinto, Y.; Seeman, N. C.; Musier-Forsyth, K.; Taton, T. A.; Kiehl, R. A. *Nano Letters* **2004**, *4*, 2343-2347.
- (5) Sharma, J.; Chhabra, R.; Liu, Y.; Ke, Y.; Yan, H. *Angew. Chem., Int. Ed.* **2006**, *45*, 730-735.
- (6) Sharma, J.; Chhabra, R.; Andersen, C. S.; Gothelf, K. V.; Yan, H.; Liu, Y. *J. Am. Chem. Soc.* **2008**, *130*, 7820-7821.
- (7) Li, H.; Park, S. H.; Reif, J. H.; LaBean, T. H.; Yan, H. *J. Am. Chem. Soc.* **2004**, *126*, 418-419.
- (8) Chhabra, R.; Sharma, J.; Ke, Y.; Liu, Y.; Rinker, S.; Lindsay, S.; Yan, H. *J. Am. Chem. Soc.* **2007**, *129*, 10304-10305.
- (9) Ke, Y.; Lindsay, S.; Chang, Y.; Liu, Y.; Yan, H. *Science* **2008**, *319*, 180-183.
- (10) Rinker, S.; Ke, Y.; Liu, Y.; Chhabra, R.; Yan, H. *Nature Nanotechnology* **2008**, *3*, 418-422.
- (11) Winfree, E.; Liu, F.; Wenzler, L. A.; Seeman, N. C. *Nature* **1998**, *394*, 539-544.
- (12) Mao, C.; Sun, W.; Seeman, N. C. *J. Am. Chem. Soc.* **1999**, *121*, 5437-5443.
- (13) LaBean, T. H.; Yan, H.; Kopatsch, J.; Liu, F.; Winfree, E.; Reif, J. H.; Seeman, N. C. *J. Am. Chem. Soc.* **2000**, *122*, 1848-1860.
- (14) Yan, H.; Park, S. H.; Finkelstein, G.; Reif, J. H.; LaBean, T. H. *Science* **2003**, *301*, 1882-1884.
- (15) Liu, D.; Wang, M.; Deng, Z.; Walulu, R.; Mao, C. *J. Am. Chem. Soc.* **2004**, *126*, 2324-2325.
- (16) Ding, B.; Sha, R.; Seeman, N. C. *J. Am. Chem. Soc.* **2004**, *126*, 10230-10231.

- (17) Rothemund, P. W. K.; Papadakis, N.; Winfree, E. *PLoS Biology* **2004**, *2*, 2041-2053.
- (18) Shih, W. M.; Quispe, J. D.; Joyce, G. F. *Nature* **2004**, *427*, 618-621.
- (19) Chelyapov, N.; Brun, Y.; Gopalkrishnan, M.; Reishus, D.; Shaw, B.; Adleman, L. *J. Am. Chem. Soc.* **2004**, *126*, 13924-13925.
- (20) Malo, J.; Mitchell, J. C.; Venien-Bryan, C.; Harris, J. R.; Wille, H.; Sherratt, D. J.; Turberfield, A. J. *Angew. Chem., Int. Ed.* **2005**, *44*, 3057-3061.
- (21) Mathieu, F.; Liao, S.; Kopatsch, J.; Wang, T.; Mao, C.; Seeman, N. C. *Nano Lett.* **2005**, *5*, 661-665.
- (22) Park, S. H.; Barish, R.; Li, H.; Reif, J. H.; Finkelstein, G.; Yan, H.; LaBean, T. H. *Nano Lett.* **2005**, *5*, 693-696.
- (23) Chworos, A.; Severcan, I.; Koyfman, A. Y.; Weinkam, P.; Oroudjev, E.; Hansma, H. G.; Jaeger, L. *Science* **2004**, *306*, 2068-2072.
- (24) Ke, Y.; Liu, Y.; Zhang, J.; Yan, H. *J. Am. Chem. Soc.* **2006**, *128*, 4414-4421.
- (25) Rothemund, P. W. K. *Nature* **2006**, *440*, 297-302.
- (26) Chen, J.; Seeman, N. C. *Nature* **1991**, *350*, 631-633.
- (27) Zhang, Y.; Seeman, N. C. *J. Am. Chem. Soc.* **1994**, *116*, 1661-1669.
- (28) Goodman, R. P.; Berry, R. M.; Turberfield, A. J. *Chem. Comm.* **2004**, 1372-1373.
- (29) Shih, W. M.; Quispe, J. D.; Joyce, G. F. *Nature* **2004**, *427*, 618-621.
- (30) Goodman, R. P.; Schaap, I. A. T.; Tardin, C. F.; Erben, C. M.; Berry, R. M.; Schmidt, C. F.; Turberfield, A. J. *Science* **2005**, *310*, 1661-1665.
- (31) He, Y.; Ye, T.; Su, M.; Zhang, C.; Ribbe, A. E.; Jiang, W.; Mao, C. *Nature* **2008**, *452*, 198-201.
- (32) Bhatia, D.; Mehtab, S.; Krishnan, R.; Indi, S. S.; Basu, A.; Krishnan, Y. *Angew. Chem., Int. Ed.* **2009**, *48*, 4134-4137.
- (33) Mastroianni, A. J.; Claridge, S. A.; Alivisatos, P. A. *J. Am. Chem. Soc.* **2009**, *131* (24), 8455-8459.
- (34) Anderson, E. S. et al. *Nature* **2009**, *459*, 73-76.

- (35) Ke, Y.; Sharma, J.; Liu, M.; Jahn, K.; Liu, Y.; Yan, H. *Nano Lett.* **2009**, *6*, 2445-2447.
- (36) Lin, C.; Rinker, S.; Wang, X.; Liu, Y.; Seeman, N. C.; Yan, H. *Proc. Natl. Acad. Sci. USA* **2008**, *105*, 17626-17631.
- (37) Wei, B.; Wang, Z.; Mi, Y. *J. Comput. Theor. Nanosci.*, **2007**, *4*, 133-141.

## Chapter 3

### Molecular Behavior of DNA Origami in Higher-Order Self-assembly

Adapted with permission from Li, Z.; Liu, M.; Wang, L.; Nangreave, J.; Liu, Y.; Yan, H.: Molecular Behavior of DNA Origami in Higher-Order Self-assembly, *J. Am. Chem. Soc.* **2010**, *132*, 13545-13552. Copyright 2010 American Chemical Society.

#### 3.1. Abstract

DNA-based self-assembly is a unique method for achieving higher-order molecular architectures made possible by the fact that DNA is a programmable information-coding polymer. In the past decade, two main types of DNA nanostructures have been developed: branch-shaped DNA tiles with small dimensions (commonly up to ~20 nm) and DNA origami tiles with larger dimensions (up to ~100 nm). Here we aim to determine the important factors involved in the assembly of DNA origami superstructures. We constructed a new series of rectangular-shaped DNA origami tiles in which parallel DNA helices are arranged in a zigzag pattern when viewed along the DNA helical axis, a design conceived to relax an intrinsic global twist found in the original planar, rectangular origami tiles. Self-associating zigzag tiles were found to form linear arrays in both diagonal directions, while planar tiles showed significant growth in only one direction. Although the series of zigzag tiles were designed to promote two-dimensional array formation, one-dimensional linear arrays and tubular structures were observed instead. We discovered that the dimensional aspect ratio of the origami unit tiles and intertile connection design play important roles in

determining the final products, as revealed by atomic force microscope imaging. This study provides insight into the formation of higher-order structures from self-assembling DNA origami tiles, revealing their unique behavior compared to conventional DNA tiles of smaller dimensions.

### **3.2. Introduction**

DNA self-assembly has shown great promise for the construction of nanoscale architectures. A large variety of one-, two-, and even three-dimensional (1D, 2D and 3D) DNA nanostructures<sup>1-27</sup> have been successfully assembled using branched motifs (tiles) as the basic structural units, and these nanostructures have been used to precisely organize a variety of functional materials.<sup>28-39</sup> Among the many exciting achievements, scaffolded DNA origami is especially remarkable for its capacity to yield complex and fully addressable patterns. In this method, a long, single-strand of DNA (e.g. 7.2 kb genome of phage M13mp18) is folded into 2D or 3D<sup>40-48</sup> structures by hundreds of short, complementary DNA strands (staples). Each staple strand occupies a specific position as a result of its unique sequence complementary to the genomic DNA strand; thus, DNA origami tiles exhibit fully addressable surfaces that can be used to organize proteins, nanoparticles, carbon nanotubes and carry out single molecule chemical reactions with spatial control.<sup>32, 49-57</sup>

One of the central goals in nanotechnology is to assemble unit building blocks into higher-order periodic or nonperiodic architectures. With the proper sticky end design, individual DNA origami tiles could act as basic structural units and self-assemble into larger 1D, 2D and 3D structures. However, reports of large

arrays formed from DNA origami tiles have been quite limited. In one example, Rothemund demonstrated that triangular-shaped DNA origami tiles can be connected through stable strand linkages to form fixed sized 2D arrays, although the size and yield of the arrays was quite small<sup>40</sup>. In another study, rectangular shaped DNA origami tiles originally designed by Rothemund were successfully used to construct 1D arrays,<sup>58</sup> but efforts to make 2D arrays with dimensions larger than 1  $\mu\text{m}$  using these rectangular tiles have proven difficult (See Appendix B). Collectively, these observations suggest that DNA origami, with its large dimensions and unique characteristics, behaves somewhat differently from small DNA tiles. It is worth pointing out that the systematic study of the higher-order self-assembly of small DNA tiles has been performed by various groups, and abundant information has been gathered<sup>15, 16, 20, 37</sup> that has led to greater control over product assembly. In contrast, the study of the higher-order assembly of large DNA origami tiles is lacking. Can the knowledge gained from small tiles be directly applied to large origami tiles when creating higher-order superstructures? This work aimed to address this critical question in a systematic way, and determine the important factors involved in the assembly of DNA origami tiles into higher-order superstructures.

In an attempt to establish the significant structural properties of origami tiles, a close examination of Rothemund's original design for rectangular-shaped DNA origami tiles was carried out. One important aspect of the original design relates to the crossovers between parallel helices: periodic crossovers are separated by odd numbers of half-turns, with 16 base pairs (bp) considered as 1.5

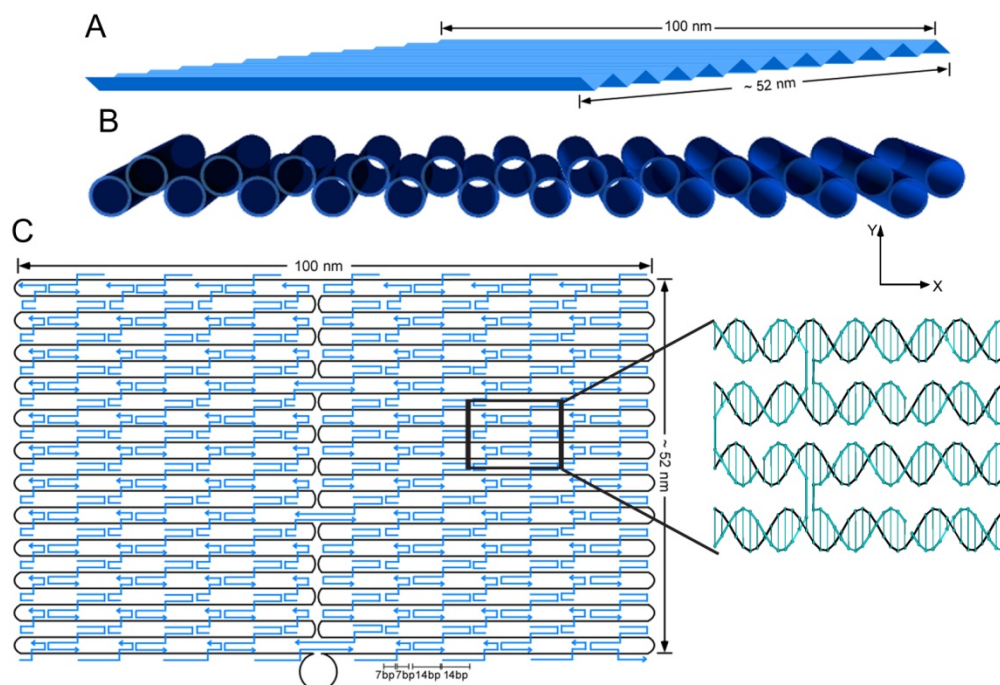


turns. This results in a twist density of 10.67 bp per turn (16 bp/1.5 turns), which represents a slight underwinding of all of the DNA helices as compared to the 10.5 bp per turn in B-form DNA. Since there are over 200 crossovers in a single tile structure, the local underwinding per helical turn may lead to a considerable global twist deformation, preventing the formation of planar, 2D lattice superstructures.

Here we present a new design for the rectangular-shaped DNA origami that is intended to relieve the deformation; it contains dihedral angles of  $120^\circ$  when viewed along the helical axes (Figure 3.1A, B), and is hereafter called “zigzag DNA origami”. The number of base pairs between consecutive crossovers of neighboring helices alternates between 14 bp and 28 bp (Figure 3.1C), corresponding to exactly  $4/3$  or  $8/3$  turns, respectively.<sup>18, 20, 43</sup> 14 bp is equal to one full turn plus  $120^\circ$ , and 28 bp is two full turns plus  $240^\circ$ . Thus, two adjacent crossovers within the same helix are spaced exactly four turns apart. The twist density of this design is 10.5 bp per turn,<sup>20</sup> the same as in B-form DNA, so that the global twisting of the structure should be minimized.

Figure 3.1C illustrates the folding path of the zigzag origami, in which 7056 nucleotides (nt) strand of M13mp18 (black) was folded into a rectangular structure using 168 staples (blue), with individual staples spanning three helices and containing either  $7n$  or  $14n$  ( $n = 3, 4$  or  $5$ ) nucleotides. The remaining nucleotides of the scaffold strand were left as an unpaired loop bridging the starting and ending points of the folding path. The length of the DNA origami tile in the direction parallel to the helical axis (the x-direction) was  $\sim 100$  nm. In the

y-direction, with an assumed interhelical distance of 0.5 nm,<sup>40</sup> the 24 parallel helices should have formed a corrugated structure with the length of ~52 nm. However, once the origami tile was deposited on a mica substrate and scanned using AFM in tapping mode, the dimensions of the origami tiles were measured to be ~100 nm x 60 nm. The stretching in the y-direction may have been due to attractive interactions with the hydrophilic mica surface, where the DNA tiles were presumably flattened to maximize contact.



**Figure 3.1.** Design of the zigzag DNA origami. (A) Schematic drawing of the rectangular-shaped corrugated tile having dimensions of 100 nm by 52 nm. (B) Side view of the tile illustrating the  $120^\circ$  dihedral angle formed between helices. (C) Folding path of the zigzag origami. A 7056 nt strand of M13mp18 (black) is folded into a rectangular structure using 168 staples (blue). The arrow on each staple strand indicates its 5' to 3' direction. The zoom-in view on the right shows structural details of selected staples.

### 3.3. Materials and Methods

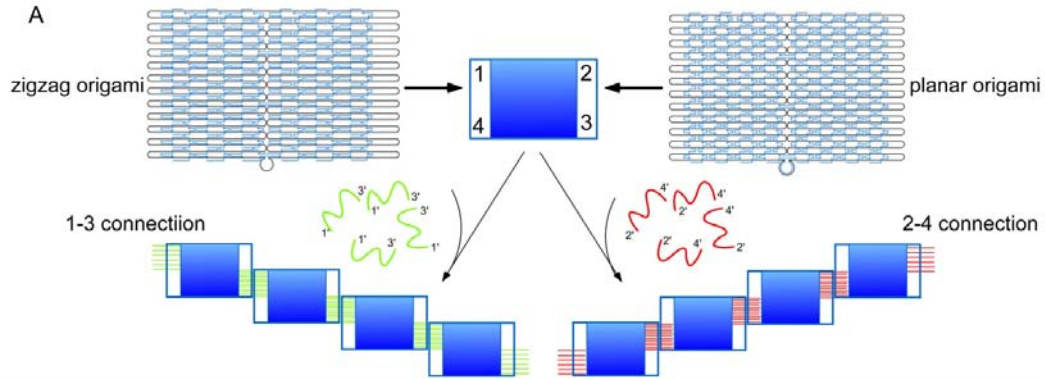
See Appendix B

### 3.4. Results and Discussion

**3.4.1. Assembly of Stairlike 1D Arrays.** First, the planar and zigzag DNA origami tiles were designed to self-associate through linker strands bridging diagonal corners and assemble into stairlike linear arrays. Figure 3.2A illustrates the assembly strategy. For both types of origami tiles, the core structures (with the far left and right column of staples omitted) were first assembled following a standard origami annealing protocol (see Appendix B for details). Unpaired regions of M13 in the four corners of the tiles are numbered as 1, 2, 3, and 4, each spanning 12 helices. Two sets of 12 linker strands were deliberately designed, one to link corner 1 to corner 3, and the other to link corner 2 to corner 4. The individual linker strands consisted of two binding domains: one containing a sequence complementary to the unpaired region of M13 in one corner, and the second containing a sequence complementary to the unpaired region of M13 in the opposite diagonal corner. When the “1-3” set of strands were added to the preannealed origami cores and incubated at room temperature overnight, the result was a stairlike array connected in the 1-3 direction. Similarly, the “2-4” linkers will connect the preannealed origami cores in the other diagonal direction.

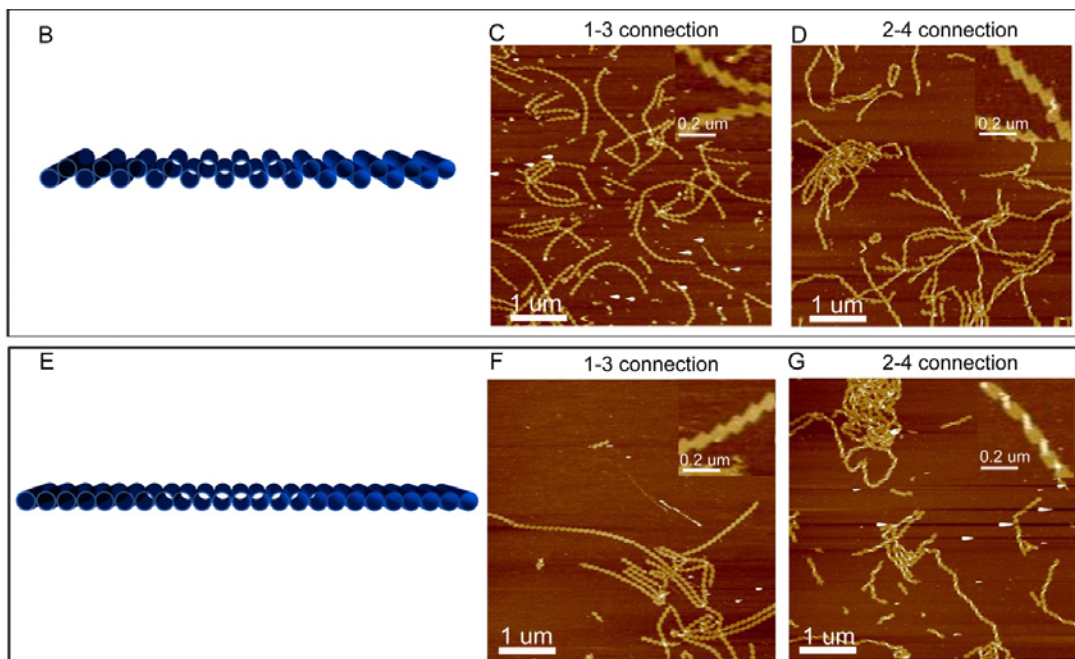
AFM imaging of the final structures revealed that employing 1-3 connections resulted in stairlike 1D arrays with a maximum length of ~40 tiles for both the zigzag origami (Figure 3.2C) and the planar origami (Figure 3.2F). In contrast, the 1D arrays formed from zigzag and planar origami connected through

corners 2 and 4 were distinct. The zigzag origami assembled into long, linear arrays similar to those formed through 1-3 connections (Figure 3.2D), while the planar origami assembled into twisted (right-handed) helical superstructures (Figure 3.2G), with every other tile forming a half twist (see the inset of Figure 3.2G). This observation supports our assumption that planar DNA origami does not adopt a perfectly flat arrangement, but instead displays a global pucker. This also indicates that the bending of the tile is severe in the 2-4 diagonal direction, but minimal in the 1-3 diagonal direction. The observation of a right-handed twist agrees with the results reported by Shih's group,<sup>43</sup> in which an origami structure with a helical twist density of greater than 10.5 bp per turn was used. It should be pointed out that the long linear arrays formed by the zigzag origami in the 2-4 direction also display some degree of twisting at certain sites (Figure 3.2D), but with a much lower frequency. A side-by-side comparison of these two designs indicated that the zigzag origami did not experience as much structural strain as the planar origami, with less twisting and bending out of the plane; therefore, the zigzag origami tile was presumed to be more suitable to serve as a basic structural unit for higher-order assembly purposes and was utilized for all subsequent assembly experiments.



**Figure 3.2.** Stairlike 1D DNA arrays assembled from the rectangular origami tiles.

(A) For both designs, the core of the origami tiles was assembled with the staple strands on the left and right edges omitted. The four corners involved in connecting individual origami tiles are numbered as 1, 2, 3, and 4, each spanning 12 helices. Two sets of linker strands were designed, one to join corners 1 and 3, and the other corners 2 and 4. When all 12 linkers of the same set were added to the preannealed origami core structures, the cores were diagonally connected into stairlike ribbons.



**Figure 3.2. Continued** (B, E) Side views of the zigzag origami and planar origami, respectively. (C, F) AFM images of DNA ribbons formed by zigzag DNA origami and planar DNA origami, respectively, with 1-3 connections. Both tiles formed long ribbons, with the longest composed of  $\sim 40$  tiles. (D, G) AFM images of DNA ribbons formed by zigzag DNA origami and planar DNA origami, respectively, with 2-4 connections. The zigzag origami formed long ribbons, similar to the case of 1-3 connections; the planar origami assembles into right-handed spiral ribbons, with every two or three tiles forming a half-turn twist. Insets in (C, D, F, and G) are zoom-in images.

**3.4.2. Formation of DNA Origami Tubes.** Experiments were conducted in which both sets of linker strands (for 1-3 connections and 2-4 connections) were added to preformed zigzag core structures, and rather than the expected 2D lattices, the formation of tubes was observed. The tubes were assembled by two independent methods: either by combining all 24 linkers simultaneously with the core structures, or using a stepwise assembly approach. For the stepwise method, stairlike arrays were first formed in one direction using one set of linkers, after which the second set of linkers was added. The two methods yielded similar tube structures as shown in Figure 3.3A, with most of the tubes having lengths of 1-3  $\mu\text{m}$ . Individual origami tiles are clearly visible in the zoom-in insets in Figure 3.3A, with the observed length in agreement with the expected 100 nm. The profile of a cross section of a single tube (Figure 3.3B) shows that the tube was 3 nm in height (double the height of an individual origami tile) and  $\sim 30$  nm in width (about half the width).

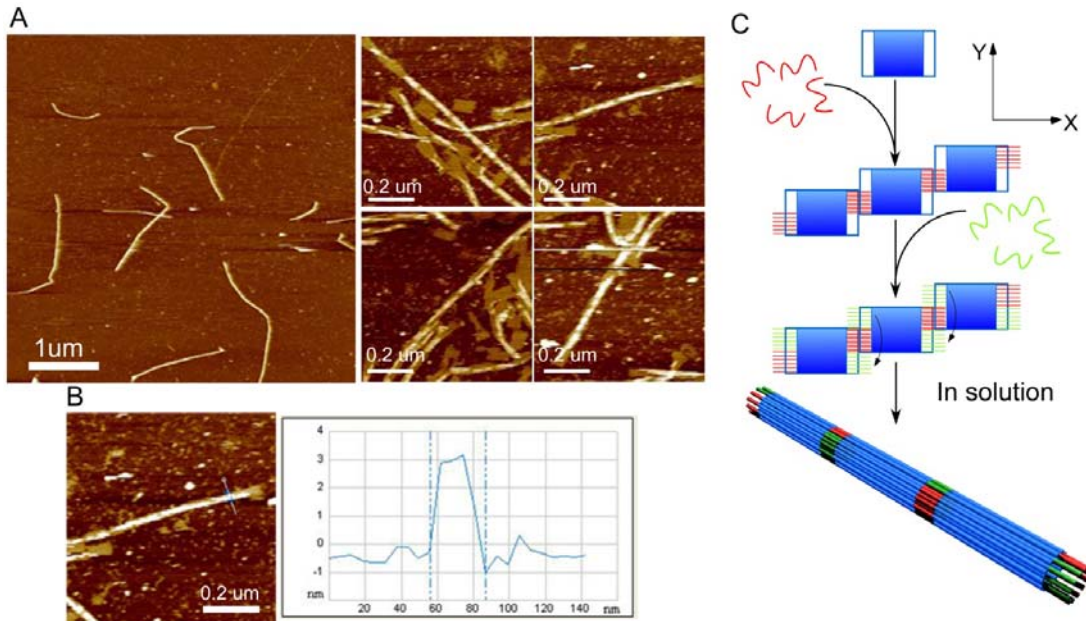
Figure 3.3C illustrates one possible mechanism for the formation of the observed tube structures. One set of linkers first recognizes the corresponding complementary regions of the origami core structures, initially connecting several origami tiles into a stairlike ribbon; similarly, recognition by the other set of linkers forms a stairlike ribbon with the opposite connectivity. Once they are assembled into a stairlike ribbon, it is then presumably faster and easier for the linkers that are not involved in the intertile connections to bind to M13 in an adjacent tile within the same ribbon than in a different ribbon, which would require travel over a much greater distance, considering the low concentration



(nM). Formation of a tube may also be thermodynamically preferred because tube closure is the most efficient process to minimize the number of unpaired DNA strands. Because of the intrinsic flexibility of origami tiles (resulting from the numerous nick points within the structure), bending of the origami tile in both the x and y direction is possible. Apparently, the preferred bending path for the 24-helix tiles is in the y direction, which might be a result of the shorter distance the linkers must traverse to form a closed structure. This interaction rolls the connected ribbons into a tube, whose axis is parallel to the helical axis of the tiles, and whose circumference is equal to the width of a single tile. Additionally, the tubes are not completely sealed, as there is no linkage between the top and bottom edges of each origami tile; thus, they are readily opened by AFM imaging, providing further evidence of tube morphology.

For comparison, surface-mediated assembly of origami core structures together with all 24 linkers was also performed.<sup>59</sup> Rather than forming tubes as seen in the solution-based assembly, the formation of small pieces (~10 tiles) of 2D arrays was observed because the solid support provided many nucleation points (see Appendix B for details). The attractive interactions between the origami tiles and the flat, hydrophilic solid support must restrict the bending of each tile and render them inflexible, causing the intertile interaction to dominate, and ultimately lead to the formation of 2D lattices. However, the size of the 2D lattices obtained using this method shows no improvement over those in existing reports. The relative low efficiency of the surface-mediated self-assembly for origami tiles relative to that of small DNA tiles or short DNA strands could be

due to the low concentration (nM vs  $\mu\text{M}$ ) and the large unit size of the origami tiles, which results in reduced lateral mobility on the mica surface.

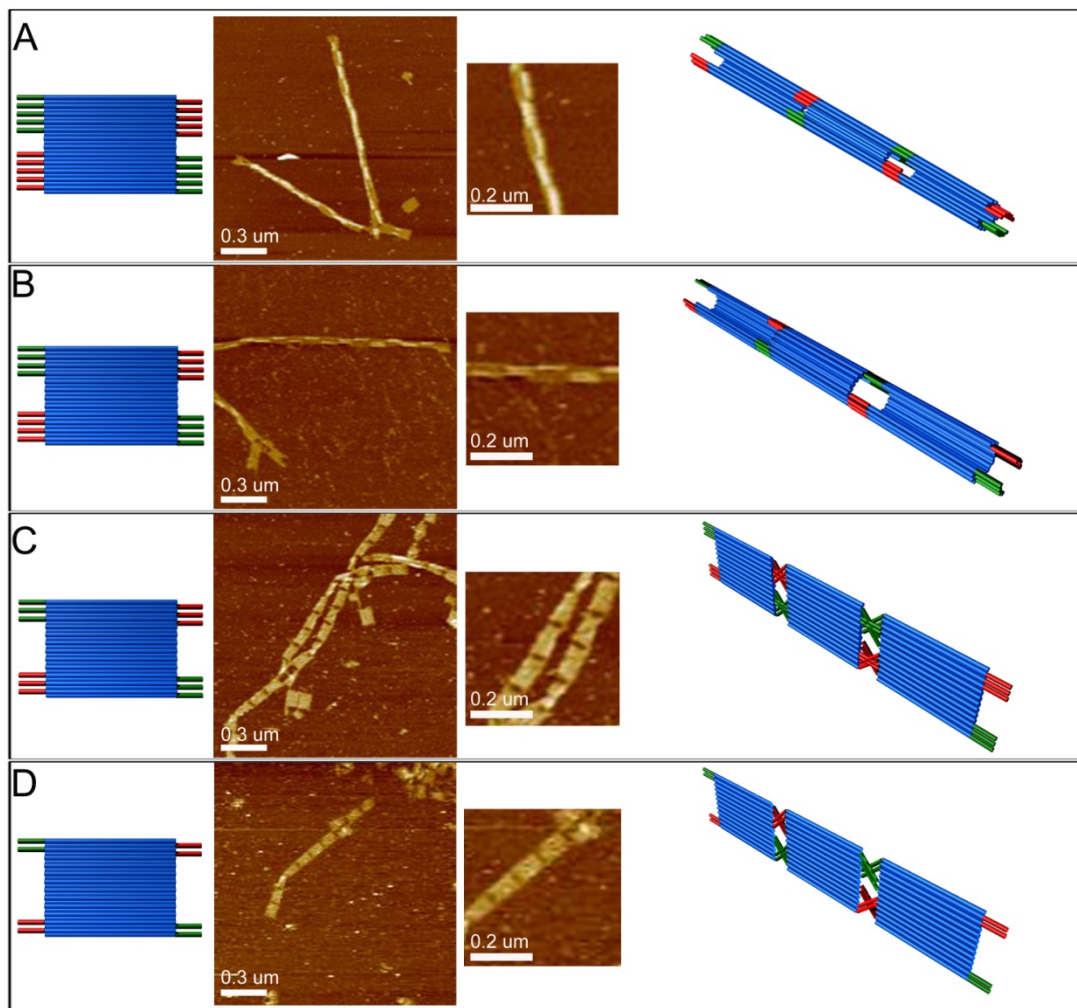


**Figure 3.3.** DNA origami tubes. (A) AFM images of the tubular structure formed after the addition of both sets of linkers into the zigzag origami core. Segments with lengths 100 nm can be observed in the zoom-in images. (B) Cross-sectional profile of a tube measured along the thin white line in the image to the left of the profile: the height was 3 nm and the width  $\sim$ 30 nm. (C) Proposed mechanism for the formation of the origami tubes. Initially, one set of linkers binds to the complementary regions of neighboring core structures, creating a stairlike ribbon. Next, one binding domain in the other set of linkers binds to its complementary region of the core structure while the other binding domain subsequently binds to its complement in the adjacent tile. This interaction rolls the connected tiles into a tube, whose axis is parallel to the origami helical axis, and whose circumference equals the width of one tile.

**3.4.3. Tailoring the Structural Features of Origami Tubes by Varying the Dimensions and Intertile Connections of the Zigzag Tile Units.** On the basis of the proposed tube formation mechanism, several structural factors could be varied to manipulate the assembly process and obtain unique products. We hypothesized that the number and position of the linker strands would control the morphology of the final structures. In addition, we presumed that tiles with varying dimensional aspect ratios would also generate unique tube structures.

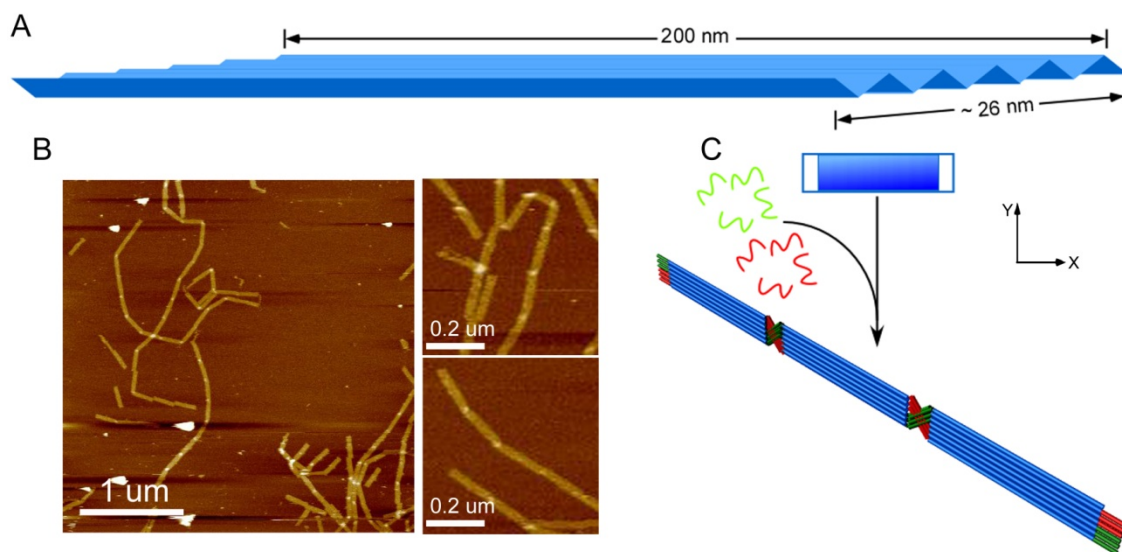
We first examined how varying the number of linkers between tiles would impact the final structures. A gap between corners 1 and 4, and corners 2 and 3 of the origami tile is formed when less than 24 linkers are used, and a smaller number of linkers between tiles produces a wider gap, as illustrated in the schemes in Figure 3.4. Upon addition of 20 linkers (10 strands from each set) to the preformed zigzag core structures, formation of origami tubes with the expected four-helix gap ( $\sim 6.5$  nm) was observed (Figure 3.4A). The zoom-in image shows alternating single-layer and double-layer regions, confirming the existence of the gaps, as schematically illustrated in Figure 4A. Similarly, tubes were also observed when 16 linkers were used (Figure 3.4B). However, when the number of linker strands was reduced to 12 or 8, 1D origami chains rather than tubes were observed (Figure 3.4C, D, respectively). It may be that when the number of linker strands is decreased this much, the free energy that is gained through intertile bond associations is not enough to pay the energy penalty for bending of the origami tiles into tubes. In this case, a half-turn twist in the linker region between two neighboring tiles yields a planar structure, as shown in Figure

3.4C, D. It is also possible that tubular structures actually form but that the wide gap makes the tubes susceptible to deformation, causing them to collapse when they are deposited onto the mica before imaging can confirm their existence.



**Figure 3.4.** The number of linkers impacts the morphology of the resulting structures. (A, B) Use of 20 or 16 linkers results in the formation of tubes with broad circumferences. Shown in each panel from left to right are a schematic drawing of the number and position of linkers used for the connections between origami tiles, a zoom-out AFM image, a zoom-in AFM image, and a schematic drawing showing the assembled structure. (C, D) Use of 12 or 8 linkers results in the assembly of 1D chains.

To investigate the effect of tile dimension on superstructure assembly, we first designed a zigzag origami tile containing 12 parallel helices that had dimensions of 200 nm by 26 nm (Figure 3.5A). In comparison with the 24-helix zigzag origami, the new design was twice as long in the x direction and half as wide in the y direction. After the assembly of the core structures, 12 linkers (six strands of each set) were added to the solution to link diagonal corners of the tile following the same design strategy as for the 24-helix tiles. However, rather than 2D arrays or tubes, only 1D chains were observed by AFM (Figure 3.5B). The decreased width of the origami tile significantly increases the energy required to bend the tile in the y direction, making it harder to roll into a tube. It is intriguing to notice that bright spots between adjacent tiles are clearly visible along the chain, corresponding to an increase in height from 1.5 nm (single-layer origami tiles) to  $\sim 3$  nm at these connection points. On the basis of this observation, we illustrate the possible formation mechanism in Figure 3.5C. For kinetic reasons, the linkers may prefer to bind to complementary regions within the same chain by attaching to the next tile end-to-end, rather than binding to a third tile. The linker strands appear to cross in the center between two neighboring tiles, though an energy penalty to bend the helices of the linker strands in the plane of the tile is required. The overlap of the linkers at the connection points between neighboring tiles forms the high spots observed by AFM.

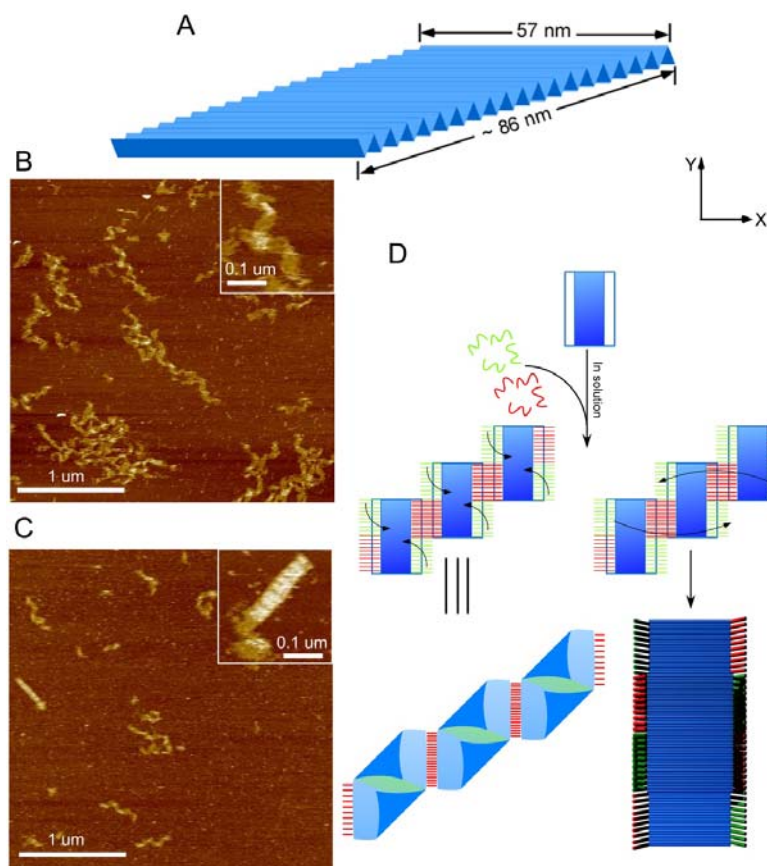


**Figure 3.5.** Formation of 1D chains by 12-helix zigzag origami tiles. (A) Schematic drawing of the 12-helix tile. (B) AFM images of the resulting 1D origami chains after the addition of 12 linker strands. Higher spots between two neighboring tiles can be clearly observed. (C) Hypothetical mechanism for the formation of 1D chains. The decreased width reduces the flexibility of origami tiles significantly, so folding them in the y direction becomes unfavorable. Instead, the linkers prefer to cross in the center to connect origami tiles end-to-end into a chain. The overlapping linker strands form the two-layer regions between neighboring tiles.



To further test the effect of varying the dimensional aspect ratio, we designed a third version of the zigzag origami tile containing 40 helices (Figure 3.6A) with dimensions of  $\sim 57$  nm by 86 nm, which is shorter in the x direction and wider in the y direction than the 24-helix tile. The dominant structures that were formed when all 40 linker strands were added to the core structure were ribbons with periodic one- and two-layer height changes (Figure 3.6B). In addition, a small fraction of linear, double-layered ribbons having a width equal to the x dimension of the unit tile were observed (Figure 3.6C).

The proposed mechanisms of formation of these two ribbon products are shown in Figure 3.6D. The initial assembly is very similar to that of the 24-helix origami in which one set of linkers recognizes the complementary regions in the origami core structures, yielding a staggered ribbon. However, rather than bending the tiles in the y direction in the same manner as the 24 helix tile, the subsequent binding of the second set of linkers results in two other types of connections. In the first case, the origami tiles bend, with sticky ends within the same tile binding at diagonal corners, resulting in the double-layer regions observed in the ribbon. In this way, all the sticky ends travel the shortest distance to bind to complementary regions of the core, but this requires overcoming the energy barrier for bending and twisting the origami tile. In the second case, linear double-layer ribbons (or tubes) with a circumference equal to twice the width of the tile that grow in the y direction are observed. We observed far fewer double-layer linear ribbons than twisted ribbons, which is likely a result of the greater bending energy required for the parallel helices to bend out of the plane of the tile.

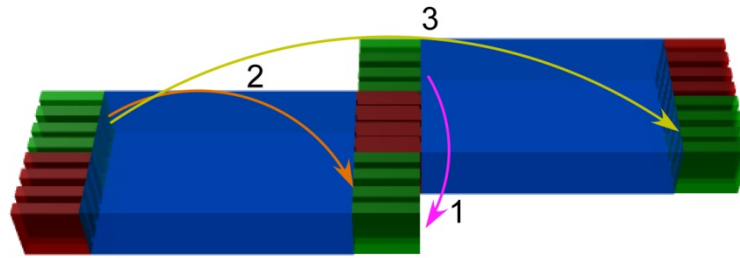









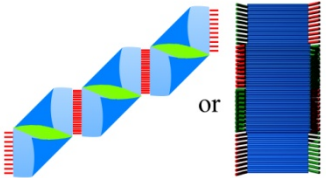
**Figure 3.6.** Formation of zigzag ribbons or double-layered linear ribbons by 40-helix zigzag origami tiles. (A) Schematic drawing of the 40-helix origami tile. (B, C) AFM images of the resulting zigzag origami ribbons and double-layered linear ribbons, respectively. (D) Hypothetical mechanism for formation of these two structures. First, one set of linkers recognizes the complementary regions of the origami core, yielding staggered ribbons, after which the other set of linkers binds to complementary regions within the same tile or an adjacent tile. Binding to the same tile causes bulges within the staggered ribbons, giving a zigzag appearance, while binding to an adjacent tile results in linear, double-layered ribbons with growth in the y direction.

### 3.5. Conclusion

We have designed and characterized a new family of rectangular-shaped DNA origami tiles in which the global twist found in typical “planar” origami has been relaxed, yielding a structural unit with the potential to self-assemble into larger and more complex nanostructures. When a linker-strand connection strategy was used, the formation of either tubular structures or 1D arrays was observed (Figure 3.7), depending on the dimensional aspect ratio of the origami DNA tiles and the number of linker strands utilized. Our observations indicate that the higher-order assembly process for origami tiles (~7000 bp per tile) is markedly different from that for small DNA tiles (80-400 bp per tile), although it follows the same thermodynamic guidelines to minimize the free energy of the system. We postulate that the kinetics of assembly is the major determining factor in the distribution of final products when multiple reaction paths are thermodynamically possible. It may be the case that the products that dominate assembly are obtained via the fastest route with the shortest distance for linkers to traverse and the smallest energy barrier to overcome. It is also likely that the larger size of the origami tiles results in slower diffusion in solution, both laterally and rotationally, which affects the kinetics of the reaction. We stress that it is difficult to access the real-time dynamics of higher-order DNA self-assembly in solution because of the sophisticated nature of the tile-tile interactions, especially with the simultaneous association of multiple sticky ends. Nevertheless, analysis of the final products using AFM imaging still provides useful information about the assembly mechanism. As DNA origami tiles are gaining attention as potential

building blocks for the bottom-up self-assembly of large superstructures, studies that reveal the influence of structural parameters such as dimensions, geometry, interunit connection strategies, and reaction conditions on assembly are imperative. Furthermore, by enhancing the rigidity of an origami tile to significantly increase the cost of bending or twisting the tile, we may be able to control the superstructure formation more reliably and avoid undesired reaction pathways. Our report highlights the need for the careful design of origami structures and assembly routes to achieve predictable products.



| Origami tile   | Linker number | Connection | Resulting structure  |
|--|---------------|------------|--|
| <br>100 nm X 52 nm  | 24            | 1          |         |
|  | 16 or 20      | 1          |         |
|  | 8 or 12       | 1          |         |
| <br>200 nm X 26 nm  | 12            | 1          |         |
| <br>57 nm X 86 nm | 40            | 2 or 3     | <br>or |

**Figure 3.7.** Summary of the impact of varying the dimensional aspect ratio and intertile connection scheme of zigzag origami tile units on the resulting structures. The arrows labeled 1, 2 and 3 specifies three different linking pathways.

### 3.6. References

- (1) Seeman, N. C. *Nature* **2003**, *421*, 427-431.
- (2) Gothelf, K. V. and LaBean, T. H. *Organic and Biomolecular Chemistry* **2005**, *3*, 4023-4037.
- (3) Deng, Z.; chen, Y.; Tian, Y. and Mao, C. *Nanotechnology: Science and Computation* **2006**, 23-34.
- (4) Aldaye, F. A.; Palmer, A.; Sleiman, H. F. *Science* **2008**, *321*, 1795-1799.
- (5) Lin, C.; Liu, Y. and Yan, H. *Biochemistry* **2009**, *48*, 1663-1674.
- (6) Fu, T. J. and Seeman, N. C. *Biochemistry* **1993**, *32*, 3211-3220.
- (7) Winfree, E.; Liu, F.; Wenzler, L. A.; Seeman, N. C. *Nature* **1998**, *394*, 539-544.
- (8) Mao, C.; Sun, W.; Seeman, N. C. *J. Am. Chem. Soc.* **1999**, *121*, 5437-5443.
- (9) LaBean, T. H.; Yan, H.; Kopatsch, J.; Liu, F.; Winfree, E.; Reif, J. H.; Seeman, N. C. *J. Am. Chem. Soc.* **2000**, *122*, 1848-1860.
- (10) Yan, H.; Park, S. H.; Finkelstein, G.; Reif, J. H.; LaBean, T. H. *Science* **2003**, *301*, 1882-1884.
- (11) Liu, D.; Wang, M.; Deng, Z.; Walulu, R.; Mao, C. *J. Am. Chem. Soc.* **2004**, *126*, 2324-2325.
- (12) Ding, B.; Sha, R.; Seeman, N. C. *J. Am. Chem. Soc.* **2004**, *126*, 10230-10231.
- (13) Rothmund, P. W. K.; Papadakis, N.; Winfree, E. *PLoS Biology* **2004**, *2*, 2041-2053.
- (14) Chelyapov, N.; Brun, Y.; Gopalkrishnan, M.; Reishus, D.; Shaw, B.; Adleman, L. *J. Am. Chem. Soc.* **2004**, *126*, 13924-13925.
- (15) Rothmund, P.; Ekani-Nkodo, A.; Papadakis, N.; Kumar, A.; Fygenson, D.; Winfree, E. *J. Am. Chem. Soc.* **2004**, *126*, 16344-16352.
- (16) Mitchell, J. C.; Harris, J. R.; Malo, J.; Bath, J.; Turberfield, A. J. *J. Am. Chem. Soc.* **2004**, *126*, 16342-14363.
- (17) Malo, J.; Mitchell, J. C.; Venien-Bryan, C.; Harris, J. R.; Wille, H.; Sherratt, D. J.; Turberfield, A. J. *Angew. Chem., Int. Ed.* **2005**, *44*, 3057-3061.

- (18) Mathieu, F.; Liao, S.; Kopatsch, J.; Wang, T.; Mao, C.; Seeman, N. C. *Nano Lett.* **2005**, *5*, 661-665.
- (19) Park, S. H.; Barish, R.; Li, H.; Reif, J. H.; Finkelstein, G.; Yan, H.; LaBean, T. H. *Nano Lett.* **2005**, *5*, 693-696.
- (20) Ke, Y.; Liu, Y.; Zhang, J.; Yan, H. *J. Am. Chem. Soc.* **2006**, *128*, 4414-4421.
- (21) Chen, J.; Seeman, N. C. *Nature* **1991**, *350*, 631-633.
- (22) Zhang, Y.; Seeman, N. C. *J. Am. Chem. Soc.* **1994**, *116*, 1661-1669.
- (23) Goodman, R. P.; Berry, R. M.; Turberfield, A. J. *Chem. Comm.* **2004**, 1372-1373.
- (24) Shih, W. M.; Quispe, J. D.; Joyce, G. F. *Nature* **2004**, *427*, 618-621.
- (25) Goodman, R. P.; Schaap, I. A. T.; Tardin, C. F.; Erben, C. M.; Berry, R. M.; Schmidt, C. F.; Turberfield, A. J. *Science* **2005**, *310*, 1661-1665.
- (26) He, Y.; Ye, T.; Su, M.; Zhang, C.; Ribbe, A. E.; Jiang, W.; Mao, C. *Nature* **2008**, *452*, 198-201.
- (27) Zheng, J.; Birktoft, J. J.; Chen, Y.; Wang, T.; Sha, R.; Constantinou, P. E.; Ginell, S. L.; Mao, C. and Seeman, N. C. *Nature* **2009**, *461*, 74-77.
- (28) Mirkin, C. A.; Letsinger, R. L.; Mucic, R. C.; Storhoff, J. J. *Nature* **1996**, *382*, 607-609.
- (29) Alivisatos, A. P.; Johnsson, K. P.; Peng, X.; Wilson, T. E.; Loweth, C. J.; Bruchez Jr, M. P.; Schultz, P. G. *Nature*, **1996**, *382*, 609-611.
- (30) Le, J. D.; Pinto, Y.; Seeman, N. C.; Musier-Forsyth, K.; Taton, T. A.; Kiehl, R. A. *Nano Letters* **2004**, *4*, 2343-2347.
- (31) Li, H.; Park, S. H.; Reif, J. H.; LaBean, T. H.; Yan, H. *J. Am. Chem. Soc.* **2004**, *126*, 418-419.
- (32) Sharma, J.; Chhabra, R.; Liu, Y.; Ke, Y.; Yan, H. *Angew. Chem., Int. Ed.* **2006**, *45*, 730-735.
- (33) Zheng, J.; Constantinou, P. E.; Micheel, C.; Alivisatos, A. P.; Kiehl, P. A. and Seeman, N. C. *Nano Letters* **2006**, *6*, 1502-1504.
- (34) Chhabra, R.; Sharma, J.; Ke, Y.; Liu, Y.; Rinker, S.; Lindsay, S.; Yan, H. *J. Am. Chem. Soc.* **2007**, *129*, 10304-10305.

- (35) Sharma, J.; Chhabra, R.; Andersen, C. S.; Gothelf, K. V.; Yan, H.; Liu, Y. *J. Am. Chem. Soc.* **2008**, *130*, 7820-7821.
- (36) Rinker, S.; Ke, Y.; Liu, Y.; Chhabra, R.; Yan, H. *Nature Nanotechnology* **2008**, *3*, 418-422.
- (37) Sharma, J.; Chhabra, R.; Cheng, A.; Brownell, J.; Liu, Y. and Yan, H. *Science* **2009**, *323*, 112-116.
- (38) Bhatia, D.; Mehtab, S.; Krishnan, R.; Indi, S. S.; Basu, A.; Krishnan, Y. *Angew. Chem., Int. Ed.* **2009**, *48*, 4134-4137.
- (39) Mastroianni, A. J.; Claridge, S. A.; Alivisatos, P. A. *J. Am. Chem. Soc.* **2009**, *131* (24), 8455-8459.
- (40) Rothmund, P. W. K. *Nature* **2006**, *440*, 297-302.
- (41) Anderson, E. S. et al. *Nature* **2009**, *459*, 73-76.
- (42) Douglas, S. M.; Dietz, H.; Liedl, T.; Högberg, B.; Graf, F.; Shih, W. M. *Nature* **2009**, *459*, 414-418.
- (43) Dietz, H.; Douglas, S. M.; Shih, W. M. *Science* **2009**, *325*, 725-730.
- (44) Pound, E.; Ashton, J. R.; Becerril, H. A. and Woolley, A. T. *Nano Letter* **2009**, *9*, 4302-4305.
- (45) Kuzuya, A. and Komiyama, M. *Chem Comm* **2009**, *28*, 4182-4184.
- (46) Ke, Y.; Douglas, S. M.; Liu, M.; Sharma, J.; Cheng, A.; Leung, A.; Liu, Y.; Shih, W. M.; Yan, H. *J. Am. Chem. Soc.* **2009**, *131*, 15903-15908.
- (47) Zhao, Z.; Yan, H.; Liu, Y. *Angew Chem Int Ed* **2010**, *49*, 1414-1417.
- (48) Liedl, T.; Högberg, B.; Tytell, J.; Ingber, D. E. and Shih, W. M. *Nature Nanotechnology* **2010**, *5*, 520-524.
- (49) Ke, Y.; Lindsay, S.; Chang, Y.; Liu, Y.; Yan, H. *Science* **2008**, *319*, 180-183.
- (50) Shen, W.; Zhong, H.; Neff, D. and Norton, M. L. *J. Am. Chem. Soc.* **2009**, *131*, 6660-6661.
- (51) Kuzyk, A.; Laitinen, K. T.; Törmä, P. *Nanotechnology* **2009**, *2*, 235305-235310.
- (52) Kuzuya, A.; Kimura, M.; Numajiri, K.; Koshi, N.; Ohnishi, T.; Okada, F. and Komiyama, M. *ChemBioChem* **2009**, *10*, 1811-1815.



- (53) Maune, H. T.; Han, S.; Barish, R. D.; Bockrath, M.; Goddard III, W. A.; Rothmund, P. W. K.; and Winfree, E. *Nature Nanotechnology* **2010**, *5*, 61-66.
- (54) Ding, B.; Deng, Z.; Yan, H.; Cabrini, S.; Zuckermann, R. N.; Bokor, J. *J Am Chem Soc* **2010**, *132*, 3248-3249.
- (55) Pal, S.; Deng, Z.; Ding, B.; Yan, H.; Liu, Y. *Angew Chem Int Ed* **2010**, *49*, 2700-2704.
- (56) Voigt, N. V.; Tørring, T.; Rotaru, A.; Jacobsen, M. F.; Ravnsbæk, J. B.; Subramani, R.; Mamdouh, W.; Kjems, J.; Mokhir, A.; Basenbacher, F.; and Gothelf, K. V. *Nature Nanotechnology* **2010**, *5*, 200-203.
- (57) Lund, K.; Manzo, A. J.; Dabby, N.; Michelotti, N.; Johnson-Buck, A.; Nangreave, J.; Taylor, S.; Pei, R.; Stojanovic, M. N.; Walter, N. G.; Winfree, E.; Yan, H. *Nature* **2010**, *465*, 206-210.
- (58) Endo, M.; Sugita, T.; Katsuda, Y.; Hidaka, K. and Sugiyama, H. *Chem. Eur. J.* **2010**, *16*, 5362-5368.
- (59) Sun, X.; Ko, S. H.; Zhang, C.; Ribbe, A. E.; Mao, C. *J. Am. Chem. Soc.* **2009**, *131*, 13248-13249.

## Chapter 4

### Effect of DNA Hairpin Loops on the Twist of Planar DNA Origami Tiles

Adapted with permission from Li, Z.; Wang, L.; Yan, H.; Liu, Y.: Effect of DNA Hairpin Loops on the Twist of Planar DNA Origami Tiles, *Langmuir* **2012**, 28, 1959-1965. Copyright 2011 American Chemical Society.

#### 4.1. Abstract

The development of scaffolded DNA origami, a technique in which a long single-stranded viral genome is folded into arbitrary shapes by hundreds of short synthetic oligonucleotides, represents an important milestone in DNA nanotechnology. Recent findings have revealed that two-dimensional (2D) DNA origami structures based on the original design parameters adopt a global twist with respect to the tile plane, which may be because the conformation of the constituent DNA (10.67 bp/turn) deviates from the natural B-type helical twist (10.4 bp/turn). Here we aim to characterize the effects of DNA hairpin loops on the overall curvature of the tile and explore their ability to control, and ultimately eliminate any unwanted curvature. A series of dumbbell-shaped DNA loops were selectively displayed on the surface of DNA origami tiles with the expectation that repulsive interactions among the neighboring dumbbell loops and between the loops and the DNA origami tile would influence the structural features of the underlying tiles. A systematic, atomic force microscopy (AFM) study of how the number and position of the DNA loops influenced the global twist of the structure was performed, and several structural models to explain the results were proposed. The observations unambiguously revealed that the first generation of rectangular-

shaped origami tiles adopt a conformation in which the upper right (corner 2) and bottom left (corner 4) corners bend upward out of the plane, causing linear superstructures attached by these corners to form twisted ribbons. Our experimental observations are consistent with the twist model predicted by the DNA mechanical property simulation software CanDo. Through the systematic design and organization of various numbers of dumbbell loops on both surfaces of the tile, a nearly planar rectangular origami tile was achieved.

#### **4.2. Introduction**

Over the past three decades, DNA molecules have been rationally designed to self-assemble into various one-, two-, and three-dimensional (1D, 2D and 3D) DNA nanostructures through sequence specific hybridization.<sup>1-26</sup> A large variety of chemical and biological components have been precisely organized into functional nanomaterials by these nanostructures.<sup>27-38</sup> Recently, various scaffolded DNA origami strategies have been developed to create complex and fully addressable patterns that have been widely utilized to design 2D and 3D<sup>39-48</sup> structures for the organization of functional molecules including proteins, nanoparticles and carbon nanotubes, and to perform single molecule chemical reactions with spatial control.<sup>31, 49-57</sup>

The self-assembly of homogeneous or heterogeneous structural units into higher-order periodic or aperiodic architectures is one of the major challenges in nanotechnology. Similar to small branched DNA motifs, individual DNA origami tiles with the proper sticky end design will also self-assemble into larger

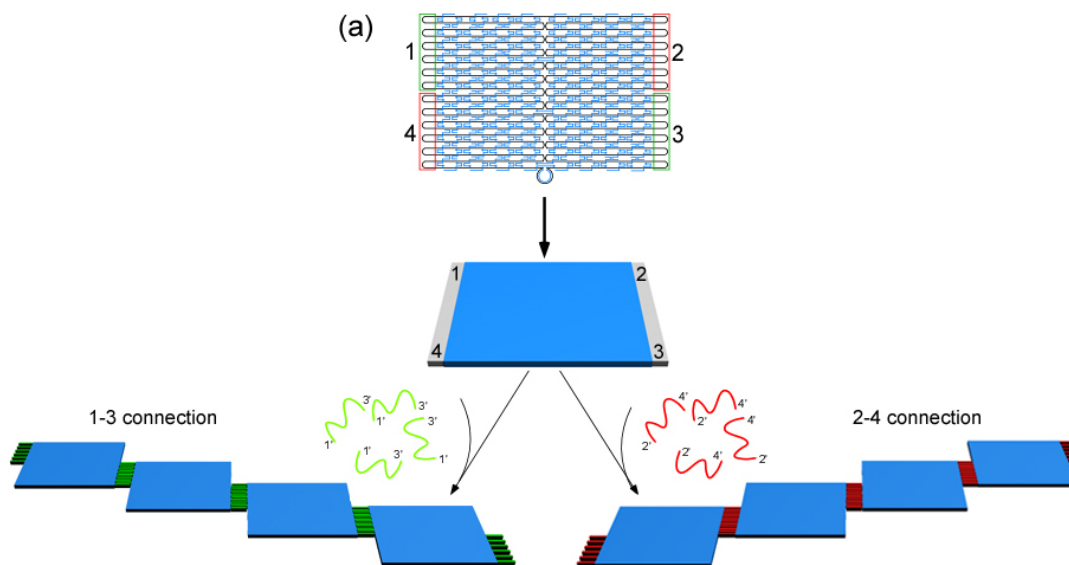
superstructures with more complex structural features.<sup>39, 58, 59</sup> A simple example of this is the assembly of elongated nanoribbons.<sup>60, 61</sup>

In a recent study we observed that planar, rectangular-shaped DNA origami tiles (based on original design specifications) formed both straight and twisted nanoribbon superstructures when assembled by complementary sticky end association.<sup>60</sup> The hierarchical assembly strategy of the tiles is illustrated in Figure 4.1. First, the core of the origami tiles are assembled, excluding the extreme left and right columns of staples. Each of the four corners of the tiles are specified as 1, 2, 3, and 4, and contain 6 sections (16 nt each) of unpaired M13 scaffold strand. Linker strands are designed with two binding domains, one complementary to the unpaired region of M13 in one corner (e.g. corner 1), and the other complementary to the unpaired region of M13 in the opposite, diagonal corner (e.g. corner 3). Thus, 12 1'-3' linker strands are used to arrange the preassembled origami cores into a stairlike ribbon structure (1-3 direction). Similarly, 12 2'-4' linker strands connect the origami cores in the 2-4 direction.

1D stairlike ribbons with a maximum length of ~40 tiles were observed when linked by corners 1 and 3, while right-handed helical super-structures, with a half twist every other tile, were the product of linking corners 2 and 4. These observations suggested a significant twisting within the tile, very obvious in the 2-4 direction but negligible in the 1-3 direction. The conclusion was that the global twist deformation in the origami unit tile prevented extended growth of nanoribbons in the 2-4 direction.<sup>60</sup>

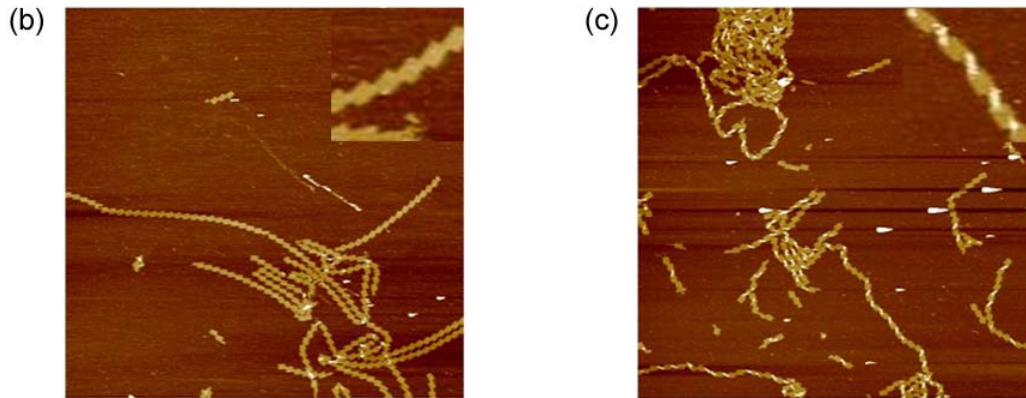
Single stranded DNA loops that adopt a dumbbell shaped structure are

commonly utilized as topographic markers in DNA self-assembly.<sup>49</sup> However, attaching such a structure to the surface of a DNA tile can influence the features of the underlying tile because of the repulsive interactions among neighboring loops and between the loops and the tile. The magnitude of the repulsion likely depends on the interloop distance and relative position on the DNA tile. In this report we show that the undesired structural curvature of a rectangular shaped DNAorigami tile can be rationally manipulated by attaching a series of dumbbell-shaped DNA loops at selected positions on the surface of the tiles. A systematic study was performed to determine how the number and position of the loops affect the degree of global twisting of the underlying tile. Several arrangements of loops were successfully used to diminish the undesired curvature of a rectangular origami tile.



**Figure 4.1.** 1D stairlike DNA ribbons assembled from rectangular origami tiles.

(a) The origami tile cores are assembled with the staple strands on the left and right edges omitted. The four corners that contain sections of unpaired M13 are denoted 1, 2, 3, and 4, each spanning 12 helices. Two sets of linker strands are designed to join corners 1 and 3, or 2 and 4 respectively. After the addition of a set of 12 1'-3' linkers to preassembled origami cores, the tiles are diagonally connected to form stairlike ribbons in the 1-3 direction. Similarly, a set of 2'-4' linkers connect origami cores in the 2-4 direction (where 1' denotes complementarity with corner 1).



**Figure 4.1. Continued** (b) AFM images of long DNA ribbons formed from rectangular origami connected by corners 1 and 3. (c) AFM images of right-handed spiral ribbons formed by origami tiles connected by corners 2 and 4. All AFM images are  $5\ \mu\text{m} \times 5\ \mu\text{m}$ . Insets in are zoom-in images,  $300\ \text{nm} \times 300\ \text{nm}$ .

### **4.3. Materials and Methods**

**4.3.1. Materials.** DNA strands were purchased from Integrated DNA Technology ([www.idtdna.com](http://www.idtdna.com)) in 96-well plates, normalized to 100  $\mu$ M. M13 viral DNA was purchased from New England Biolabs, Inc. (NEB, Catalog number: #N4040S). Microcon Centrifugal Filter Devices (100 000 MWCO, Catalog number: 42413) were purchased from Millipore.

**4.3.2. Assembly of DNA Origami.** The sequences used to form the unmodified rectangular DNA origami were reported previously.<sup>39</sup> DNA origami cores were assembled by mixing a 1:10 molar ratio of M13 viral DNA to each helper strand in 1xTAE/Mg buffer (20 mM Tris, pH 7.6, 2mM EDTA, 12.5mM MgCl<sub>2</sub>). Helper strands corresponding to the far left and right edges in each tile were not included. The final concentration of origami was 5 nM. The DNA mixtures were heated to 90 °C and slowly cooled to 4 °C in a thermal cycler over 12 h. After the formation of the origami cores, purification was performed using Microcon centrifugal filter devices (100 000 MWCO, 300g speed, 10 min) to remove excess helper strands. Then linker strands were added to the solution of origami cores with a 5:1 molar ratio of linker strands to core structure. The mixture was incubated at room temperature overnight.

**4.3.3. AFM Imaging.** For AFM imaging, 2  $\mu$ L of sample was deposited onto a freshly cleaved piece of mica (Ted Pella, Inc.) and left for 2 min. Thirty microliters of 1xTAE/Mg buffer was then deposited onto the mica surface. Imaging was performed using a MultiMode V AFM (Veeco Instruments, now Bruker) in tapping mode, with SNL tips (Veeco Probes).



## 4.4. Results and Discussion

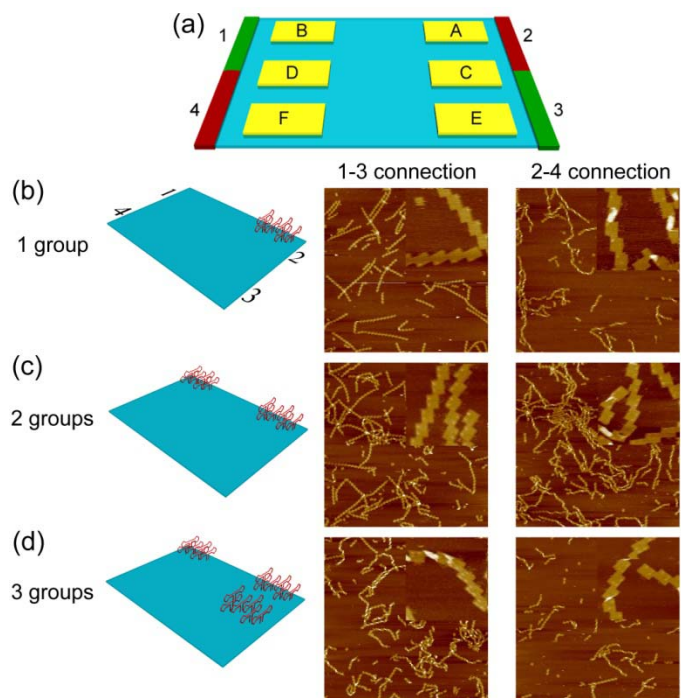
**4.4.1. Effects of DNA Hairpin Loops.** The top and bottom surfaces of rectangular shaped DNA origami tiles are distinct from each other. Moving clockwise, the surface in which corners 1-4 are consecutively encountered is specified as the top or upper surface, and the opposite surface is subsequently referred to as the bottom or lower surface. A set of topographical markers is introduced to either surface of the rectangular origami tile at six unique positions, labeled as A-F in Figure 4.2. Each set contains six individual DNA loops with the same 28-nucleotide-long sequence, directly attached to the underlying staple strands at designated positions. The sequence is designed to fold into two stem-loop structures, forming a dumbbell-shaped index. Within each group, the 6 loops are extending away from the surface of the tile in the same direction, upward or downward. We explore how the global curvature of the tile and, thus, superstructure formation is influenced by the presence, absence, and arrangement of loop structures. The degree of influence was evaluated from atomic force microscopy (AFM) images of superstructures formed from the various monomer units.

In the first set of experiments, the upper surfaces of the origami tiles were decorated with anywhere from one to six sets of dumbbell structures. When only group A dumbbell loops (corner 2) are introduced, the resulting superstructures exhibit no obvious differences from the unmodified origami tile system (no dumbbell structures in the monomers): straight ribbons are observed for the 1-3 connection, and twisted structures are observed for the 2-4 connection (Figure

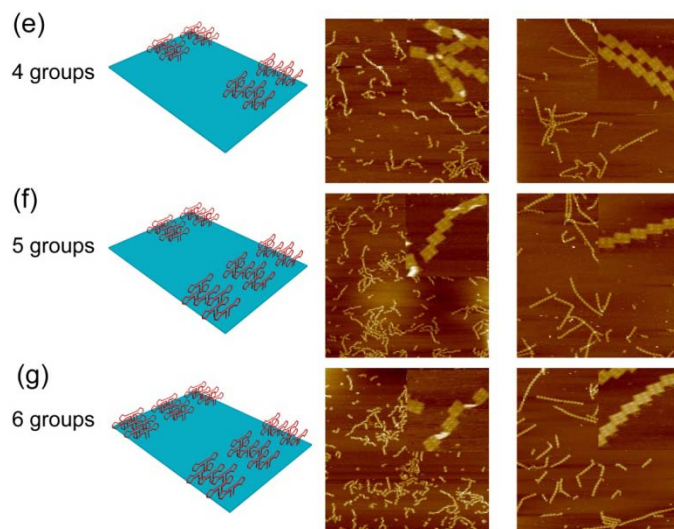
4.2b), suggesting that the origami tiles do not have significantly different conformations. Similarly, when both group A and B (corner 1) loops are both displayed, straight and twisted ribbons were observed in the 1-3 and 2-4 direction, respectively. However, the degree of twisting was reduced from a half twist per 2-3 tiles to a half twist per 4-5 tiles (Figure 4.2c). This result is consistent with the hypothesis that the repulsive interactions among neighboring loops and, between the loops and the tile, actually reduce the out-of-plane twisting of the origami tile in the 2-4 diagonal direction.

The addition of group C loops (in the middle of the right side) results in a dramatically different 1-3 connected superstructure compared to that assembled with unmodified origami tiles; twisted superstructures are observed rather than linear ribbons. On the other hand, the 2-4 connected ribbons become further unwound (Figure 4.2d). This indicates that the presence of three sets of dumbbell structures extended from the upper surface induces a twisting in 1-3 connected superstructures while reducing the degree of twisting in 2-4 connected structures.

On the opposite side of the tile (the left side), the addition of group D dumbbell loops reverses the twisting in 2-4 connected superstructures, resulting in linear ribbons. Meanwhile, 1-3 connected structures appear more tightly twisted (Figure 4.2e). Upon further addition of group E and group F dumbbell loops, similar products were observed; however, the 1-3 connected twisted ribbon structures were shorter, likely because overtwisting in the 1-3 direction interferes with the association between the tiles. The average length and period between full twists of each structure are summarized in Table S1, Appendix C.

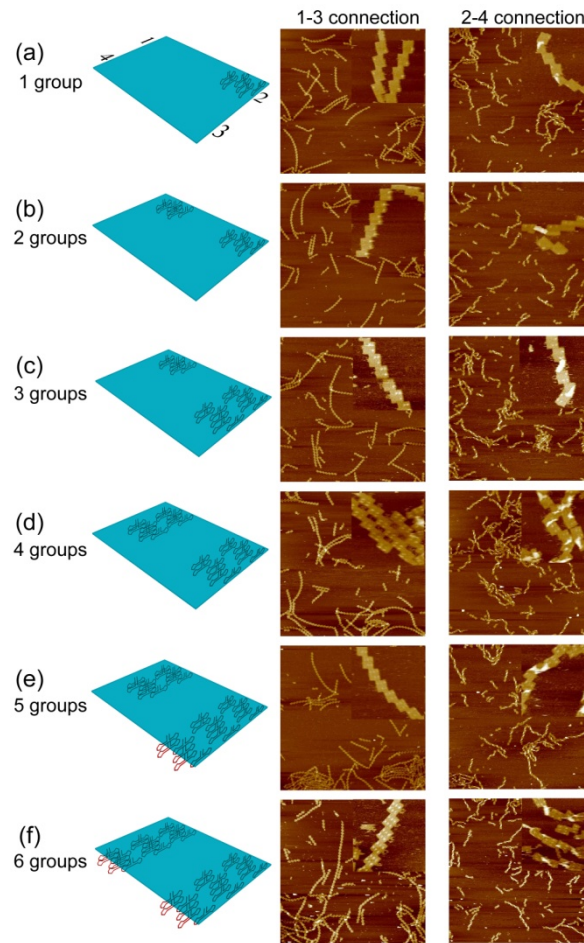


**Figure 4.2.** AFM images of 1D DNA ribbons assembled from rectangular origami tiles with different numbers of dumbbell loops on the top surface. (a) Scheme shows the position of each of the 6 sets of loops (in yellow) on the origami tile (in blue). (b) The display of group A loops on origami tiles does not substantially change their association. Straight ribbons are formed from 1-3 connected tiles, while 2-4 connected tiles form twisted structures. (c) After the addition of group B loops, sections of the 2-4 connected ribbons are unwound. (d) The addition of group C loops results in twisted ribbons in 1-3 connected tiles, and additional sections of 2-4 connected ribbons are unwound.



**Figure 4.2. Continued** (e) With addition of group D loops, straight ribbons are assembled from 2-4 connected tiles, and twisted ribbons are observed from 1-3 connected tiles. (f, g) The addition of group E and F loops results in a shortening of 1-3 connected ribbons. All AFM images are  $5\ \mu\text{m} \times 5\ \mu\text{m}$ . Insets in are zoom-in images,  $500\ \text{nm} \times 500\ \text{nm}$ ; each bright spot on origami tiles represents one group of dumbbell loops that contains 6 individual loops.

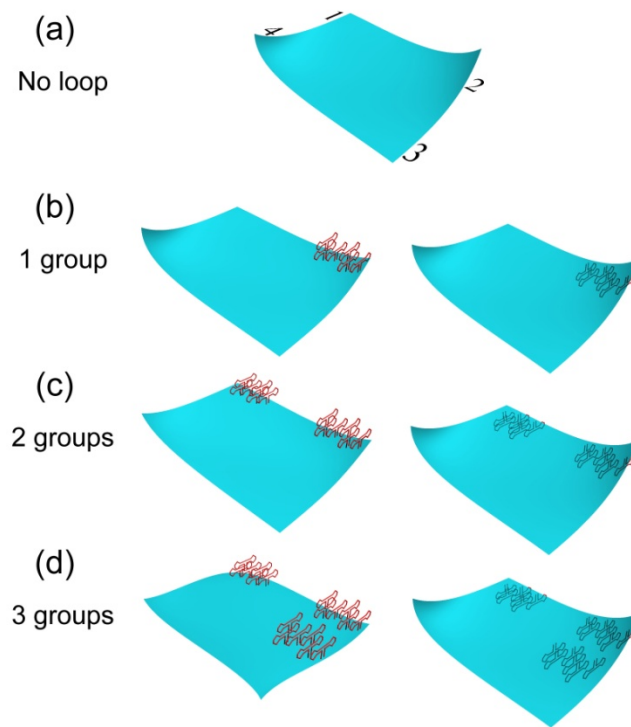
On the basis of these observations, it was expected that adding dumbbell loops on the bottom surface of the origami tiles, rather than the top surface as shown above, should change the curvature of origami tiles in the opposite direction. In the same manner previously described, one to six sets of dumbbell loops were displayed on the bottom surface of the tiles (Figure 4.3, left), at the same positions within the tiles, except extending downward. The AFM images shown in Figure 4.3 (right) reveal that the addition of linker strands (either 1-3 or 2-4 linkers) results in final structures that are nearly the same as those formed from unmodified tiles, regardless of the number or position of the dumbbell loops. A summary of the average length and period between full twists of each structure is located in Table S2 in Appendix C. This result suggests that the repulsive interactions between dumbbell loops displayed on the bottom surface of the origami tiles do not significantly influence the global twist of the tiles, which can be understood if we assume that corners 2 and 4 curl upward in unmodified tiles.



**Figure 4.3.** AFM images of 1D DNA ribbons assembled from the rectangular origami tiles with different numbers of dumbbell loops on the bottom surface. (a-f) The addition of loops has no effect on the final structures that are assembled in either direction. In all cases, straight ribbons are formed from 1-3 connected tiles, while twisted structures are assembled from 2-4 connected tiles, the same as for the unmodified tiles. All AFM images are  $5\ \mu\text{m} \times 5\ \mu\text{m}$ . Insets in are zoom-in images,  $500\ \text{nm} \times 500\ \text{nm}$ ; each bright spot on origami tiles represents one group of dumbbell loops.

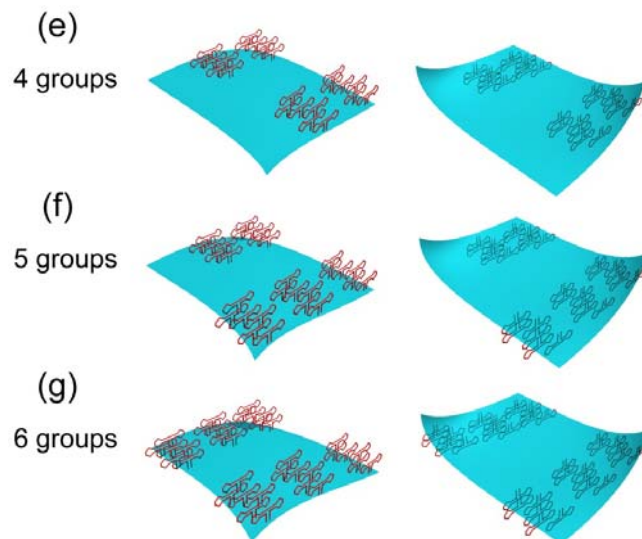
Figure 4.4 contains models illustrating the proposed change in the tiles as groups of dumbbell loop are added. In summary, it is clear that unmodified tiles are somewhat concave at corners 2 and 4 (viewed from the top) (Figure 4.4a) due to the out of plane bending of the corners, while corners 1 and 3 appear to lie in the same plane as the rest of the tile. This is consistent with the observation that introducing loops to the convex surface (bottom) does not significantly affect the overall curvature (Figure 4.4b-g, right columns). In contrast, increasing the number of dumbbell loops on the concave surface (top) helps to flatten the structure and eventually results in a “flip” of the curvature in the opposite direction, likely due to the repulsion between the loops (Figure 4.4b-g left column).

More specifically, displaying group A and B dumbbell loops on the top surface of the origami tiles provides the necessary force to untwist the structure, although the force is not strong enough to cause significant conformational changes (Figure 4.4b and c, left columns). The addition of group C loops in the middle of the right side continues to drive corner 2 into the plane, while simultaneously causing corner 3 to bend out of the plane (Figure 4.4d, left column). The additional influence from group D loops, in the middle of the left side, allows corners 2 and 4 to become coplanar. However, this situation forces corners 1 and 3 to bend downward (Figure 4.4e, left column). The overall conformation of the tile follows the same trend with the addition of group E and F loops, provoking corners 1 and 3 to bend even further downward (Figure 4.4f and g, left columns).



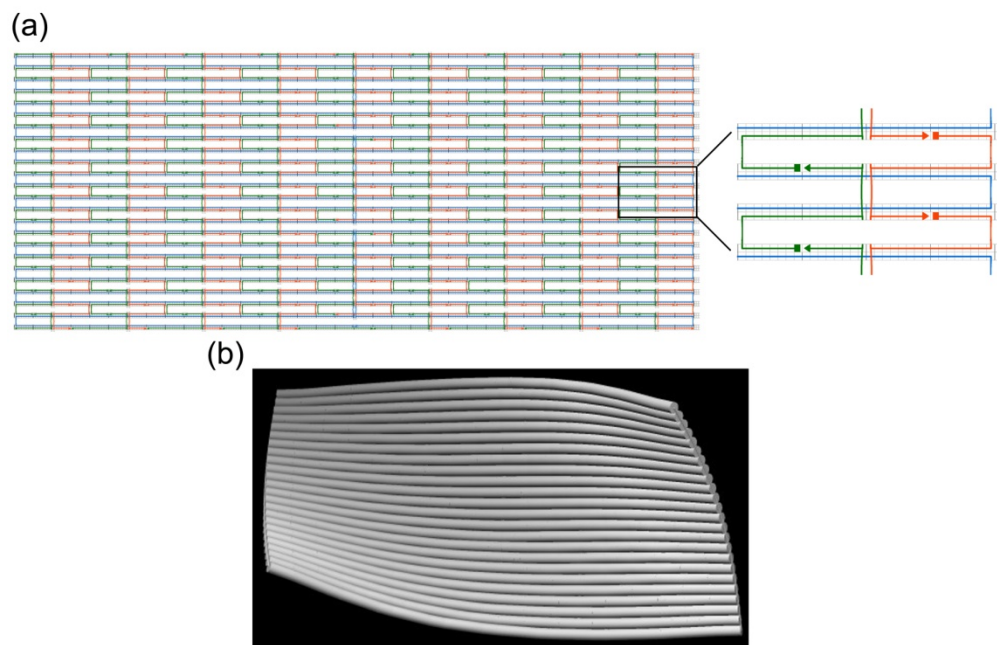
**Figure 4.4.** Control of the conformation of a DNA origami tile through the addition of topographical features. (a) The unmodified origami tile has a twisted conformation in which corners 2 and 4 bend upwards. (b, c) The addition of group A and B loops result in no significant conformational changes, regardless of which surface they are displayed on. (d) When group C loops are added to the upper surface, corners 1 and 3 begin to bend downwards.





**Figure 4.4. Continued** (e) The addition of group D loops to the upper surface results in a coplanar organization of corners 2 and 4. (f, g) The addition of group E and F loops to the upper surface causes additional downward bending of corners 1 and 3. There are no significant conformational changes when the loops are added to the lower surface.

It should be noted that the ensuing conformations of the origami tiles are a consequence of the collective effects of all of the loops sets, including their interactions with the origami tiles as well as among themselves. Although this provides a fairly thorough qualitative assessment, it is still difficult to predict what the effect of loops located at arbitrary positions would be. We also stress that it is difficult to visualize the particular conformation of a single origami tile in solution by AFM imaging. For AFM imaging, the structures are adsorbed to a solid mica substrate, and they are inclined to maximize contact with the hydrophilic mica surface thereby distorting their native conformations. Nevertheless, analysis of the final products of origami tile assembly by AFM does provide useful information that can be used to construct probable models of the tiles. In fact, with the help of computational tools such as caDNAo<sup>62</sup> and CanDo,<sup>63</sup> the 3D structure of DNA origami tiles can be modeled. As shown in Figure 4.5b, CanDo indeed predicts that unmodified rectangular shaped origami tiles will adopt a structure with corners 2 and 4 bent upward out of the plane while corners 1 and 3 remain largely in the plane, consistent with the models shown in Figure 4.4a. However, all current software still lacks the ability to predict the conformation of structures that contain topographical features including DNA stem-loops.



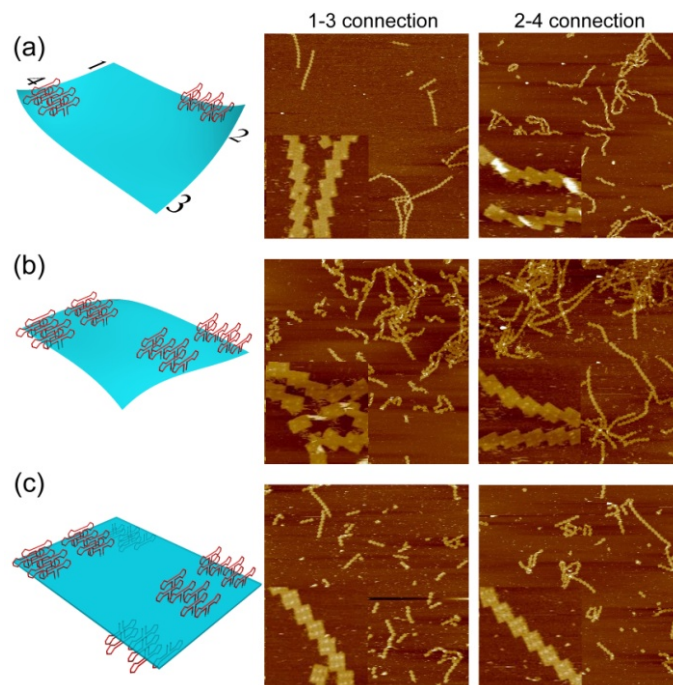
**Figure 4.5.** Predicted structural model of the rectangular shaped DNA origami tile. (a) caDNAno design diagram of unmodified rectangular DNA origami. (b) CanDo analysis predicts that the rectangular origami tile exhibits a non-planar conformation in which corners 2 and 4 bend upwards out of the plane, while corners 1 and 3 remain in plane.

**4.4.2. Rational Design of Planar Origami Tiles.** All the above results demonstrate that the rectangular origami tile is not perfect planar but possesses a global curvature, and this twisting can be varied by introducing other structural components, such as dumbbell loops to the structure. Therefore, we hypothesized that a planar origami tile could be achieved by deliberately selecting the number and positions of the dumbbell loop structures within the origami tile. Considering that corners 2 and 4 are naturally bent upward, it was reasonable to predict that group A and F loops would direct the corners into the plane of the tile. However, the AFM images in Figure 4.6a reveal that, although tiles with group A and F loops form straight ribbons when connected by corners 1 and 3, 2-4 connected tiles form twisted ribbons. This suggests that the repulsive force provided by the two groups of loops is not sufficient to flatten the tiles. It is noted that for nontwisted stairlike ribbons, the origami tile surface can face both up and down, as evidenced in Figure 4.6a.

Next, in addition to groups A and F, group C and loops were also added to the upper surface of the origami tile (Figure 4.6b). In this case, the 1-3 connected tiles formed twisted structures, while 2-4 connected tiles formed straight ribbons. Apparently, the repulsive force of the loops was greater than what was required to bring corners 1 and 3 into the plane, and thus, corners 1 and 3 were forced to bend downward.

The design was further modified by adding dumbbell loops to group B and E loops to the lower surface of the tile, as illustrated in Figure 4.6c, to compensate for the downward bending caused by the excess repulsive forces from the upper

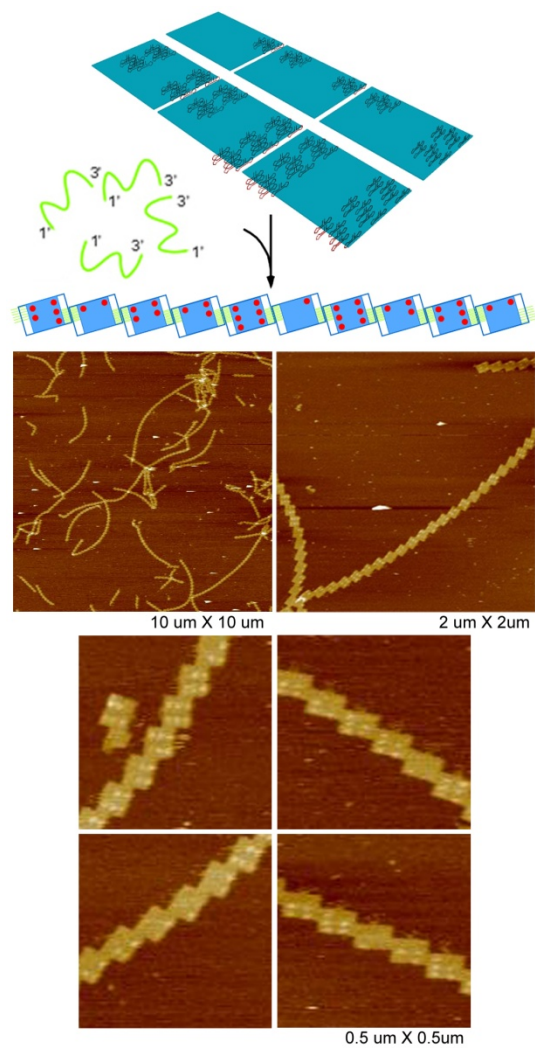
surface. AFM images reveal that both 1-3 and 2-4 connected tiles formed straight ribbons, suggesting that the overall conformation of the adapted tile is near planar. Therefore, we have demonstrated that the rational design of topographical features can be used to influence the conformation of the underlying DNA origami tile and create planar tiles. More sophisticated control over the tile structure may be possible by introducing loops to additional locations on the tile.



**Figure 4.6.** A planar rectangular origami tile was achieved by controlling the number and position of dumbbell loops. (a) Adding group A and F loops to the upper surface did not disrupt the upward bending at the corners 2 and 4. (b) The addition of group C and D loops over-corrected the bending and caused corners 1 and 3 to bend downward. (c) With groups A, C, D and F loops on the upper surface and groups B and E on the lower surface, the overall tile is nearly planar. All AFM images are  $5\ \mu\text{m} \times 5\ \mu\text{m}$ . Insets in are zoom-in images,  $500\ \text{nm} \times 500\ \text{nm}$ ; each bright spot on origami tiles represents one group of dumbbell loops.

#### **4.4.3. Heterogeneous Origami for Information Storage and**

**Computation.** As shown in Figure 4.3, origami tiles with various dumbbell loops decorated on the bottom surface are always assembled into straight ribbons when connected by corners 1 and 3. The reliability of this behavior can be exploited to efficiently assemble heterogeneous origami tiles, each with a unique number of dumbbell loops. When six unique origami tiles with different numbers of dumbbell loops displayed from the bottom surface were mixed in equal molar ratios and linked through corners 1 and 3, very long ribbons (up to 40 tiles long) were formed. Each of these ribbons contained a random sequence of the tiles that was easily read from the AFM images (Figure 4.7a). The randomness of the tile organization is a result of the equal opportunity of each tile to be incorporated at any given position.



**Figure 4.7.** Heterogeneous assembly of six different origami tiles. Origami tiles were decorated with one to six dumbbell loops on the bottom surface and connected by corners 1 and 3 to form very long ribbons. Scales of AFM images are labeled. Inset is zoom-in image, 500 nm  $\times$  500 nm.



It is possible to apply this strategy to perform parallel molecular computation by DNA tile self-assembly, in which a large number of distinct inputs may be simultaneously processed. For example, one may design individual tiles that carry sticky ends to represent two rows of input as well as one row of output, so that a truth table can be encoded. Linear self-assembly of such tiles into chains would perform XOR calculations. With a unique tile at one end of the assembly serving as the initial input, many different origami tiles can be connected by corners 1 and 3 to form straight 1D ribbons. Readout of the calculations can be achieved by AFM imaging to reveal all possible outputs.

#### **4.5. Conclusion**

In this study, we unambiguously revealed that the rectangular shaped origami tile based on original design parameters adopts a conformation in which the upper right (corner 2) and bottom left (corner 4) corners bend upward out of plane, which causes 2-4 connected superstructures to adopt twisted ribbon arrangements. The same nonplanar origami structure was also predicted using the software CanDo, consistent with our experimental observations. A series of dumbbell-shaped DNA loops were introduced to the rectangular origami tiles, yielding a series of tiles with varying degrees of planarity that self-assemble into either straight or twisted ribbons. The curvature of each origami tile can be customized by deliberately displaying various structural components, such as DNA dumbbell loops, at desired locations to provide repulsive forces that will either diminish or enhance the curvature. A nearly planar rectangular origami tile was achieved through rational design, with the placement of specific numbers of

dumbbell loops at certain positions on both surfaces of the tile. The linear nanoribbons may be used for many functional applications, including molecular computation or as tracks for DNA robots or circuits. Other nanoscale structural features, such as ligand protected metallic nanoparticles or inorganic nanocrystals are also known to experience repulsive interactions when they are brought into close vicinity on a DNA scaffold, and may also be used to manipulate the underlying tile.<sup>36,64</sup> In addition, interactions between the DNA scaffold and the selected structural components (i.e., loops, nanoparticles, etc), and among the components themselves, should be considered in the design so that precise control of the positioning, including the relative orientations, distances, and 3D geometry can be achieved.

#### **4.6. References**

- (1) Seeman, N. C. *Nature* **2003**, *421*, 427-431.
- (2) Gothelf, K. V. and LaBean, T. H. *Organic and Biomolecular Chemistry* **2005**, *3*, 4023-4037.
- (3) Aldaye, F. A.; Palmer, A.; Sleiman, H. F. *Science* **2008**, *321*, 1795-1799.
- (4) Lin, C.; Liu, Y. and Yan, H. *Biochemistry* **2009**, *48*, 1663-1674.
- (5) Fu, T. J. and Seeman, N. C. *Biochemistry* **1993**, *32*, 3211-3220.
- (6) Winfree, E.; Liu, F.; Wenzler, L. A.; Seeman, N. C. *Nature* **1998**, *394*, 539-544.
- (7) Mao, C.; Sun, W.; Seeman, N. C. *J. Am. Chem. Soc.* **1999**, *121*, 5437-5443.
- (8) LaBean, T. H.; Yan, H.; Kopatsch, J.; Liu, F.; Winfree, E.; Reif, J. H.; Seeman, N. C. *J. Am. Chem. Soc.* **2000**, *122*, 1848-1860.
- (9) Yan, H.; Park, S. H.; Finkelstein, G.; Reif, J. H.; LaBean, T. H. *Science* **2003**, *301*, 1882-1884.

- (10) Liu, D.; Wang, M.; Deng, Z.; Walulu, R.; Mao, C. Tensegrity: *J. Am. Chem. Soc.* **2004**, *126*, 2324-2325.
- (11) Ding, B.; Sha, R.; Seeman, N. C. *J. Am. Chem. Soc.* **2004**, *126*, 10230-10231.
- (12) Rothmund, P. W. K.; Papadakis, N.; Winfree, E. *PLoS Biology* **2004**, *2*, 2041-2053.
- (13) Chelyapov, N.; Brun, Y.; Gopalkrishnan, M.; Reishus, D.; Shaw, B.; Adleman, L. *J. Am. Chem. Soc.* **2004**, *126*, 13924-13925.
- (14) Rothmund, P.; Ekani-Nkodo, A.; Papadakis, N.; Kumar, A.; Fygenson, D.; Winfree, E. *J. Am. Chem. Soc.* **2004**, *126*, 16344-16352.
- (15) Mitchell, J. C.; Harris, J. R.; Malo, J.; Bath, J.; Turberfield, A. J. *J. Am. Chem. Soc.* **2004**, *126*, 16342-14363.
- (16) Malo, J.; Mitchell, J. C.; Venien-Bryan, C.; Harris, J. R.; Wille, H.; Sherratt, D. J.; Turberfield, A. J. *Angew. Chem., Int. Ed.* **2005**, *44*, 3057-3061.
- (17) Mathieu, F.; Liao, S.; Kopatsch, J.; Wang, T.; Mao, C.; Seeman, N. C. *Nano Lett.* **2005**, *5*, 661-665.
- (18) Park, S. H.; Barish, R.; Li, H.; Reif, J. H.; Finkelstein, G.; Yan, H.; LaBean, T. H. *Nano Lett.* **2005**, *5*, 693-696.
- (19) Ke, Y.; Liu, Y.; Zhang, J.; Yan, H. *J. Am. Chem. Soc.* **2006**, *128*, 4414-4421.
- (20) Chen, J.; Seeman, N. C. *Nature* **1991**, *350*, 631-633.
- (21) Zhang, Y.; Seeman, N. C. *J. Am. Chem. Soc.* **1994**, *116*, 1661-1669.
- (22) Goodman, R. P.; Berry, R. M.; Turberfield, A. J. *Chem. Comm.* **2004**, 1372-1373.
- (23) Shih, W. M.; Quispe, J. D.; Joyce, G. F. *Nature* **2004**, *427*, 618-621.
- (24) Goodman, R. P.; Schaap, I. A. T.; Tardin, C. F.; Erben, C. M.; Berry, R. M.; Schmidt, C. F.; Turberfield, A. J. *Science* **2005**, *310*, 1661-1665.
- (25) He, Y.; Ye, T.; Su, M.; Zhang, C.; Ribbe, A. E.; Jiang, W.; Mao, C. *Nature* **2008**, *452*, 198-201.
- (26) Zheng, J.; Birktoft, J. J.; Chen, Y.; Wang, T.; Sha, R.; Constantinou, P. E.; Ginell, S. L.; Mao, C. and Seeman, N. C. *Nature* **2009**, *461*, 74-77.

- (27) Mirkin, C. A.; Letsinger, R. L.; Mucic, R. C.; Storhoff, J. J. *Nature* **1996**, 382, 607-609.
- (28) Alivisatos, A. P.; Johnsson, K. P.; Peng, X.; Wilson, T. E.; Loweth, C. J.; Bruchez Jr, M. P.; Schultz, P. G. *Nature*, **1996**, 382, 609-611.
- (29) Le, J. D.; Pinto, Y.; Seeman, N. C.; Musier-Forsyth, K.; Taton, T. A.; Kiehl, R. A. *Nano Letters* **2004**, 4, 2343-2347.
- (30) Li, H.; Park, S. H.; Reif, J. H.; LaBean, T. H.; Yan, H. *J. Am. Chem. Soc.* **2004**, 126, 418-419.
- (31) Sharma, J.; Chhabra, R.; Liu, Y.; Ke, Y.; Yan, H. *Angew. Chem., Int. Ed.* **2006**, 45, 730-735.
- (32) Zheng, J.; Constantinou, P. E.; Micheel, C.; Alivisatos, A. P.; Kiehl, P. A. and Seeman, N. C. *Nano Letters* **2006**, 6, 1502-1504.
- (33) Chhabra, R.; Sharma, J.; Ke, Y.; Liu, Y.; Rinker, S.; Lindsay, S.; Yan, H. *J. Am. Chem. Soc.* **2007**, 129, 10304-10305.
- (34) Sharma, J.; Chhabra, R.; Andersen, C. S.; Gothelf, K. V.; Yan, H.; Liu, Y. *J. Am. Chem. Soc.* **2008**, 130, 7820-7821.
- (35) Rinker, S.; Ke, Y.; Liu, Y.; Chhabra, R.; Yan, H. *Nature Nanotechnology* **2008**, 3, 418-422.
- (36) Sharma, J.; Chhabra, R.; Cheng, A.; Brownell, J.; Liu, Y. and Yan, H. *Science* **2009**, 323, 112-116.
- (37) Bhatia, D.; Mehtab, S.; Krishnan, R.; Indi, S. S.; Basu, A.; Krishnan, Y. *Angew. Chem., Int. Ed.* **2009**, 48, 4134-4137.
- (38) Mastroianni, A. J.; Claridge, S. A.; Alivisatos, P. A. *J. Am. Chem. Soc.* **2009**, 131 (24), 8455-8459.
- (39) Rothmund, P. W. K. *Nature* **2006**, 440, 297-302.
- (40) Anderson, E. S.; Dong, M.; Nielsen, M. M.; Jahn, K.; Subramani, R.; Mamdouh, W.; Golas, M.m.; Sander, B.; Stark, H.; Oliveira, C. L. P. and *et al.* *Nature* **2009**, 459, 73-76.
- (41) Douglas, S. M.; Dietz, H.; Liedl, T.; Högberg, B.; Graf, F.; Shis, W. M. *Nature* **2009**, 459, 414-418.
- (42) Dietz, H.; Douglas, S. M.; Shih, W. M. *Science* **2009**, 325, 725-730.

- (43) Pound, E.; Ashton, J. R.; Becerril, H. A. and Woolley, A. T. *Nano Letter* **2009**, *9*, 4302-4305.
- (44) Kuzuya, A. and Komiyama, M. *Chem Comm* **2009**, *28*, 4182-4184.
- (45) Ke, Y.; Douglas, S. M.; Liu, M.; Sharma, J.; Cheng, A.; Leung, A.; Liu, Y.; Shih, W. M.; Yan, H. *J. Am. Chem. Soc.* **2009**, *131*, 15903-15908.
- (46) Zhao, Z.; Yan, H.; Liu, Y.. *Angew Chem Int Ed* **2010**, *49*, 1414-1417.
- (47) Liedl, T.; Högberg, B.; Tytell, J.; Ingber, D. E. and Shih, W. M. *Nature Nanotechnology* **2010**, *5*, 520-524.
- (48) Han, D.; Pal, S.; Liu, Y. and Yan, H. *Nature Nanotechnology* **2010**, *5*, 712-717.
- (49) Ke, Y.; Lindsay, S.; Chang, Y.; Liu, Y.; Yan, H. *Science* **2008**, *319*, 180-183.
- (50) Shen, W.; Zhong, H.; Neff, D. and Norton, M. L. *J. Am. Chem. Soc.* **2009**, *131*, 6660-6661.
- (51) Kuzyk, A.; Laitinen, K. T.; Törmä, P. *Nanotechnology* **2009**, *2*, 235305-235310.
- (52) Kuzuya, A.; Kimura, M.; Numajiri, K.; Koshi, N.; Ohnishi, T.; Okada, F. and Komiyama, M. *ChemBioChem* **2009**, *10*, 1811-1815.
- (53) Maune, H. T.; Han, S.; Barish, R. D.; Bockrath, M.; Goddard III, W. A.; Rothmund, P. W. K.; and Winfree, E. *Nature Nanotechnology* **2010**, *5*, 61-66.
- (54) Ding, B.; Deng, Z.; Yan, H.; Cabrini, S.; Zuckermann, R. N.; Bokor, J. *J Am Chem Soc* **2010**, *132*, 3248-3249.
- (55) Pal, S.; Deng, Z.; Ding, B.; Yan, H.; Liu, Y. *Angew Chem Int Ed* **2010**, *49*, 2700-2704.
- (56) Voigt, N. V.; Tørring, T.; Rotaru, A.; Jacobsen, M. F.; Ravnsbæk, J. B.; Subramani, R.; Mamdouh, W.; Kjems, J.; Mokhir, A.; Basenbacher, F. and *et al.* *Nature Nanotechnology* **2010**, *5*, 200-203.
- (57) Lund, K.; Manzo, A. J.; Dabby, N.; Michelotti, N.; Johnson-Buck, A.; Nangreave, J.; Taylor, S.; Pei, R.; Stojanovic, M. N.; Walter, N. G.; Winfree, E.; Yan, H. *Nature* **2010**, *465*, 206-210.
- (58) Endo, M.; Sugita, T.; Katsuda, Y.; Hidaka, K. and Sugiyama, H. *Chem. Eur. J.* **2010**, *16*, 5362-5368.

- (59) Liu, W.; Zhong, H.; Wang, R. and Seeman, N.C. *Angew Chem Int Ed* **2011**, *50*, 264-267.
- (60) Li, Z.; Liu, M.; Wang, L.; Nangreave, J.; Yan, H. and Liu, Y. *J. Am. Chem. Soc.* **2010**, *132*, 13545-13552.
- (61) Jungmann, R.; Scheible, M.; Kuzyk, A.; Pardatscher, G.; Castro, C. E. and Simmel, F. C. *Nanotechnology* **2011**, *22*, 275301.
- (62) Douglas, S. M.; Marblestone, A. H.; Teerapittayanon, S.; Vazquez, A.; Church, G. M. and Shih, W. M. *Nucleic Acids Res.* **2009**, *37*, 5001-5006.
- (63) Castro, C. E.; Kilchherr, F.; Kim, D.; Shiao, E. L.; Wauer, T.; Wortmann, P.; Bathe, M. and Dietz, H. *Nature Methods*. **2011**, *8*, 221-229.
- (64) Zhang, J.; Liu, Y.; Ke, Y. and Yan, H. *Nano Lett.* **2006**, *6*, 248-251.

## Chapter 5

### Summary

The past 30 years have witnessed the fast development of structural DNA nanotechnology. Today, researchers are able to construct 2D and 3D nanostructures with considerable complexity and addressability using DNA as building blocks. These DNA structures serve as scaffolds of a large variety of functional molecules, for a broad range of applications such as biosensing, controlled macromolecular interactions, and nanoelectronics. However, a number of challenges remain to be addressed for its further progress, including in vivo assembly of DNA nanostructures, cost reduction of synthetic DNA molecules, size expanding of the assemblies, and accurate controls of the assembly process and products.

The research presented in this dissertation represents fundamental steps toward solving these issues. First, we designed and constructed a tetrahedron composed of a single-stranded DNA, which was the first example of a complete 3D nanostructure assembled from the minimum number of DNA strands. The correct assembly of the tetrahedron was verified by restriction enzyme digestion, Ferguson analysis, and AFM imaging. This ss-tetrahedron was able to be replicated through standard molecular cloning techniques in *E. coli* cells with high efficiency and fidelity, indicating the biocompatibility of DNA nanostructures, as well as suggesting a feasible low-cost method of scaling up the preparation of synthetic DNA, which was especially ideal for strands with long sequences and high complexity.

Next, the higher-order self-assembly, one of the central goals in nanotechnology, of DNA origami tiles was systematically studied. We designed a family of rectangular-shaped DNA origami tiles, and introduced a linker-strand connection strategy to assemble them into larger patterns. Various 1D arrays and tubular structures were formed, depending on the dimensional aspect ratio of the origami tiles and intertile connection. Our observations suggested that the thermodynamic guidelines to minimize the free energy as well as the kinetic requirements to minimize the travel distance and energy barrier were both essential to determine the assembled products. These results provided the insight to control the formation of superstructures by carefully designing suitable geometries and assembly pathways.

In a following study, the effects of DNA hairpin loops on the conformations of origami tiles as well as the higher-order assembled structures were discussed. The first generation of rectangular-shaped DNA origami tile was found to adopt a global twist, while dumbbell-shaped DNA loops on its surface were expected to influence its overall curvature because of the repulsive interactions between the loops and the tile. The effects of the number and position of the DNA loops were systematically studied, and the results were explained by several structural models. Our observations indicated that the upper right and bottom left corners of the origami tile bent upward out of the plane, resulting in twisted ribbons when connecting multiple tiles by these corners. The results suggested that to control the formation of superstructures, the interactions between DNA scaffolds and structural components should also be considered.



## Bibliography

### Chapter 1 References

- (1) Seeman, N. C. *Nature* **2003**, *421*, 427–431.
- (2) Aldaye, F. A.; Palmer, A.; Sleiman, H. F. *Science* **2008**, *321*, 1795-1799.
- (3) Lin, C.; Liu, Y. and Yan, H. *Biochemistry* **2009**, *48*, 1663-1674.
- (4) Watson, J. D.; Crick, F. H. C. *Nature* **1953**, *171*, 737-738.
- (5) Seeman, N. C. *J. Theor. Biol.* **1982**, *99*, 237–247.
- (6) Fu, T-J.; Seeman, N. C. *Biochemistry* **1993**, *32*, 3211–3220.
- (7) Winfree, E.; Liu, F.; Wenzler, L.A.; Seeman, N. C. *Nature* **1998**, *394*, 539–544.
- (8) LaBean, T.; Yan, H.; Kopatsch, J.; Liu, F.; Winfree, E.; Reif, J. H.; Seeman, N. C. *J. Am. Chem. Soc.* **2000**, *122*, 1848–1860.
- (9) Reishus, D.; Shaw, B.; Brun, Y.; Chelyapov, N.; Adleman, L. *J. Am. Chem.Soc.* **2005**, *127*, 17590–17591.
- (10) Ke, Y.; Liu, Y.; Zhang, J.; Yan, H. *J. Am. Chem. Soc.* **2006**, *128*, 4414–4421.
- (11) Mao, C.; Sun, W.; Seeman, N. C. *J. Am. Chem. Soc.* **1999**, *121*, 5437-5443.
- (12) Liu, D.; Wang, M.; Deng, Z.; Walulu, R.; Mao, C. *J. Am. Chem. Soc.* **2004**, *126*, 2324-2325.
- (13) Park, S. H.; Barish, R.; Li, H. Y.; Reif, J. H.; Finkelstein, G.; Yan, H.; LaBean, T. H. *Nano Lett.* **2005**, *5*, 693–696.
- (14) Mathieu, F.; Liao, S. P.; Kopatscht, J.; Wang, T.; Mao, C. D.; Seeman, N. C. *Nano Lett.* **2005**, *5*, 661–665.
- (15) Yan, H.; Park, S. H.; Ginkelstein, G.; Reif, J. H.; LaBean, T. H. *Science* **2003**, *301*, 1882–1884.
- (16) He, Y.; Tian, Y.; Chen, Y.; Deng, Z. X.; Ribbe, A. E.; Mao, C. D. *Angew. Chem. Int. Ed.* **2005**, *44*, 6694–6696.
- (17) He, Y.; Chen, Y.; Liu, H.; Ribbe, A. E.; Mao, C. *J. Am. Chem. Soc.* **2005**, *127*, 12202–12203.

- (18) He, Y.; Tian, Y.; Ribbe, A. E.; Mao, C. *J. Am. Chem. Soc.* **2006**, *128*, 15978–15979.
- (19) Lund, K.; Liu, Y.; Lindsay, S.; Yan, H. *J. Am. Chem. Soc.* **2005**, *127*, 17606–17607.
- (20) Park, S. H.; Pistol, C.; Ahn, S. J.; Reif, J. H.; Lebeck, A. R.; Dwyer, C.; LaBean, T. H. *Angew. Chem. Int. Ed.* **2006**, *45*, 735–739.
- (21) Rothmund, P. W. K.; Papadakis, N.; Winfree, E. *PLoS Biol.* **2004**, *2*, 2041–2053.
- (22) Yan, H.; LaBean, T. H.; Feng, L. P.; Reif, J. H. *Proc. Natl. Acad. Sci. USA* **2003**, *100*, 8103–8108.
- (23) Rothmund, P. W. K. *Nature* **2006**, *440*, 297–302.
- (24) Endo, M.; Sugita, T.; Katsuda, Y.; Hidaka, K. and Sugiyama, H. *Chem. Eur. J.* **2010**, *16*, 5362–5368.
- (25) Li, Z.; Liu, M.; Wang, L.; Nangreave, J.; Yan, H. and Liu, Y. *J. Am. Chem. Soc.* **2010**, *132*, 13545–13552.
- (26) Liu, W.; Zhong, H.; Wang, R. and Seeman, N.C. *Angew Chem Int Ed* **2011**, *50*, 264–267.
- (27) Zhao, Z.; Yan, H.; Liu, Y. *Angew Chem Int Ed* **2010**, *49*, 1414–1417.
- (28) Zhao, Z.; Yan, H.; Liu, Y. *Nano Lett.* **2011**, *11*, 2997–3002.
- (29) Chen, J.; Seeman, N. C. *Nature* **1991**, *350*, 631–633.
- (30) Zhang, Y.; Seeman, N. C. *J. Am. Chem. Soc.* **1994**, *116*, 1661–1669.
- (31) Goodman, R. P.; Berry, R. M.; Turberfield, A. J. *Chem. Commun.*, **2004**, 1372–1373.
- (32) Goodman, R. P.; Schaap, I. A. T.; Tardin, C. F.; Erben, C. M.; Berry, R. M.; Schmidt, C. F.; Turberfield, A. J. *Science* **2005**, *310*, 1661–1665.
- (33) Goodman, R. P.; Heilemann, M.; Doose, S.; Erben, C. M.; Kapanidis, A. N.; Turberfield, A. J. *Nat. Nanotechnol* **2008**, *3*, 93–96.
- (34) Aldaye, F. A.; Sleiman, H. F. *J. Am. Chem. Soc.* **2007**, *129*, 13376–13377.
- (35) He, Y.; Ye, T.; Su, M.; Zhang, C.; Ribbe, A. E.; Jiang, W.; Mao, C. *Nature* **2008**, *452*, 198–202.

- (36) Zhang, C.; Su, M.; He, Y.; Zhao, X.; Fang, P.; Ribbe, A. E.; Jiang, W.; Mao, C. *Proc. Natl. Acad. Sci. U.S.A.* **2008**, *105*, 10665–10669.
- (37) Li, Z.; Wei, B.; Nangreave, J.; Lin, C.; Liu, Y.; Mi, Y.; Yan, H. *J. Am. Chem. Soc.* **2009**, *131*, 13093–13098.
- (38) Shih, W. M.; Quispe, J. D.; Joyce, G. F. *Nature* **2004**, *427*, 618–621.
- (39) Shen, Z.; Yan, H.; Wang, T.; Seeman, N. C. *J. Am. Chem. Soc.* **2004**, *126*, 1666–1674.
- (40) Andersen, E. S.; Dong, M.; Nielsen, M. M.; Jahn, K.; Subramani, R.; Mamdouh, W.; Golas, M. M.; Sander, B.; Stark, H.; Oliveira, C. L. P.; Pedersen, J. S.; Birkedal, V.; Besenbacher, F.; Gothelf, K. V.; Kjems, J. *Nature* **2009**, *459*, 73-76.
- (41) Ke, Y.; Sharma, J.; Liu, M.; Jahn, K.; Liu, Y.; Yan, H. *Nano Lett.* **2009**, *6*, 2445-2447.
- (42) Ke, Y.; Douglas, S. M.; Liu, M.; Sharma, J.; Cheng, A.; Leung, A.; Liu, Y.; Shih, W. M.; Yan, H. *J. Am. Chem. Soc.* **2009**, *131*, 15903-15908.
- (43) Douglas, S. M.; Dietz, H.; Liedl, T.; Högberg, B.; Graf, F.; Shis, W. M. *Nature* **2009**, *459*, 414-418.
- (44) Douglas, S. M.; Marblestone, A. H.; Teerapittayanon, S.; Vazquez, A.; Church, G. M.; Shis, W. M. *Nucleic Acids Research* **2009**, *37*, 5001-5006.
- (45) Dietz, H.; Douglas, S. M.; Shih, W. M. *Science* **2009**, *325*, 725-730.
- (46) Liedl, T.; Högberg, B.; Tytell, J.; Ingber, D. E. and Shih, W. M. *Nature Nanotechnology* **2010**, *5*, 520-524.
- (47) Han, D.; Pal, S.; Nangreave, J.; Deng, Z.; Liu, Y.; Yan, H. *Science* **2011**, *332*, 342-346.
- (48) Mirkin, C. A.; Letsinger, R. L.; Mucic, R. C.; Storhoff, J. J. *Nature* **1996**, *382*, 607-609.
- (49) Alivisatos, A. P.; Johnsson, K. P.; Peng, X.; Wilson, T. E.; Loweth, C. J.; Bruchez Jr, M. P.; Schultz, P. G. *Nature*, **1996**, *382*, 609-611.
- (50) Le, J. D.; Pinto, Y.; Seeman, N. C.; Musier-Forsyth, K.; Taton, T. A.; Kiehl, R. A. *Nano Letters* **2004**, *4*, 2343-2347.
- (51) Li, H.; Park, S. H.; Reif, J. H.; LaBean, T. H.; Yan, H. *J. Am. Chem. Soc.* **2004**, *126*, 418-419.

- (52) Sharma, J.; Chhabra, R.; Liu, Y.; Ke, Y.; Yan, H. *Angew. Chem., Int. Ed.* **2006**, *45*, 730-735.
- (53) Zheng, J.; Constantinou, P. E.; Micheel, C.; Alivisatos, A. P.; Kiehl, P. A. and Seeman, N. C. *Nano Letters* **2006**, *6*, 1502-1504.
- (54) Sharma, J.; Chhabra, R.; Andersen, C. S.; Gothelf, K. V.; Yan, H.; Liu, Y. *J. Am. Chem. Soc.* **2008**, *130*, 7820-7821.
- (55) Sharma, J.; Chhabra, R.; Cheng, A.; Brownell, J.; Liu, Y. and Yan, H. *Science* **2009**, *323*, 112-116.
- (56) Bhatia, D.; Mehtab, S.; Krishnan, R.; Indi, S. S.; Basu, A.; Krishnan, Y. *Angew. Chem., Int. Ed.* **2009**, *48*, 4134-4137.
- (57) Mastroianni, A. J.; Claridge, S. A.; Alivisatos, P. A. *J. Am. Chem. Soc.* **2009**, *131* (24), 8455-8459.
- (58) Ding, B.; Deng, Z.; Yan, H.; Cabrini, S.; Zuckermann, R. N.; Bokor, J. *J Am Chem Soc* **2010**, *132*, 3248-3249.
- (59) Pal, S.; Deng, Z.; Ding, B.; Yan, H.; Liu, Y. *Angew Chem Int Ed* **2010**, *49*, 2700-2704.
- (60) Sharma, J.; Ke, Y.; Lin, C.; Chhabra, R.; Wang, Q.; Nangreave, J.; Liu, Y.; Yan, H. *Angew Chem Int Ed* **2008**, *47*, 5157-5159.
- (61) Maune, H. T.; Han, S.; Barish, R. D.; Bockrath, M.; Goddard III, W. A.; Rothmund, P. W. K.; and Winfree, E. *Nature Nanotechnology* **2010**, *5*, 61-66.
- (62) Lund, K.; Manzo, A. J.; Dabby, N.; Michelotti, N.; Johnson-Buck, A.; Nangreave, J.; Taylor, S.; Pei, R.; Stojanovic, M. N.; Walter, N. G.; Winfree, E.; Yan, H. *Nature* **2010**, *465*, 206-210.
- (63) Park, S. H.; Yin, P.; Liu, Y.; Reif, J. H.; LaBean, T. H.; Yan, H. *Nano Lett.* **2005**, *5*, 729-733.
- (64) Liu, Y.; Lin, C.; Li, H.; Yan, H. *Angew. Chem. Int. Ed.* **2005**, *44*, 4333-4338.
- (65) Lin, C.; Xie, M.; Chen, J. J.-L.; Liu, Y.; Yan, H. *Angew. Chem. Int. Ed.* **2006**, *45*, 7537-7539.
- (66) Lin, C.; Liu, Y.; Yan, H. *Nano Lett.* **2007**, *7*, 507-512.

- (67) Malo, J.; Mitchell, J. C.; Vénien-Bryan, C.; Harris, J. R.; Wille, H.; Sherratt, D. J.; Turberfield, A. J. *Angew. Chem. Int. Ed.* **2005**, *44*, 3057–3061.
- (68) Erben, C. M.; Goodman, R. P.; Turberfield, A. J. *Angew. Chem. Int. Ed.* **2006**, *45*, 7414–7417.
- (69) Wilner, O. I.; Weizmann, Y.; Gill, R.; Lioubashevski, O.; Freeman, R.; Willner, I. *Nature Nanotechnology* **2009**, *4*, 249–254.
- (70) Ke, Y.; Lindsay, S.; Chang, Y.; Liu, Y.; Yan, H. *Science* **2008**, *319*, 180–183.
- (71) Rinker, S.; Ke, Y.; Liu, Y.; Chhabra, R.; Yan, H. *Nat. Nanotechnol* **2008**, *3*, 418–422.
- (72) Sacca, B.; Meyer, R.; Erkelenz, M.; Kiko, K.; Arndt, A.; Schroeder, H.; Rabe, K. S.; Niemeyer, C. M. *Angew. Chem. Int. Ed.* **2010**, *49*, 9378–9383.
- (73) Douglas, S. M.; Bachelet, I.; Church, G. M. *Science* **2012**, *335*, 831–834.
- (74) Pinheiro, A. V.; Han, D.; Shih, W. M.; Yan, H. *Nat. Nanotechnol* **2011**, *6*, 763–772.
- (75) Delebecque, C. J.; Lindner, A. B.; Silver, P. A.; Aldaye, F. A. *Science* **2011**, *333*, 470–474.
- (76) Mei, Q.; Wei, X.; Su, F.; Liu, Y.; Youngbull, C.; Johnson, R.; Lindsay, S.; Yan, H.; Meldrum, D. *Nano Lett.* **2011**, *11*, 1477–1482.
- (77) Lin, C.; Rinker, S.; Wang, X.; Liu, Y.; Seeman, N. C.; Yan, H. *Proc. Natl. Acad. Sci. U.S.A.* **2008**, *105*, 17626–17631.

## Chapter 2 References

- (1) Seeman, N. C. *Nature* **2003**, *421*, 427–431.
- (2) Mirkin, C. A.; Letsinger, R. L.; Mucic, R. C.; Storhoff, J. J. *Nature* **1996**, *382*, 607–609.
- (3) Alivisatos, A. P.; Johnsson, K. P.; Peng, X.; Wilson, T. E.; Loweth, C. J.; Bruchez Jr, M. P.; Schultz, P. G. *Nature*, **1996**, *382*, 609–611.
- (4) Le, J. D.; Pinto, Y.; Seeman, N. C.; Musier-Forsyth, K.; Taton, T. A.; Kiehl, R. A. *Nano Letters* **2004**, *4*, 2343–2347.
- (5) Sharma, J.; Chhabra, R.; Liu, Y.; Ke, Y.; Yan, H. *Angew. Chem., Int. Ed.* **2006**, *45*, 730–735.

- (6) Sharma, J.; Chhabra, R.; Andersen, C. S.; Gothelf, K. V.; Yan, H.; Liu, Y. *J. Am. Chem. Soc.* **2008**, *130*, 7820-7821.
- (7) Li, H.; Park, S. H.; Reif, J. H.; LaBean, T. H.; Yan, H. *J. Am. Chem. Soc.* **2004**, *126*, 418-419.
- (8) Chhabra, R.; Sharma, J.; Ke, Y.; Liu, Y.; Rinker, S.; Lindsay, S.; Yan, H. *J. Am. Chem. Soc.* **2007**, *129*, 10304-10305.
- (9) Ke, Y.; Lindsay, S.; Chang, Y.; Liu, Y.; Yan, H. *Science* **2008**, *319*, 180-183.
- (10) Rinker, S.; Ke, Y.; Liu, Y.; Chhabra, R.; Yan, H. *Nature Nanotechnology* **2008**, *3*, 418-422.
- (11) Winfree, E.; Liu, F.; Wenzler, L. A.; Seeman, N. C. *Nature* **1998**, *394*, 539-544.
- (12) Mao, C.; Sun, W.; Seeman, N. C. *J. Am. Chem. Soc.* **1999**, *121*, 5437-5443.
- (13) LaBean, T. H.; Yan, H.; Kopatsch, J.; Liu, F.; Winfree, E.; Reif, J. H.; Seeman, N. C. *J. Am. Chem. Soc.* **2000**, *122*, 1848-1860.
- (14) Yan, H.; Park, S. H.; Finkelstein, G.; Reif, J. H.; LaBean, T. H. *Science* **2003**, *301*, 1882-1884.
- (15) Liu, D.; Wang, M.; Deng, Z.; Walulu, R.; Mao, C. *J. Am. Chem. Soc.* **2004**, *126*, 2324-2325.
- (16) Ding, B.; Sha, R.; Seeman, N. C. *J. Am. Chem. Soc.* **2004**, *126*, 10230-10231.
- (17) Rothmund, P. W. K.; Papadakis, N.; Winfree, E. *PLoS Biology* **2004**, *2*, 2041-2053.
- (18) Shih, W. M.; Quispe, J. D.; Joyce, G. F. *Nature* **2004**, *427*, 618-621.
- (19) Chelyapov, N.; Brun, Y.; Gopalkrishnan, M.; Reishus, D.; Shaw, B.; Adleman, L. *J. Am. Chem. Soc.* **2004**, *126*, 13924-13925.
- (20) Malo, J.; Mitchell, J. C.; Venien-Bryan, C.; Harris, J. R.; Wille, H.; Sherratt, D. J.; Turberfield, A. J. *Angew. Chem., Int. Ed.* **2005**, *44*, 3057-3061.
- (21) Mathieu, F.; Liao, S.; Kopatsch, J.; Wang, T.; Mao, C.; Seeman, N. C. *Nano Lett.* **2005**, *5*, 661-665.
- (22) Park, S. H.; Barish, R.; Li, H.; Reif, J. H.; Finkelstein, G.; Yan, H.; LaBean, T. H. *Nano Lett.* **2005**, *5*, 693-696.

- (23) Chworos, A.; Severcan, I.; Koyfman, A. Y.; Weinkam, P.; Oroudjev, E.; Hansma, H. G.; Jaeger, L. *Science* **2004**, *306*, 2068-2072.
- (24) Ke, Y.; Liu, Y.; Zhang, J.; Yan, H. *J. Am. Chem. Soc.* **2006**, *128*, 4414-4421.
- (25) Rothmund, P. W. K. *Nature* **2006**, *440*, 297-302.
- (26) Chen, J.; Seeman, N. C. *Nature* **1991**, *350*, 631-633.
- (27) Zhang, Y.; Seeman, N. C. *J. Am. Chem. Soc.* **1994**, *116*, 1661-1669.
- (28) Goodman, R. P.; Berry, R. M.; Turberfield, A. J. *Chem. Comm.* **2004**, 1372-1373.
- (29) Shih, W. M.; Quispe, J. D.; Joyce, G. F. *Nature* **2004**, *427*, 618-621.
- (30) Goodman, R. P.; Schaap, I. A. T.; Tardin, C. F.; Erben, C. M.; Berry, R. M.; Schmidt, C. F.; Turberfield, A. J. *Science* **2005**, *310*, 1661-1665.
- (31) He, Y.; Ye, T.; Su, M.; Zhang, C.; Ribbe, A. E.; Jiang, W.; Mao, C. *Nature* **2008**, *452*, 198-201.
- (32) Bhatia, D.; Mehtab, S.; Krishnan, R.; Indi, S. S.; Basu, A.; Krishnan, Y. *Angew. Chem., Int. Ed.* **2009**, *48*, 4134-4137.
- (33) Mastroianni, A. J.; Claridge, S. A.; Alivisatos, P. A. *J. Am. Chem. Soc.* **2009**, *131* (24), 8455-8459.
- (34) Anderson, E. S. et al. *Nature* **2009**, *459*, 73-76.
- (35) Ke, Y.; Sharma, J.; Liu, M.; Jahn, K.; Liu, Y.; Yan, H. *Nano Lett.* **2009**, *6*, 2445-2447.
- (36) Lin, C.; Rinker, S.; Wang, X.; Liu, Y.; Seeman, N. C.; Yan, H. *Proc. Natl. Acad. Sci. USA* **2008**, *105*, 17626-17631.
- (37) Wei, B.; Wang, Z.; Mi, Y. *J. Comput. Theor. Nanosci.*, **2007**, *4*, 133-141.

### Chapter 3 References

- (1) Seeman, N. C. *Nature* **2003**, *421*, 427-431.
- (2) Gothelf, K. V. and LaBean, T. H. *Organic and Biomolecular Chemistry* **2005**, *3*, 4023-4037.
- (3) Deng, Z.; chen, Y.; Tian, Y. and Mao, C. *Nanotechnology: Science and Computation* **2006**, 23-34.

- (4) Aldaye, F. A.; Palmer, A.; Sleiman, H. F. *Science* **2008**, *321*, 1795-1799.
- (5) Lin, C.; Liu, Y. and Yan, H. *Biochemistry* **2009**, *48*, 1663-1674.
- (6) Fu, T. J. and Seeman, N. C. *Biochemistry* **1993**, *32*, 3211-3220.
- (7) Winfree, E.; Liu, F.; Wenzler, L. A.; Seeman, N. C. *Nature* **1998**, *394*, 539-544.
- (8) Mao, C.; Sun, W.; Seeman, N. C. *J. Am. Chem. Soc.* **1999**, *121*, 5437-5443.
- (9) LaBean, T. H.; Yan, H.; Kopatsch, J.; Liu, F.; Winfree, E.; Reif, J. H.; Seeman, N. C. *J. Am. Chem. Soc.* **2000**, *122*, 1848-1860.
- (10) Yan, H.; Park, S. H.; Finkelstein, G.; Reif, J. H.; LaBean, T. H. *Science* **2003**, *301*, 1882-1884.
- (11) Liu, D.; Wang, M.; Deng, Z.; Walulu, R.; Mao, C. *J. Am. Chem. Soc.* **2004**, *126*, 2324-2325.
- (12) Ding, B.; Sha, R.; Seeman, N. C. *J. Am. Chem. Soc.* **2004**, *126*, 10230-10231.
- (13) Rothmund, P. W. K.; Papadakis, N.; Winfree, E. *PLoS Biology* **2004**, *2*, 2041-2053.
- (14) Chelyapov, N.; Brun, Y.; Gopalkrishnan, M.; Reishus, D.; Shaw, B.; Adleman, L. *J. Am. Chem. Soc.* **2004**, *126*, 13924-13925.
- (15) Rothmund, P.; Ekani-Nkodo, A.; Papadakis, N.; Kumar, A.; Fygenson, D.; Winfree, E. *J. Am. Chem. Soc.* **2004**, *126*, 16344-16352.
- (16) Mitchell, J. C.; Harris, J. R.; Malo, J.; Bath, J.; Turberfield, A. J. *J. Am. Chem. Soc.* **2004**, *126*, 16342-14363.
- (17) Malo, J.; Mitchell, J. C.; Venien-Bryan, C.; Harris, J. R.; Wille, H.; Sherratt, D. J.; Turberfield, A. J. *Angew. Chem., Int. Ed.* **2005**, *44*, 3057-3061.
- (18) Mathieu, F.; Liao, S.; Kopatsch, J.; Wang, T.; Mao, C.; Seeman, N. C. *Nano Lett.* **2005**, *5*, 661-665.
- (19) Park, S. H.; Barish, R.; Li, H.; Reif, J. H.; Finkelstein, G.; Yan, H.; LaBean, T. H. *Nano Lett.* **2005**, *5*, 693-696.
- (20) Ke, Y.; Liu, Y.; Zhang, J.; Yan, H. *J. Am. Chem. Soc.* **2006**, *128*, 4414-4421.
- (21) Chen, J.; Seeman, N. C. *Nature* **1991**, *350*, 631-633.



- (22) Zhang, Y.; Seeman, N. C. *J. Am. Chem. Soc.* **1994**, *116*, 1661-1669.
- (23) Goodman, R. P.; Berry, R. M.; Turberfield, A. J. *Chem. Comm.* **2004**, 1372-1373.
- (24) Shih, W. M.; Quispe, J. D.; Joyce, G. F. *Nature* **2004**, *427*, 618-621.
- (25) Goodman, R. P.; Schaap, I. A. T.; Tardin, C. F.; Erben, C. M.; Berry, R. M.; Schmidt, C. F.; Turberfield, A. J. *Science* **2005**, *310*, 1661-1665.
- (26) He, Y.; Ye, T.; Su, M.; Zhang, C.; Ribbe, A. E.; Jiang, W.; Mao, C. *Nature* **2008**, *452*, 198-201.
- (27) Zheng, J.; Birktoft, J. J.; Chen, Y.; Wang, T.; Sha, R.; Constantinou, P. E.; Ginell, S. L.; Mao, C. and Seeman, N. C. *Nature* **2009**, *461*, 74-77.
- (28) Mirkin, C. A.; Letsinger, R. L.; Mucic, R. C.; Storhoff, J. J. *Nature* **1996**, *382*, 607-609.
- (29) Alivisatos, A. P.; Johnsson, K. P.; Peng, X.; Wilson, T. E.; Loweth, C. J.; Bruchez Jr, M. P.; Schultz, P. G. *Nature*, **1996**, *382*, 609-611.
- (30) Le, J. D.; Pinto, Y.; Seeman, N. C.; Musier-Forsyth, K.; Taton, T. A.; Kiehl, R. A. *Nano Letters* **2004**, *4*, 2343-2347.
- (31) Li, H.; Park, S. H.; Reif, J. H.; LaBean, T. H.; Yan, H. *J. Am. Chem. Soc.* **2004**, *126*, 418-419.
- (32) Sharma, J.; Chhabra, R.; Liu, Y.; Ke, Y.; Yan, H. *Angew. Chem., Int. Ed.* **2006**, *45*, 730-735.
- (33) Zheng, J.; Constantinou, P. E.; Micheel, C.; Alivisatos, A. P.; Kiehl, P. A. and Seeman, N. C. *Nano Letters* **2006**, *6*, 1502-1504.
- (34) Chhabra, R.; Sharma, J.; Ke, Y.; Liu, Y.; Rinker, S.; Lindsay, S.; Yan, H. *J. Am. Chem. Soc.* **2007**, *129*, 10304-10305.
- (35) Sharma, J.; Chhabra, R.; Andersen, C. S.; Gothelf, K. V.; Yan, H.; Liu, Y. *J. Am. Chem. Soc.* **2008**, *130*, 7820-7821.
- (36) Rinker, S.; Ke, Y.; Liu, Y.; Chhabra, R.; Yan, H. *Nature Nanotechnology* **2008**, *3*, 418-422.
- (37) Sharma, J.; Chhabra, R.; Cheng, A.; Brownell, J.; Liu, Y. and Yan, H. *Science* **2009**, *323*, 112-116.
- (38) Bhatia, D.; Mehtab, S.; Krishnan, R.; Indi, S. S.; Basu, A.; Krishnan, Y. *Angew. Chem., Int. Ed.* **2009**, *48*, 4134-4137.

- (39) Mastroianni, A. J.; Claridge, S. A.; Alivisatos, P. A. *J. Am. Chem. Soc.* **2009**, *131* (24), 8455-8459.
- (40) Rothmund, P. W. K. *Nature* **2006**, *440*, 297-302.
- (41) Anderson, E. S. et al. *Nature* **2009**, *459*, 73-76.
- (42) Douglas, S. M.; Dietz, H.; Liedl, T.; Högberg, B.; Graf, F.; Shis, W. M. *Nature* **2009**, *459*, 414-418.
- (43) Dietz, H.; Douglas, S. M.; Shih, W. M. *Science* **2009**, *325*, 725-730.
- (44) Pound, E.; Ashton, J. R.; Becerril, H. A. and Woolley, A. T. *Nano Letter* **2009**, *9*, 4302-4305.
- (45) Kuzuya, A. and Komiyama, M. *Chem Comm* **2009**, *28*, 4182-4184.
- (46) Ke, Y.; Douglas, S. M.; Liu, M.; Sharma, J.; Cheng, A.; Leung, A.; Liu, Y.; Shih, W. M.; Yan, H. *J. Am. Chem. Soc.* **2009**, *131*, 15903-15908.
- (47) Zhao, Z.; Yan, H.; Liu, Y. *Angew Chem Int Ed* **2010**, *49*, 1414-1417.
- (48) Liedl, T.; Högberg, B.; Tytell, J.; Ingber, D. E. and Shih, W. M. *Nature Nanotechnology* **2010**, *5*, 520-524.
- (49) Ke, Y.; Lindsay, S.; Chang, Y.; Liu, Y.; Yan, H. *Science* **2008**, *319*, 180-183.
- (50) Shen, W.; Zhong, H.; Neff, D. and Norton, M. L. *J. Am. Chem. Soc.* **2009**, *131*, 6660-6661.
- (51) Kuzyk, A.; Laitinen, K. T.; Törmä, P. *Nanotechnology* **2009**, *2*, 235305-235310.
- (52) Kuzuya, A.; Kimura, M.; Numajiri, K.; Koshi, N.; Ohnishi, T.; Okada, F. and Komiyama, M. *ChemBioChem* **2009**, *10*, 1811-1815.
- (53) Maune, H. T.; Han, S.; Barish, R. D.; Bockrath, M.; Goddard III, W. A.; Rothmund, P. W. K.; and Winfree, E. *Nature Nanotechnology* **2010**, *5*, 61-66.
- (54) Ding, B.; Deng, Z.; Yan, H.; Cabrini, S.; Zuckermann, R. N.; Bokor, J. *J Am Chem Soc* **2010**, *132*, 3248-3249.
- (55) Pal, S.; Deng, Z.; Ding, B.; Yan, H.; Liu, Y. *Angew Chem Int Ed* **2010**, *49*, 2700-2704.

- (56) Voigt, N. V.; Tørring, T.; Rotaru, A.; Jacobsen, M. F.; Ravnsbæk, J. B.; Subramani, R.; Mamdouh, W.; Kjems, J.; Mokhir, A.; Basenbacher, F.; and Gothelf, K. V. *Nature Nanotechnology* **2010**, *5*, 200-203.
- (57) Lund, K.; Manzo, A. J.; Dabby, N.; Michelotti, N.; Johnson-Buck, A.; Nangreave, J.; Taylor, S.; Pei, R.; Stojanovic, M. N.; Walter, N. G.; Winfree, E.; Yan, H. *Nature* **2010**, 465, 206-210.
- (58) Endo, M.; Sugita, T.; Katsuda, Y.; Hidaka, K. and Sugiyama, H. *Chem. Eur. J.* **2010**, *16*, 5362-5368.
- (59) Sun, X.; Ko, S. H.; Zhang, C.; Ribbe, A. E.; Mao, C. *J. Am. Chem. Soc.* **2009**, *131*, 13248-13249.

#### Chapter 4 References

- (1) Seeman, N. C. *Nature* **2003**, *421*, 427-431.
- (2) Gothelf, K. V. and LaBean, T. H. *Organic and Biomolecular Chemistry* **2005**, *3*, 4023-4037.
- (3) Aldaye, F. A.; Palmer, A.; Sleiman, H. F. *Science* **2008**, *321*, 1795-1799.
- (4) Lin, C.; Liu, Y. and Yan, H. *Biochemistry* **2009**, *48*, 1663-1674.
- (5) Fu, T. J. and Seeman, N. C. *Biochemistry* **1993**, *32*, 3211-3220.
- (6) Winfree, E.; Liu, F.; Wenzler, L. A.; Seeman, N. C. *Nature* **1998**, *394*, 539-544.
- (7) Mao, C.; Sun, W.; Seeman, N. C. *J. Am. Chem. Soc.* **1999**, *121*, 5437-5443.
- (8) LaBean, T. H.; Yan, H.; Kopatsch, J.; Liu, F.; Winfree, E.; Reif, J. H.; Seeman, N. C. *J. Am. Chem. Soc.* **2000**, *122*, 1848-1860.
- (9) Yan, H.; Park, S. H.; Finkelstein, G.; Reif, J. H.; LaBean, T. H. *Science* **2003**, *301*, 1882-1884.
- (10) Liu, D.; Wang, M.; Deng, Z.; Walulu, R.; Mao, C. Tensegrity: *J. Am. Chem. Soc.* **2004**, *126*, 2324-2325.
- (11) Ding, B.; Sha, R.; Seeman, N. C. *J. Am. Chem. Soc.* **2004**, *126*, 10230-10231.
- (12) Rothmund, P. W. K.; Papadakis, N.; Winfree, E. *PLoS Biology* **2004**, *2*, 2041-2053.

- (13) Chelyapov, N.; Brun, Y.; Gopalkrishnan, M.; Reishus, D.; Shaw, B.; Adleman, L. *J. Am. Chem. Soc.* **2004**, *126*, 13924-13925.
- (14) Rothmund, P.; Ekani-Nkodo, A.; Papadakis, N.; Kumar, A.; Fyngenson, D.; Winfree, E. *J. Am. Chem. Soc.* **2004**, *126*, 16344-16352.
- (15) Mitchell, J. C.; Harris, J. R.; Malo, J.; Bath, J.; Turberfield, A. J. *J. Am. Chem. Soc.* **2004**, *126*, 16342-14363.
- (16) Malo, J.; Mitchell, J. C.; Venien-Bryan, C.; Harris, J. R.; Wille, H.; Sherratt, D. J.; Turberfield, A. J. *Angew. Chem., Int. Ed.* **2005**, *44*, 3057-3061.
- (17) Mathieu, F.; Liao, S.; Kopatsch, J.; Wang, T.; Mao, C.; Seeman, N. C. *Nano Lett.* **2005**, *5*, 661-665.
- (18) Park, S. H.; Barish, R.; Li, H.; Reif, J. H.; Finkelstein, G.; Yan, H.; LaBean, T. H. *Nano Lett.* **2005**, *5*, 693-696.
- (19) Ke, Y.; Liu, Y.; Zhang, J.; Yan, H. *J. Am. Chem. Soc.* **2006**, *128*, 4414-4421.
- (20) Chen, J.; Seeman, N. C. *Nature* **1991**, *350*, 631-633.
- (21) Zhang, Y.; Seeman, N. C. *J. Am. Chem. Soc.* **1994**, *116*, 1661-1669.
- (22) Goodman, R. P.; Berry, R. M.; Turberfield, A. J. *Chem. Comm.* **2004**, 1372-1373.
- (23) Shih, W. M.; Quispe, J. D.; Joyce, G. F. *Nature* **2004**, *427*, 618-621.
- (24) Goodman, R. P.; Schaap, I. A. T.; Tardin, C. F.; Erben, C. M.; Berry, R. M.; Schmidt, C. F.; Turberfield, A. J. *Science* **2005**, *310*, 1661-1665.
- (25) He, Y.; Ye, T.; Su, M.; Zhang, C.; Ribbe, A. E.; Jiang, W.; Mao, C. *Nature* **2008**, *452*, 198-201.
- (26) Zheng, J.; Birktoft, J. J.; Chen, Y.; Wang, T.; Sha, R.; Constantinou, P. E.; Ginell, S. L.; Mao, C. and Seeman, N. C. *Nature* **2009**, *461*, 74-77.
- (27) Mirkin, C. A.; Letsinger, R. L.; Mucic, R. C.; Storhoff, J. J. *Nature* **1996**, *382*, 607-609.
- (28) Alivisatos, A. P.; Johnsson, K. P.; Peng, X.; Wilson, T. E.; Loweth, C. J.; Bruchez Jr, M. P.; Schultz, P. G. *Nature*, **1996**, *382*, 609-611.
- (29) Le, J. D.; Pinto, Y.; Seeman, N. C.; Musier-Forsyth, K.; Taton, T. A.; Kiehl, R. A. *Nano Letters* **2004**, *4*, 2343-2347.

- (30) Li, H.; Park, S. H.; Reif, J. H.; LaBean, T. H.; Yan, H. *J. Am. Chem. Soc.* **2004**, *126*, 418-419.
- (31) Sharma, J.; Chhabra, R.; Liu, Y.; Ke, Y.; Yan, H. *Angew. Chem., Int. Ed.* **2006**, *45*, 730-735.
- (32) Zheng, J.; Constantinou, P. E.; Micheel, C.; Alivisatos, A. P.; Kiehl, P. A. and Seeman, N. C. *Nano Letters* **2006**, *6*, 1502-1504.
- (33) Chhabra, R.; Sharma, J.; Ke, Y.; Liu, Y.; Rinker, S.; Lindsay, S.; Yan, H. *J. Am. Chem. Soc.* **2007**, *129*, 10304-10305.
- (34) Sharma, J.; Chhabra, R.; Andersen, C. S.; Gothelf, K. V.; Yan, H.; Liu, Y. *J. Am. Chem. Soc.* **2008**, *130*, 7820-7821.
- (35) Rinker, S.; Ke, Y.; Liu, Y.; Chhabra, R.; Yan, H. *Nature Nanotechnology* **2008**, *3*, 418-422.
- (36) Sharma, J.; Chhabra, R.; Cheng, A.; Brownell, J.; Liu, Y. and Yan, H. *Science* **2009**, *323*, 112-116.
- (37) Bhatia, D.; Mehtab, S.; Krishnan, R.; Indi, S. S.; Basu, A.; Krishnan, Y. *Angew. Chem., Int. Ed.* **2009**, *48*, 4134-4137.
- (38) Mastroianni, A. J.; Claridge, S. A.; Alivisatos, P. A. *J. Am. Chem. Soc.* **2009**, *131* (24), 8455-8459.
- (39) Rothmund, P. W. K. *Nature* **2006**, *440*, 297-302.
- (40) Anderson, E. S.; Dong, M.; Nielsen, M. M.; Jahn, K.; Subramani, R.; Mamdouh, W.; Golas, M.m.; Sander, B.; Stark, H.; Oliveira, C. L. P. and *et al.* *Nature* **2009**, *459*, 73-76.
- (41) Douglas, S. M.; Dietz, H.; Liedl, T.; Högberg, B.; Graf, F.; Shis, W. M. *Nature* **2009**, *459*, 414-418.
- (42) Dietz, H.; Douglas, S. M.; Shih, W. M. *Science* **2009**, *325*, 725-730.
- (43) Pound, E.; Ashton, J. R.; Becerril, H. A. and Woolley, A. T. *Nano Letter* **2009**, *9*, 4302-4305.
- (44) Kuzuya, A. and Komiyama, M. *Chem Comm* **2009**, *28*, 4182-4184.
- (45) Ke, Y.; Douglas, S. M.; Liu, M. ; Sharma, J.; Cheng, A.; Leung, A.; Liu, Y.; Shih, W. M.; Yan, H. *J. Am. Chem. Soc.* **2009**, *131*, 15903-15908.
- (46) Zhao, Z.; Yan, H.; Liu, Y.. *Angew Chem Int Ed* **2010**, *49*, 1414-1417.

- (47) Liedl, T.; Högberg, B.; Tytell, J.; Ingber, D. E. and Shih, W. M. *Nature Nanotechnology* **2010**, *5*, 520-524.
- (48) Han, D.; Pal, S.; Liu, Y. and Yan, H. *Nature Nanotechnology* **2010**, *5*, 712-717.
- (49) Ke, Y.; Lindsay, S.; Chang, Y.; Liu, Y.; Yan, H. *Science* **2008**, *319*, 180-183.
- (50) Shen, W.; Zhong, H.; Neff, D. and Norton, M. L. *J. Am. Chem. Soc.* **2009**, *131*, 6660-6661.
- (51) Kuzyk, A.; Laitinen, K. T.; Törmä, P. *Nanotechnology* **2009**, *2*, 235305-235310.
- (52) Kuzuya, A.; Kimura, M.; Numajiri, K.; Koshi, N.; Ohnishi, T.; Okada, F. and Komiyama, M. *ChemBioChem* **2009**, *10*, 1811-1815.
- (53) Maune, H. T.; Han, S.; Barish, R. D.; Bockrath, M.; Goddard III, W. A.; Rothmund, P. W. K.; and Winfree, E. *Nature Nanotechnology* **2010**, *5*, 61-66.
- (54) Ding, B.; Deng, Z.; Yan, H.; Cabrini, S.; Zuckermann, R. N.; Bokor, J. *J Am Chem Soc* **2010**, *132*, 3248-3249.
- (55) Pal, S.; Deng, Z.; Ding, B.; Yan, H.; Liu, Y. *Angew Chem Int Ed* **2010**, *49*, 2700-2704.
- (56) Voigt, N. V.; Tørring, T.; Rotaru, A.; Jacobsen, M. F.; Ravnsbæk, J. B.; Subramani, R.; Mamdouh, W.; Kjems, J.; Mokhir, A.; Basenbacher, F. and *et al.* *Nature Nanotechnology* **2010**, *5*, 200-203.
- (57) Lund, K.; Manzo, A. J.; Dabby, N.; Michelotti, N.; Johnson-Buck, A.; Nangreave, J.; Taylor, S.; Pei, R.; Stojanovic, M. N.; Walter, N. G.; Winfree, E.; Yan, H. *Nature* **2010**, *465*, 206-210.
- (58) Endo, M.; Sugita, T.; Katsuda, Y.; Hidaka, K. and Sugiyama, H. *Chem. Eur. J.* **2010**, *16*, 5362-5368.
- (59) Liu, W.; Zhong, H.; Wang, R. and Seeman, N.C. *Angew Chem Int Ed* **2011**, *50*, 264-267.
- (60) Li, Z.; Liu, M.; Wang, L.; Nangreave, J.; Yan, H. and Liu, Y. *J. Am. Chem. Soc.* **2010**, *132*, 13545-13552.
- (61) Jungmann, R.; Scheible, M.; Kuzyk, A.; Pardatscher, G.; Castro, C. E. and Simmel, F. C. *Nanotechnology* **2011**, *22*, 275301.

- (62) Douglas, S. M.; Marblestone, A. H.; Teerapittayanon, S.; Vazquez, A.; Church, G. M. and Shih, W. M. *Nucleic Acids Res.* **2009**, 37, 5001-5006.
- (63) Castro, C. E.; Kilchherr, F.; Kim, D.; Shiao, E. L.; Wauer, T.; Wortmann, P.; Bathe, M. and Dietz, H. *Nature Methods.* **2011**, 8, 221-229.
- (64) Zhang, J.; Liu, Y.; Ke, Y. and Yan, H. *Nano Lett.* **2006**, 6, 248-251.

APPENDIX A

SUPPLEMENTAL INFORMATION FOR CHAPTER 2



## Supplemental Information

### A Replicable Tetrahedral Nanostructure Self-Assembled from a Single DNA Strand

Zhe Li, Bryan Wei, Jeanette Nangreave, Chenxiang Lin, Yan Liu,

Yongli Mi, and Hao Yan

#### Materials.

All DNA oligonucleotides were purchased from Integrated DNA Technology and purified by polyacrylamide gel electrophoresis (PAGE). Restriction enzymes (*Pst*I, *Sac*I, *Bsr*GI, and *Bsp*HI), T4 DNA ligase, phagemid vector Litmus 28I, and helper phage M13KO7 were purchased from New England BioLabs. Competent cell line XL1-Blue was purchased from Stratagene. 10-bp DNA ladders were purchased from Invitrogen. Plasmid Spin Miniprep kit was purchased from Qiagen. All other reagents were purchased from Sigma–Aldrich.

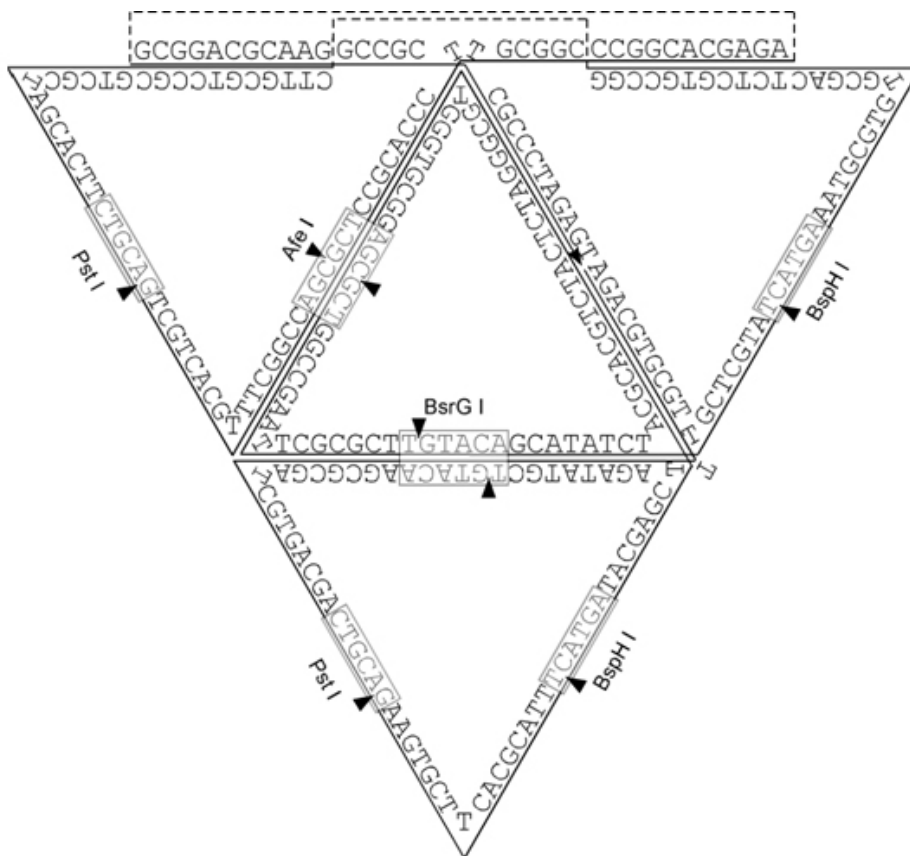
**In vivo cloning.** The process is illustrated schematically in Fig S4.

1) Preparation of double stranded insert and ligation with the plasmid: Equal amounts of sense and antisense nanostructure strands (90 nM, sequences are listed in Table S1 and S2 respectively) were annealed in a water bath from 95 °C to room temperature for about 48 hours in 1X TAE/Mg<sup>2+</sup> buffer to yield a double-stranded (DS) insert. 2 µg Litmus 28i (500 µg/mL) were digested by 20 U *Pst*I and 15 U *Sac*I in 50 µL 1X NEBuffer 1 at 37 °C for 2 hrs, and purified via agarose gel electrophoresis. 100 ng of digested vector was ligated with 0.16 pmol of pre-annealed DS insert (~ 3 fold excess) in 20 µL 1X T4 ligase buffer at 4 °C overnight.

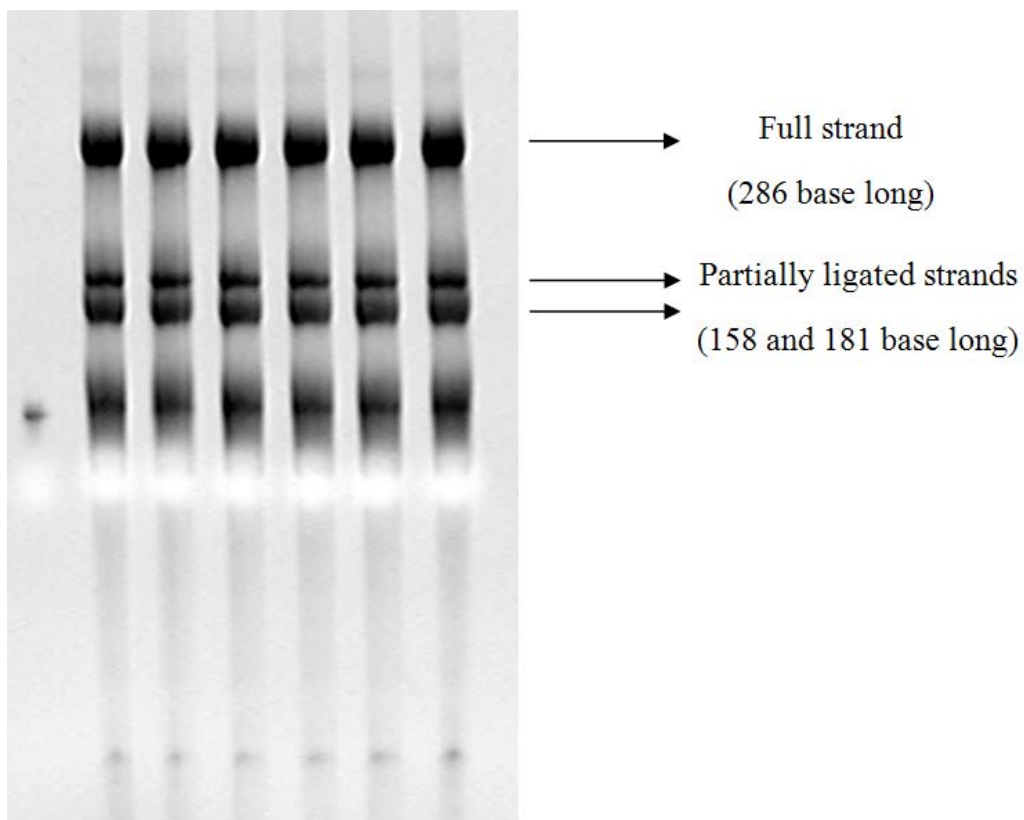
2) Transformation of the cell by the ligated vector and verification of the correct vector insertion: The ligated vector, 50 ng, was transformed into competent XL1-Blue cells by heat shock, and incubated on LB-ampicillin (LB-Amp) agar plates at 37 °C overnight. Double stranded phagemid was extracted using the plasmid miniprep kit from cells in 5 mL of saturated cultures that were amplified from a single colony picked from the agar. The correct insertion was verified by restriction enzyme digestion followed by denaturing PAGE.

3) Infection of the transformed cells with helper phage, amplification and packaging of the single stranded phage DNA: 1 mL glycerol stock of XL1-Blue cells (OD<sub>600</sub>=0.8) with correctly inserted phagemid were infected by 50 µL of 1x10<sup>11</sup> M13KO7 helper phage and incubated overnight at 37 °C in 250 mL LB-Amp culture containing 25 µg/mL Kanamycin.

4) Isolation and purification of the amplified single stranded tetrahedron DNA: The bacteriophage particles that contained single-stranded vectors were precipitated from the supernatant by addition of 10 g PEG and 7.5 g NaCl followed by centrifugation at 10,000 g. Protein shells were removed from the single-stranded vectors by phenol/chloroform extraction. DNA was recovered by ethanol precipitation, re-dissolved in 0.9 mL water, and restricted by 500 U of *Pst*I and 360 U of *Sac*I in the presence of 1 nmol of restriction helper strands in 1 mL 1X NEbuffer 1. The digested single-stranded vector was resolved on a 10% denaturing polyacrylamide gel and the correctly replicated insert was excised from the gel and eluted. Typically, about 50 pmol of ssDNA was recovered.



**Figure S1.** DNA sequence of the single-stranded tetrahedron.



**Figure S2.** Purification of the 286-nt full length strand obtained by ligation. The gel band of full strand was excised out and extracted for 48 hours in the extraction buffer.

|                                 |   |
|---------------------------------|---|
| Sense component strand 1*       | /Phos/CAGACGTGCGTTAGATATGCTGTACAAGCGC<br>GATCGTGACGACTGTAGAAGTGCTTCACGCATTT<br>ATGATACGAGCTACGCACGTCTACTCTAGGGCGTG<br>GGTGCGGAGCGCTGG |
| Sense component strand 2*       | /Phos/CCGAATTCGCGCTTGTACAGCATATCTTGCTC<br>GTATCATGAAATGCGTGTGCGACTCTCGTGCCGGC<br>TTGCGTCCGCGTCGCTAGCACTTCTACAGTCGTAC<br>GTTTCGGCCAG   |
| Sense component strand 3*       | /Phos/CGCTCCGCACCCTGCGGCCCGGCACGAGAGC<br>GGACGCAAGGCCGCTCGCCCTAGAGTCTGCA  |
| Splint between sense strand 1&2 | CTGTACAAGCGCGAATTCGGCCAGCGCTCCGCACC<br>CACGC  |
| Splint between sense strand 2&3 | GGGCCGCAGGGTGCGGAGCGCTGGCCGAAACGTG<br>ACGACT  |

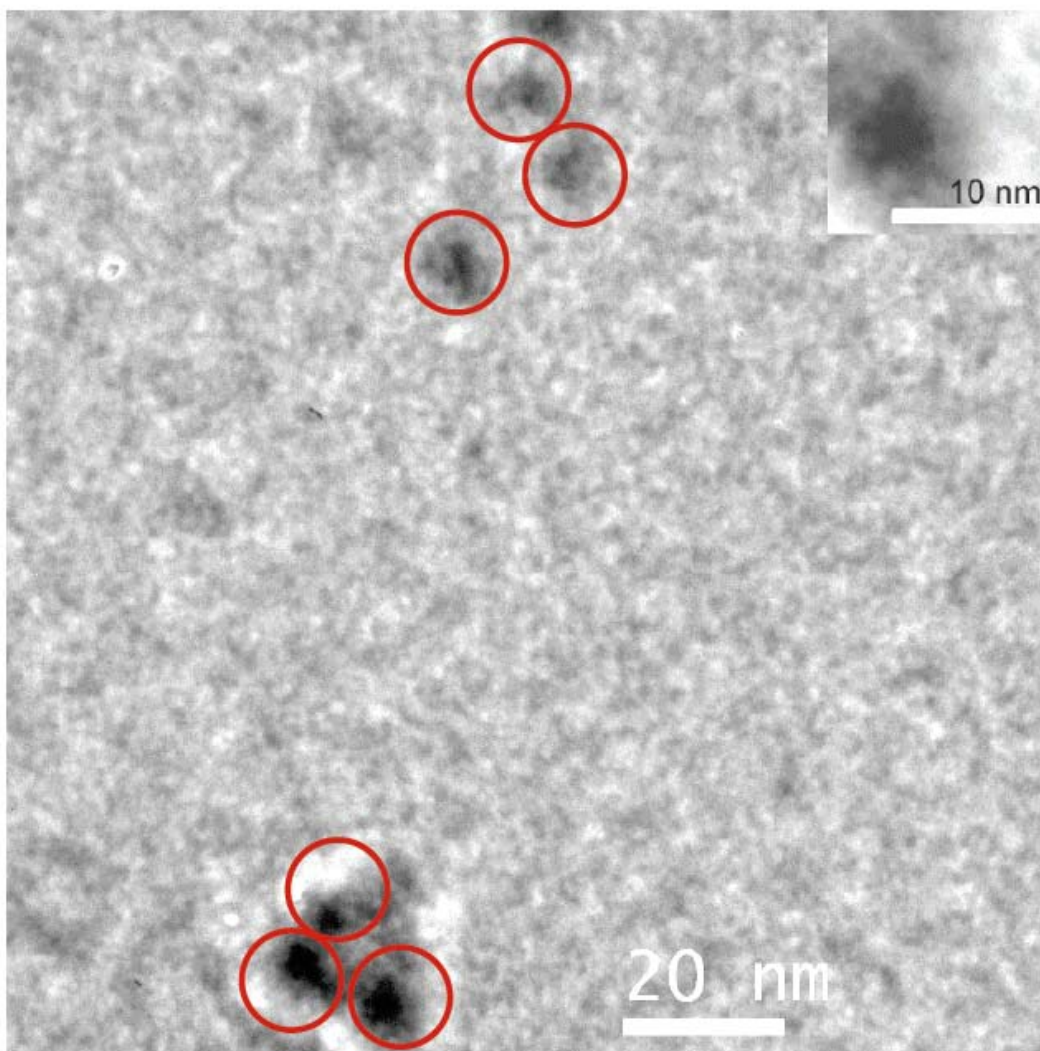
**Table S1.** Sequences of component strands of the DNA tetrahedron for sense ligation.

\* The 5' end of the strand is phosphorylated.

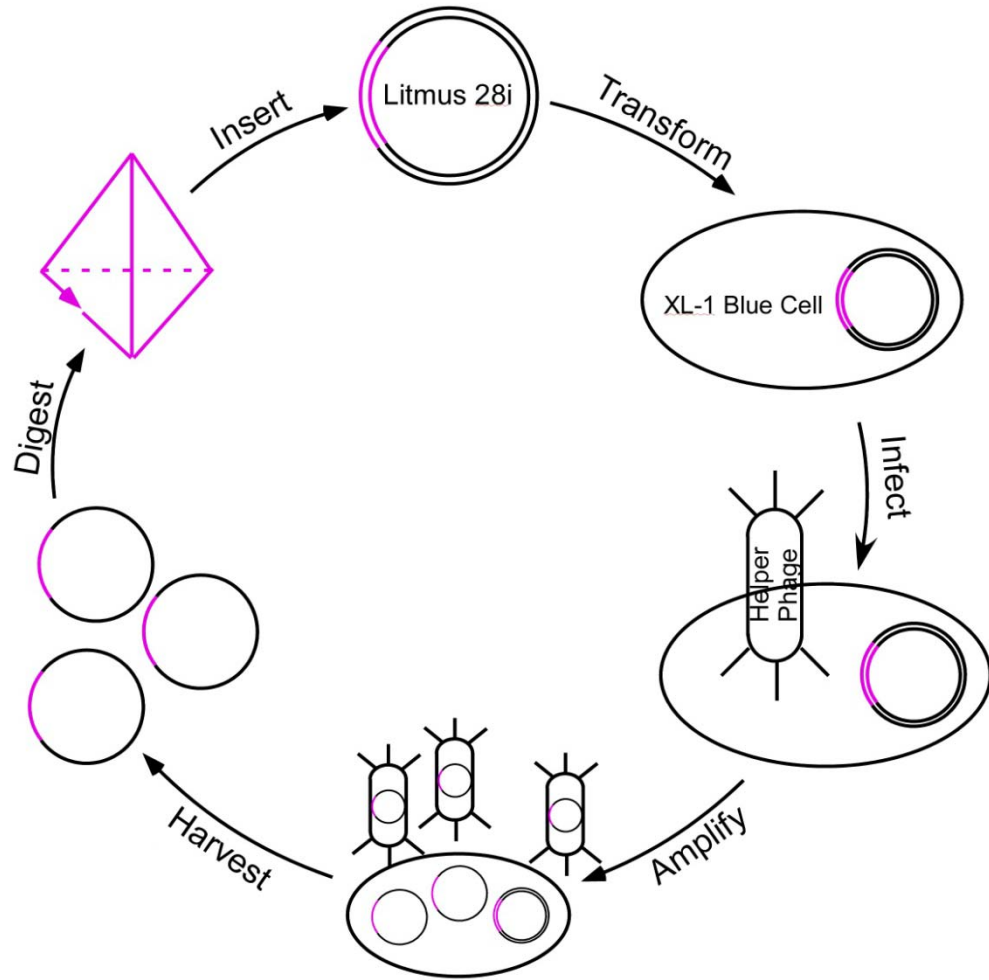
|                                     |   |
|-------------------------------------|---|
| Antisense component strand 1*       | /Phos/GACTCTAGGGCGAGCGGCCTTGCGTCCGCTCT<br>CGTGCCGGGCGCAGGGTGCGGAGCGCTGGCCGA<br>AACGTGACGACTGTAGAAGTGCTAGCGACGCGGA<br>CGCAAGCCGGCACGAG |
| Antisense component strand 2*       | /Phos/AGTCGCACACGCATTTTCATGATACGAGCAAG<br>ATATGCTGTACAAGCGCGAATTCGGCCAGCGCTCC<br>GCACCCACGCCCTAGAGTAGACGTGCGTAGCTCGT<br>ATCATGAAATGCG |
| Antisense component strand 3*       | /Phos/TGAAGCACTTCTACAGTCGTCACGATCGCGCT<br>TGTACAGCATATCTAACGCACGTCTGAGCT  |
| Splint between antisense strand 1&2 | CATGAAATGCGTGTGCGACTCTCGTGCCGGCTTGC<br>GTCCG  |
| Splint between antisense strand 2&3 | ACGACTGTAGAAGTGCTTTCACGCATTTTCATGATAC<br>GAGCT  |

**Table S2.** Sequences of constituent strands for antisense ligation.

\* The 5' end of the strand is phosphorylated.



**Figure S3.** TEM images of ss-tetrahedron DNA structures. Individual tetrahedral are circled. The size of the triangle-shaped structure was in agreement with the design ( $\sim 7.5$  nm).

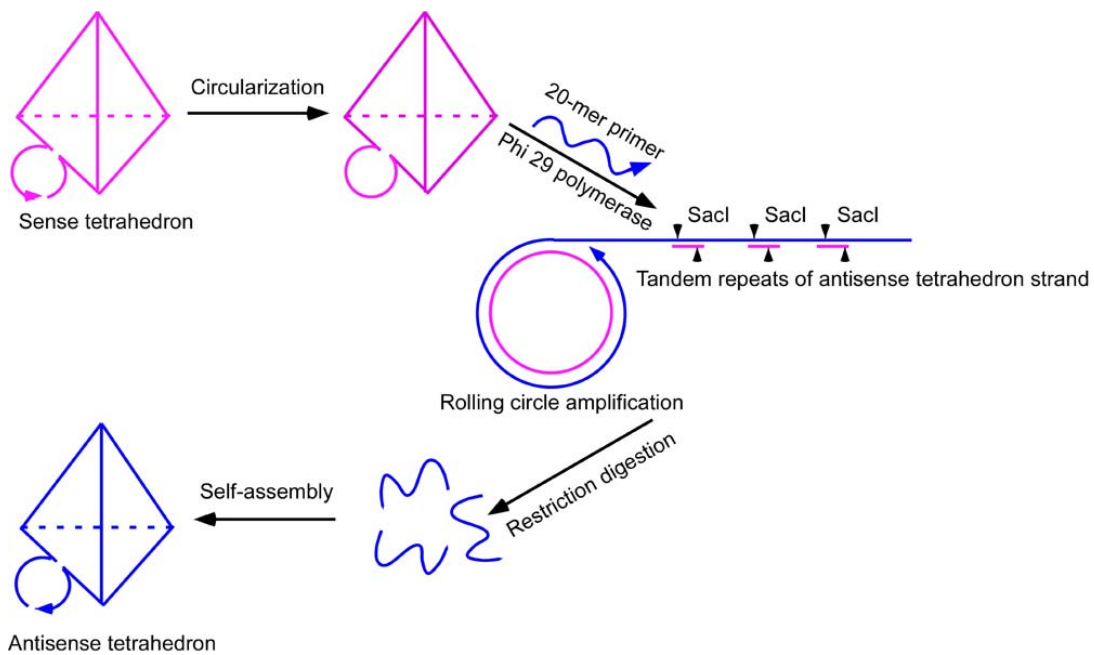


**Figure S4.** Scheme showing the in vivo replication process of the single-stranded DNA tetrahedron.

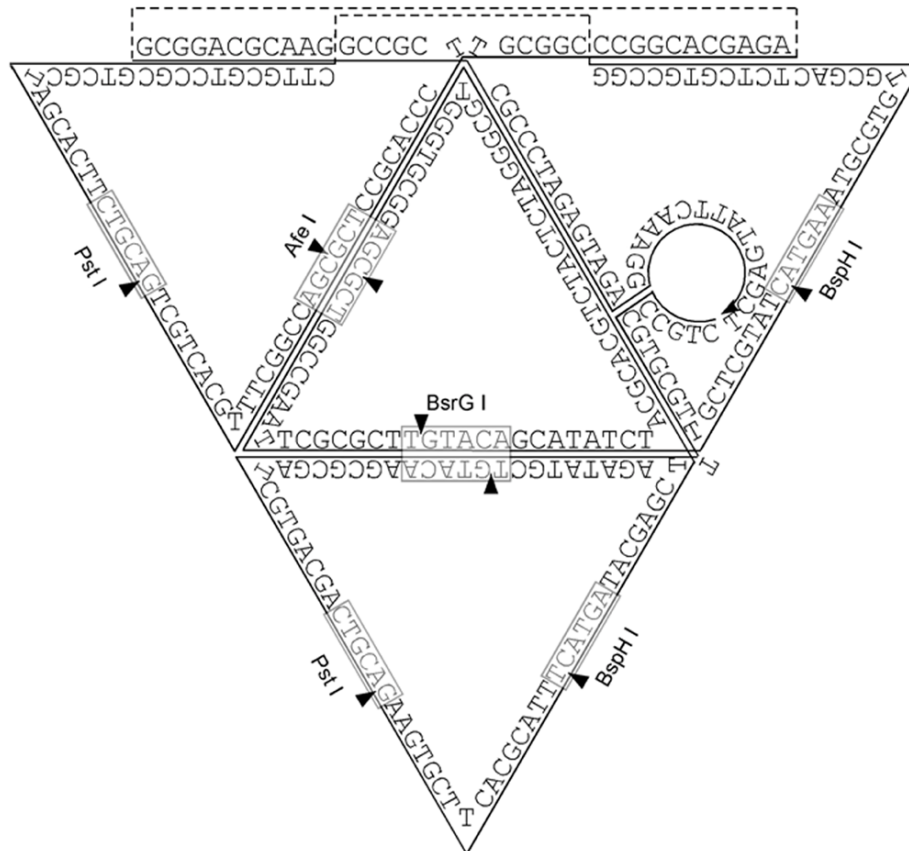


### **Rolling circle amplification of the tetrahedron.**

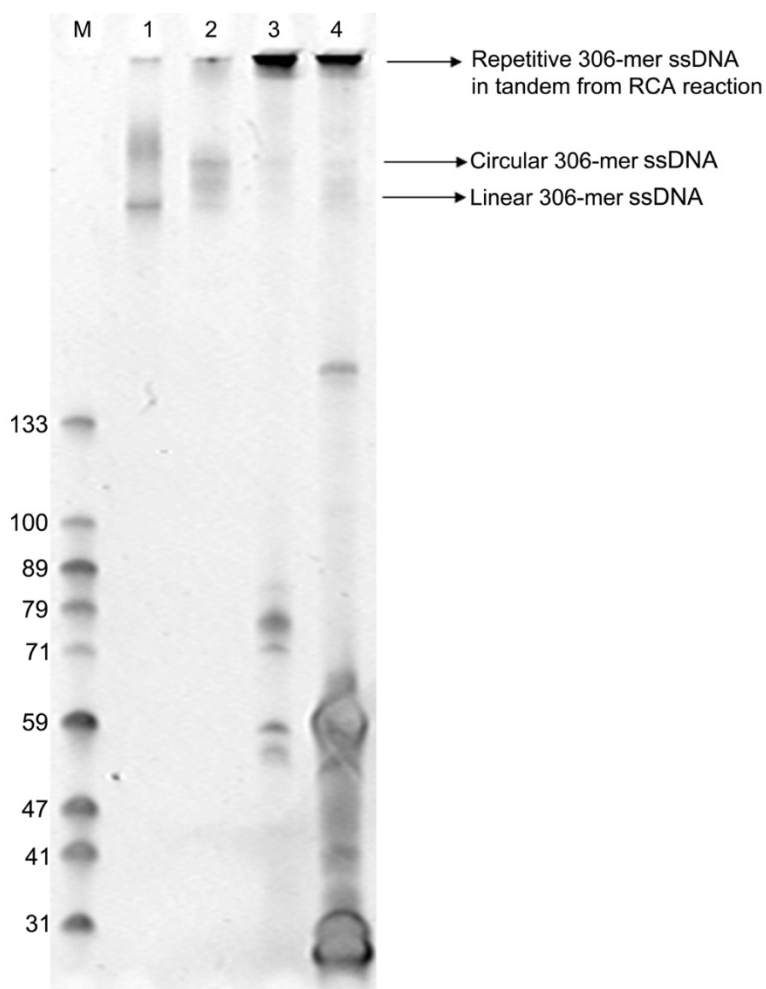
Rolling circle amplification (RCA) [S1] was attempted to propagate this strand (Fig S6). A total 20-mer loop with *SacI* recognition site was designed to extend out from one edge of the tetrahedron (Fig S5). The 5' and the 3' ends in the loop region were covalently connected by CircLigase (Epicentre Biotech). The circularized strand served as the original template for the rolling circle amplification. Phi 29 DNA polymerase then repeatedly read through the circular template for amplification after the 20-mer primer was annealed to the loop region. As a result, a long ssDNA that was composed of repetitive anti-sense strand segments was obtained. After restriction digestion by *SacI* enzyme, the product was analyzed by denaturing PAGE. However, as seen in Fig S7, this method did not result in the efficient amplification of the desired structure.



**Figure S5.** Schematic of rolling circle amplification of DNA tetrahedron.



**Figure S6.** DNA sequence of the single-stranded template for RCA.



**Figure S7.** RCA result visualized by denaturing PAGE. ssDNA markers were loaded in lane M. The linear 306-mer ssDNA was loaded in lane 1. Circular 306-mer template (cyclized by CircLigase) was loaded in lane 2. RCA product and its *SacI* digested product were loaded in lane 3 and 4 respectively. The intensity of the linear 306-mer band was expected to be much higher in lane 4 than in lane 1 if the amplification was successful. The result was opposite with mostly truncated products, indicating extremely low yield of the full length product of this procedure.

#### Reference

[S1] C. Lin, M. Xie, J. J. L. Chen, Y. Liu, H. Yan, *Angew. Chem.* **2006**, 45, 7537-7539.

APPENDIX B

SUPPLEMENTAL INFORMATION FOR CHAPTER 3

## Supplemental Information

### Molecular Behavior of DNA Origami in Higher Order Self-assembly

Zhe Li, Minghui Liu, Lei Wang, Jeanette Nangreave, Hao Yan, Yan Liu

#### Material

DNA strands were purchased from Integrated DNA Technology (www.idtdna.com) in 96-well plates, normalized to 100  $\mu$ M. Microcon Centrifugal Filter Devices (100,000 MWCO, Catalog number: 42413) were purchased from Millipore. M13 viral DNA was purchased from New England Biolabs, Inc. (NEB, Catalog number: #N4040S).

#### Assembly of DNA Origami

The modeling of 12, 24, and 40 helix zigzag DNA origami structures and the generation of strand sequences were performed using Tiamat software developed in the Yan lab (Williams, S.; Lund, K.; Lin, C.; Wonka, P.; Lindsay, S.; and Yan, H. LNCS 5347, DNA Computing, the program is free download from the webpage <http://yanlab.asu.edu/Resources.html>). The strand sequences of the 24 helix 'planar' rectangular shaped DNA origami are reported in previously published work (Rothemund, P. W. K. *Nature*, **440** 297 (2006)).

To assemble core structures:

DNA origami core structures were assembled by mixing a 1:10 molar ratio of M13 viral DNA to each helper strand in 1xTAE/Mg buffer (20 mM Tris, pH 7.6, 2mM EDTA, 12.5 mM MgCl<sub>2</sub>). Helper strands corresponding to the far left and right edges in each tile were not included. The final concentration of origami was 10 nM. The DNA mixtures were heated to 90 °C and slowly cooled to 4 °C in a thermal cycler over 12 hours. After the formation of the origami core structures, purification was performed using Microcon centrifugal filter devices (100,000 MWCO, 300 x g speed, 10 min) to remove excess helper strands. The purified origami core structures (~5 nM) were used in all subsequent higher order assemblies.

To assemble stair-like 1D arrays, tubes, or other 1D structures in solution:

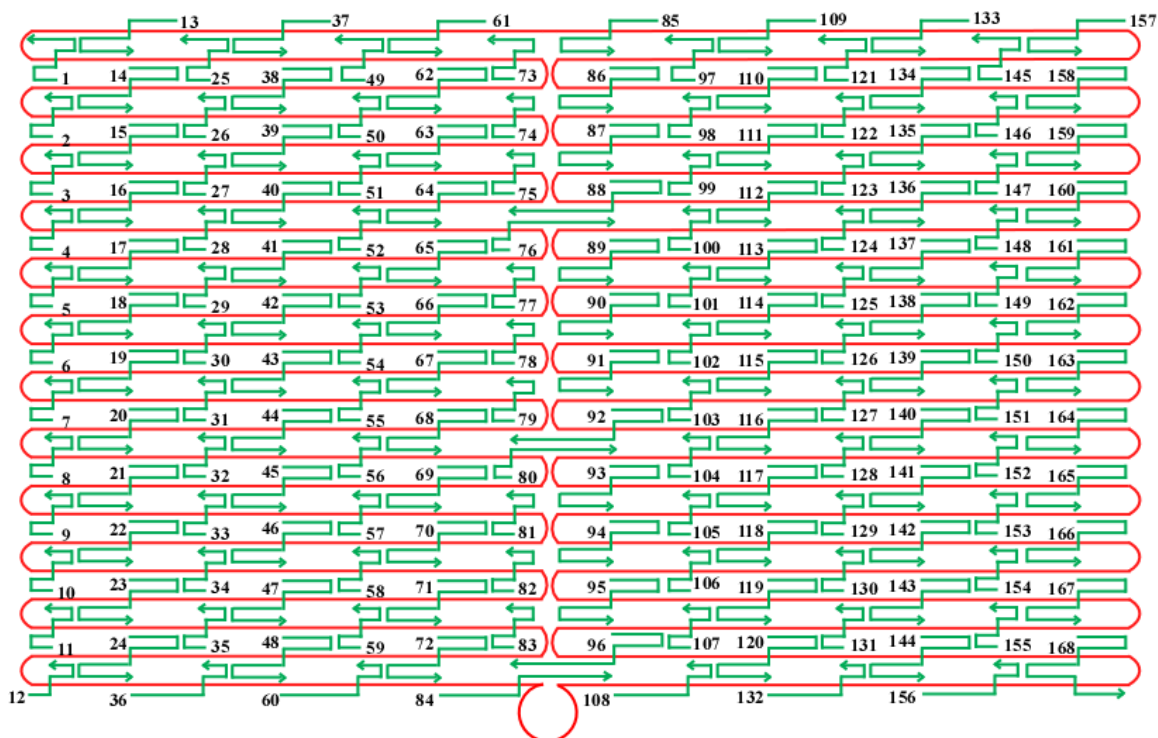
Specific linker strands were added to the solution of origami core structures with a 5:1 molar ratio of linker strands to core structure. The mixture was incubated at room temperature overnight.

For surface mediated assembly of 2D arrays from origami tile units:

2  $\mu$ L of the origami core structure (~5 nM) solution was mixed with specific linker strands (with a 5:1 molar ratio of linker strands to core structure), placed on mica and incubated at 40 °C in a humid chamber for 12 hours to allow DNA origami tiles to assemble into 2D arrays.

## **AFM Imaging**

For AFM imaging, 2  $\mu\text{L}$  of sample was deposited onto a freshly cleaved piece of mica (Ted Pella, Inc.) and left for 2 min. 30  $\mu\text{L}$  of 1xTAE/Mg buffer was then deposited onto the mica surface. Imaging was performed using a MultiMode V AFM (Veeco Inc.) in tapping mode, with NP-S or SNL tips (Veeco Inc.).



**Figure S1.** Schematic of the 24-helix zigzag origami structure, helper strand position and numbering assignment. The continuous red strand corresponds to the circular M13 viral genome with all helper strands shown in green. The arrows indicate the 3' - ends of the oligonucleotides. Dangling loop represents unpaired sequences. Sequences of helper strands used in these experiments are given below.

**Sequences of the helper strands:**

- 1: TTTTAAATGCCAGTTACAAAATCCAGAGCCTAATT
- 2: TAAATATGAAAAGTAAGCAGAGAAGCCC
- 3: CCACCACTGACGGAAATTATTGGGAAGG
- 4: TGCCTTGCGGAACCGCCTCCCACCAGAG
- 5: AGGGATAAGTAACAGTGCCCGGGGTCAG
- 6: GGAGCCTGCAAGCCCAATAGGCATTTTC
- 7: TGCCACTTTAATTGTATCGGTTCCAAAA
- 8: AGTAATCACGAAGGCACCAACTACGTAA
- 9: GAATACCTTGACAAGAACCGGCATCAAG
- 10: ACCCTGAACATTCAACTAATGGATTTAG
- 11: ACAGTTGCTATTATAGTCAGAGGTCTTT
- 12: ATTCCAATTCTGCCCATATA
- 13: GAATCTTACCAACGCTAACGAGCGTCTTTAAACAGCCATATT
- 14: ATTTATCCCAATCCACAATGAAATAGCAATAGCTATCTTACCTAGCCG  
AACAAAGT
- 15: TACCAGAAGGAAACAAAGGGGCGACATTCAACCGATTGAGGGACATTA  
AAGTGAAT



16:  
TATCACCGTCACCGCCATCTTTTCATAATCAAAATCACCGGATCAGAG  
CCGCCACC

17:  
CTCAGAACCGCCACAGGAGTGTACTGGTAATAAGTTTTAACGTATAAA  
CAGTTAAT

18:  
GCCCCCTGCCTATTGAACCGCCACCCTCAGAGGCCACCACCCTAACCCA  
TGTACCGT

19:  
AACACTGAGTTTTCGTCACGTTGAAAATCTCCAAAAAAAAGGCTTATCA  
GCTTGCTT

20:  
TCGAGGTGAATTTCTGAGGAAGTTTCCATTAACGGGTAAAACCTAAAA  
CGAAAGAG

21:  
GCAAAGAATACACAGACCAGGCGCATAGGCTGGCTGACCTTATATTC  
ATTACCCA

22:  
AATCAACGTAACAAATTACAGGTAGAAAGATTCATCAGTTGACAGAT  
ACATAACGC

23:  
CAAAAGGAATTACGAACGAGAATGACCATAAATCAAAAATCAAGCAA  
AGCGGATTG

24:  
CATCAAAAAGATTACTAAAGTACGGTGTCTGGAAGTTTCATTGAACGA  
GTAGATTT

25: GCAAGAAAAATAAGAAACGATTACAATTTTATCCT

26: AAAGACACGAGGAAACGCAATAATAAGA

27: GCGTTTGACTTGAGCCATTTGCAGCGCC

28: ATGATACCCTCAGAGCCACCACTTATTA

29: ACCCTCATCGGAACCTATTATGCTTTTG

30: AATTTTTTACCAGTACAAACAACCGCC

31: TTTTTCATTAACAGCTTGATGAATAAT

32: GGTGTACTAAAACACTCATCTTAAAGAC

33: CAACATTAGCTGCTCATTTCAGGATGAAC

34: TTCAGAAAGGCATAGTAAGAGAACGGAA

35: TATGCAAAGAGGAAGCCCGAATAAACAG

36: AGTTTGACCATTAG ATACATTTGCAAATTTTAAA

37: CAAGATTAGTTGCTATTTTGCACCCAGCTTTTTGTTTAAACGT

38:  
CAAAAATGAAAATAAACCCACAAGAATTGAGTTAAGCCCAATAATAA  
CGGAATACC

39:  
CAAAAGAACTGGCACAATCAATAGAAAATTCATATGGTTTACGGAATT  
AGAGCCAG

40:  
CAAATCACCAGTATTTTCATCGGCATTTTTCGGTCATAGCCCCCCTCA  
GAGCCGCC

41:  
ACCAGAACCACCACTTTACCGTTCCAGTAAGCGTCATACATGTCTGAA  
ACATGAAA

42:  
GTATTAAGAGGCTGTCAGGAGGTTTAGTACCGCCACCCTCAGTACAAC  
GCCTGTAG

43:  
CATTCCACAGACAGAATAGAAAGGAACAATAAGGAATTGCACCGA  
TAGTTGCGC

44:  
CGACAATGACAACATAGCAACGGCTACAGAGGCTTTGAGGACTTGAC  
CCCCAGCGA

45:  
TTATACCAAGCGCGCCGAACTGACCAACTTTGAAAGAGGACATGAAT  
AAGGCTTGC

46:  
CCTGACGAGAAACAAGAAAAATCTACGTTAATAAAACGAACTCAACA  
CTATCATAA

47:  
CCCTCGTTTACCAGATATTCATTGAATCCCCCTCAAATGCTTAGACTTC  
AAATATC

48:  
GCGTTTTAATTCGAGCTGAATATAATGCTGTAGCTCAACATGTGGTCA  
ATAACCTG

49: GAGAGATGCAGCCTTTACAGATTGAAGCCTTAAAT

50: TTTGTCATGATTAAGACTCCTAATATCA

51: AGCGCGTGCACCATTACCATTAGTTTAT

52: CTCTGAACAGAGCCGCCGCAAGACTGT

53: ACCGTACAGACTCCTCAAGAGGCGCAGT

54: GAGTGAGCCCTCATAGTTAGCGTGTATC

55: ACGAGGGACCATCGCCCACGCTTCAGCG

56: AAGGGAAAAACAAAGTACAACCATCGGA

57: GTTGGGACCAGAACGAGTAGTCAATCAT

58: GTCATAAACGACGATAAAAACTCAGGAC

59: CTTAATTGCTTCAAAGCGAACCGGAATC

60: TTTAGCTATATTTT CATTGGGGCGCGACTTAGAG

61: TAGCGAACCTCCCGACTTGCGGGAGGTTGAGAATAACATAAA

62:  
AACAGGGAAGCGCAGAACAAAGTCAGAGGGTAATTGAGCGCTTATTA  
CGCAGTATG

63:  
TTAGCAAACGTAGAAAAAGAAACGCAAAGACACCACGGAATAAGCAA  
GGCCGGAAA

64:  
CGTCACCAATGAAACGACAGAATCAAGTTTGCCTTTAGCGTCGCATTG  
ACAGGAGG

65:  
TTGAGGCAGGTCAGTAAATCCTCATTAAAGCCAGAATGGAAAAAGGA  
TTAGGATTA

66:  
GCGGGGTTTTGCTCGGGTTGATATAAGTATAGCCCGGAATAGGTAACG  
ATCTAAAG

67:  
TTTTGTCGTCTTTCGGGATTTTGCTAAACAACCTTCAACAGTATAACCG  
ATATATT

68:  
CGGTCGCTGAGGCTGATCGTCACCCTCAGCAGCGAAAGACAGGGAGA  
TTTGTATCA

69:  
TCGCCTGATAAATTTACTTAGCCGGAACGAGGCGCAGACGGTAAATTG  
GGCTTGAG

70:  
ATGGTTTAATTCAGATTTTAAGAACTGGCTCATTATACCAGCAAAT  
AGCGAGAG

71:  
GCTTTTGCAAAGATGTTTAGACTGGATAGCGTCCAATACTGCAGACC  
GGAAGCAA

72:  
ACTCCAACAGGTCATTTGATAAGAGGTCATTTTTGCGGATGGGCTGAA  
AAGGTGGC

73: ACACCCTTTAGACGGGAGAATAACGCGAGGCGTTT

74: AACATATAAATACATAATAACTGA

75: TCAGTAGCCATCGATAGCAGCAGGTGGC

76: AAACAAAACGATTGGCCTTGACAAAGAAACCACCA

77: GTCGAGAAGTACCAGGCGGATTATTCAC

78: TCTGTATCAGACGTTAGTAAAAAGTGCC

79: TTTGCGGTGCAGGGAGTTAAATGAATTT

80: TCCATGTGTGTCGAAATCCGCATAGGGTTGAGTGT

81: CTTATGCACTTTAATCATTGTGACCTGC

82: AGTAAAAAGTTTTGCCAGAGGGAATTAC

83: TGCTCCTGGATTAGAGAGTACGGGTAAT

84: ATCAATTCTACTAA TAGTAGTAGCATTTGTGTAGGTAAAGAT

85: ATATAGAAGGCTTATCCGGTATTCTAAGCCGACAAAAGGTAA

86:  
AGTAATTCTGTCCACGAGCCAGTAATAAGAGAATATAAAGTAATCCAA  
TCGCAAGA

87:  
CAAAGAACGCGAGAATATAACTATATGTAAATGCTGATGCAATGAGC  
AAAAGAAGA

88:  
TGATGAAACAAACACAGAGGCGAATTATTCATTTCAATTACCACCGTA  
A  
89:  
GAAGGAGCGGAATTGTTTGAGTAACATTATCATTTTTCGCGGAATGCAAC  
AGTGCCAC  
90:  
GCTGAGAGCCAGCAAGGTGAGGCGGTCAGTATTAACACCGCCCCAGC  
CATTGCAAC  
91:  
AGGAAAAACGCTCAGCTGGTAATATCCAGAACAATATTACCGCGCGCT  
TAATGCGC  
92:  
CGCTACAGGGCGCGTCACGCTGCGCGTAACCACCACACCCGCGGCCG  
CT  
93:  
TGTTCCAGTTTGGACCCTTATAAATCAAAGAATAGCCCGAGCCTAAT  
GAGTGAGC  
94:  
TAACTCACATTAATGGAAGCATAAAGTGTAAGCCTGGGGTGCCATTC  
AGGCTGCG  
95:  
CAACTGTTGGGAAGTGCCGGAACCAGGCAAAGCGCCATTCGAATTTT  
TGTTAAAT  
96:  
CAGCTCATTTTTTACGTTAATATTTTGTAAATTCGCATTACTTTAAT  
97: GCATTTTGACGACGACAATAAAGCAAGCAAATCAG  
98: TTGGGTAAACTTTTTCAAATGGCAGAG  
99: AATCGCGTCAAGAAAACAAAAGCTTAGG  
100: TTAAAAATCATCATATTCCTGTTACAA  
101: AAAACAGGCAAATGAAAAATCTATTAAT  
102: CGGCCTTTGGAAATACCTACAAGAAGAT  
103: GTAGCGTACTATGGTTGCTTAAACTAT  
104: GCAAATAACAAGAGTCCACTAGGCAAGT  
105: ACGAGCCTGCGTTGCGCTCACGAAATCG  
106: CTTCTGGGGCGATCGGTGCGGACAACAT  
107: TTGTAAAACCAATAGGAACGCGGCACCG  
108: TCAAAGGGTGAGA AAGGCCGAGACAGATTTAAA  
109: CATCGTAGGAATCATTACCGCGCCCAATACAACATGTTCAGC  
110:  
TAATGCAGAACGCGATATTTAACAACGCCAACATGTAATTTAATATTT  
TAGTTAAT  
111:  
TTCATCTTCTGACCGTCTGAGAGACTACCTTTTTAACCTCCGTTAATTA  
CATTAA

112:  
CAATTTCAATTTGAAGGATTCGCCTGATTGCTTTGAATACCAAGATTATC  
AGATGAT  
113:  
GGCAATTCATCAATACTCGTATTAAATCCTTTGCCCGAACGTTAAAGC  
ATCACCTT  
114:  
GCTGAACCTCAAATCATTAAAAATACCGAACGAACCACCAGCTTTTGA  
CGCTCAAT  
115:  
CGTCTGAAATGGATAACATCACTTGCCTGAGTAGAAGAAGTCTGACGA  
GCACGTAT  
116:  
AACGTGCTTTCCTCAAGCGAAAGGAGCGGGCGCTAGGGCGCTTTAAA  
GAACGTGGA  
117:  
CTCCAACGTCAAAGGGCGAAAATCCTGTTTGATGGTGGTTCCTGCCCG  
CTTTCCAG  
118:  
TCGGGAAACCTGTCTGAAATTGTTATCCGCTCACAATTCCACGCCTCTT  
CGCTATT  
119:  
ACGCCAGCTGGCGAAGGAAGATCGCACTCCAGCCAGCTTTCCCATCAA  
AAATAATT  
120:  
CGCGTCTGGCCTTCCAAAAACAGGAAGATTGTATAAGCAAATTCAAAT  
CACCATCA  
121: AATCGCCCCTGTTTATCAACAGCCGTTTTTATTTT  
122: ATCATAGTAAATTTAATGGTTAATTGAG  
123: CAATAACTTACCTTTTTTAATTATCAAA  
124: TTCGACAATAATCCTGATTGTGGAGAAA  
125: ACATCGCATCAAACCCTCAATCAAACAA  
126: TAGTAATTATTTACATTGGCACCCCTAAA  
127: GGGAAGAGTTAGAATCAGAGCCTTTGAT  
128: CCCAGCAGGCGAAAAACCGTCAAAGGAA  
129: TCCTGTGGTGCCAGCTGCATTGGTTTGC  
130: CGGCCTCAAGGGGGATGTGCTAGCTGTT  
131: AAAGCCCCTGTAGCCAGCTTTACAGTAT  
132: ATATGATATTCAAC CGTTCTAGCTGATAAATCAGA  
133: AAGTACCGCACTCATCGAGAACAAGCAAATAGATAAGTCCTG  
134:  
AACAAAGAAAAATAAATAAAGCCAACGCTCAACAGTAGGGCTTTGAAA  
TACCGACCG  
135:  
TGTGATAAATAAGGAGACGCTGAGAAGAGTCAATAGTGAATTGGAAA  
CAGTACATA

136:  
AATCAATATATGTGATATACAGTAACAGTACCTTTTACATCGTTGGATT  
ATACTTC

137:  
TGAATAATGGAAGGTTTGAGGATTTAGAAGTATTAGACTTTACAATAT  
CTGGTCAG

138:  
TTGGCAAATCAACATATTAGTCTTTAATGCGCGAACTGATAGGATTCA  
CCAGTCAC

139:  
ACGACCAGTAATAAACGCAAATTAACCGTTGTAGCAATACTTGGGAGC  
TAAACAGG

140:  
AGGCCGATTAAAGGGACGGGGAAAGCCGGCGAACGTGGCGAGTATCA  
GGGCGATGG

141:  
CCCACTACGTGAACGAGAGAGTTGCAGCAAGCGGTCCACGCTAATGA  
ATCGGCCAA

142:  
CGCGCGGGGAGAGGCCGAGCTCGAATTCGTAATCATGGTCATGCAAG  
GCGATTAAG

143:  
TTGGGTAACGCCAGGTGCATCTGCCAGTTTGAGGGGACGACGCATCAA  
CATTAAAT

144:  
GTGAGCGAGTAACACATGTCAATCATATGTACCCCGTTGATAATTAA  
TGCCGGAG

145: TACCAGTTATCCCATCCTAATACGGGTATTAACC

146: TAGATTACGTTAAATAAGAATAAATTCT

147: CAGATGAAGTGAATAACCTTGGATAGCT

148: TAATACAGTTAGAACCTACCATTAACGT

149: GAATGGCGTTGAAAGGAATTGCAATAGA

150: GTCCATCAAGGGACATTCTGGTATTTTT

151: AGAGCTTGATTTTAGACAGGAAGAGTCT

152: TGGCCCTCATCACCCAAATCACCGATTT

153: CCGGGTACGGTTTGCGTATTGCACCGCC

154: CGTAACCGGTTTTCCAGTCAAGGATCC

155: AAAC TAGACCCGTCGGATTCTGGCGCAT

156: AGGGTAGCTATTTT TGAGAGATCTACAAAATCGTA

157: TCGGCTGTCTTTCCTTATCATTCCAAGATTACGAGCATGTAG

158:  
AAACCAATCAATAAAGCCTGTTTAGTATCATATGCGTTATACAAACAC  
CGGAATCA

159:  
TAATTA TAGAAAATTTCCCTTAGAATCCTTGAAAACATAGCCTTCTGT  
AAATCGT

160:  
CGCTATTAATTAATAATAAAGAAATTGCGTAGATTTTCAGGTTATCAA  
AATTATTT

161:  
GCACGTAAAACAGAGCACTAACAACTAATAGATTAGAGCCGTAGGAA  
GGTTATCTA

162:  
AAATATCTTTAGGAAAAGCGTAAGAATACGTGGCACAGACAACCAAC  
AGAGATAGA

163:  
ACCCTTCTGACCTGTTTATAATCAGTGAGGCCACCGAGTAAAACGGTA  
CGCCAGAA

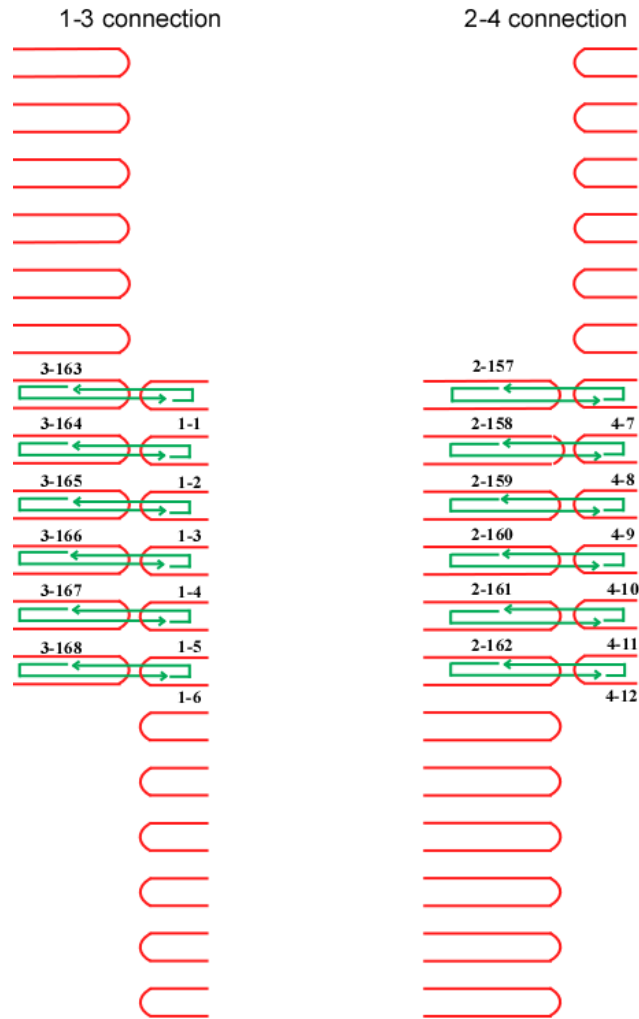
164:  
TCCTGAGAAGTGTTCACTAAATCGGAACCCTAAAGGGAGCCCAGTTTT  
TTGGGGTC

165:  
GAGGTGCCGTAAAGGTGAGACGGGCAACAGCTGATTGCCCTTGGCGC  
CAGGGTGGT

166:  
TTTTCTTTTCACCAAGCTTGCATGCCTGCAGGTCGACTCTAGCGACGTT  
GTAAAAC

167:  
GACGGCCAGTGCCAAATGGGATAGGTCACGTTGGTGTAGATGCCGTG  
GGAACAAAC

168:  
GGCGGATTGACCGTGGAGCAAACAAGAGAATCGATGAACGGTAGGCT  
ATCAGGTCA TTGCCTGAGAGTCT



**Figure S2.** Schematics of the 1-3 and 2-4 linkers of the 24-helix zigzag origami.

**Sequences of 1-3 linkers:**

1-1: TACAAAATCCAGAGCCTAATTTTTATAATCAGTGAACCCTCA  
 1-2: AAGCAGAGAAGCCCTTTTTAACACTAAATCGGAACTACCCAG  
 1-3: AATTATTGGGAAGGTAAATATGTGAGACGGGCAACCGCTGTA  
 1-4: GCCTCCCACCCAGAGCCACCACAGCTTGCATGCCTGTAGGATT  
 1-5: GTGCCCGGGTTCAGTGCCTTGAATGGGATAGGTCAACCGCGC  
 1-6: CAATAGGCATTTTCAGGGATAGGAGCAAACAAGAGATATACT

3-163: GGCCACCGAGTAAAACGGTACGCCAGAATCCTGAGAAGTGTT  
 TGCCAGTCAGTCGA  
 3-164: CCTAAAGGGAGCCCAGTTTTTTGGGGTCGAGGTGCCGTAAG  
 GAAAAGTCTGTGGG  
 3-165: AGCTGATTGCCCTTGGCGCCAGGGTGGTTTTTCTTTTCACCA  
 TGACGGACCGTTCT  
 3-166: CAGGTCGACTCTAGCGACGTTGTAAAACGACGGCCAGTGCCA  
 CGGAACCTCCGGCG



3-167: CGTTGGTGTAGATGCCGTGGGAACAAACGGCGGATTGACCGT  
AGTAACAGACTATG

3-168: AATCGATGAACGGTAGGCTATCAGGTCA TTGCCTGAGAGTCT  
GCAAGCCCTCCGCG

**Sequences of 2-4 linkers:**

2-157: TTATCATTCCAAGATTACGAGCATGTAG

AAACCAATCAATAATTAATTGGACTGCG

2-158: CATATGCGTTATACAAACACCGGAATCATAATTACTAGAAAA  
ACGAAGGATAGACC

2-159: CTTGAAAACATAGCCTTCTGTAAATCGTCGCTATTAATTAAT  
TTGACAACAGAAAC

2-160: GTAGATTTTCAGGTTATCAAAATTATTTGCACGTAAAACAGA  
ACATTCATTACAAA

2-161: TAGATTAGAGCCGTAGGAAGGTTATCTAAAATATCTTTAGGA  
CTATTATTTGGCGG

2-162: CGTGGCACAGACAACCAACAGAGATAGAACCCTTCTGACCTG  
ATTCCCAGTCGGGT

4-7: TATCGGTTCCAAAAGGAGCCTTCGGCTGTCTTTCCGCAGCTT

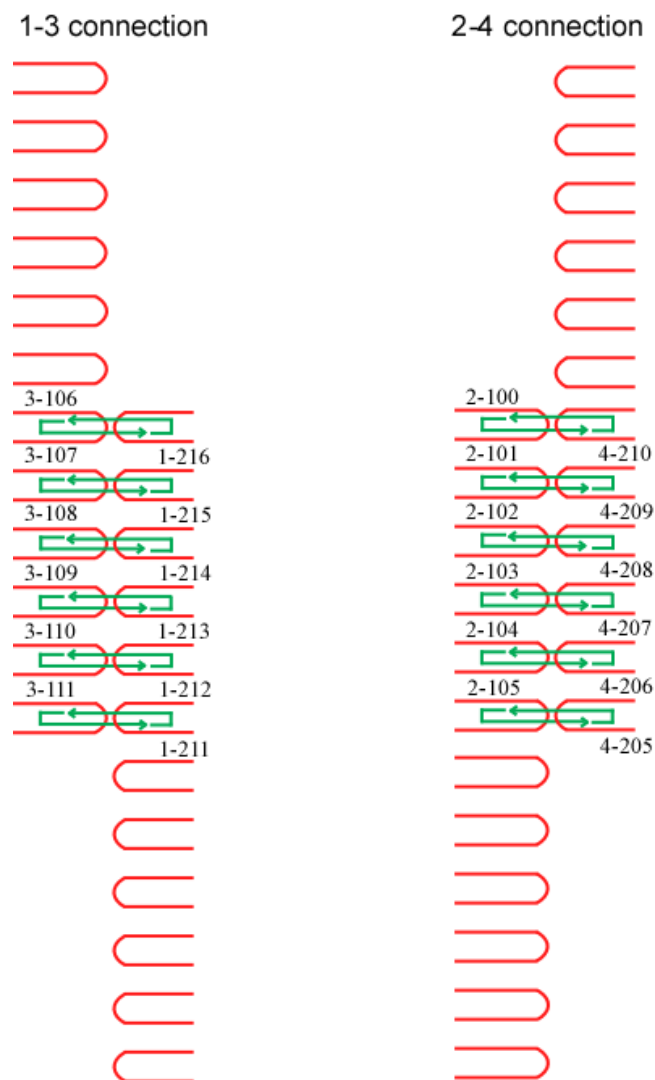
4-8: CACCAACTACGTAATGCCACTAGCCTGTTTAGTATATGGGCC

4-9: GAACCGGCATCAAGAGTAATCTTTCCCTTAGAATCAGGACAC

4-10: ACTAATGGATTTAGGAATACCAATAAAGAAATTGCTTTAAAC

4-11: AGTCAGAGGTCTTTACCCTGAGCACTAACAACTAAATCCAAT

4-12: ATTCTGCCCATATAACAGTTGAAAGCGTAAGAATAGCAGGCG



**Figure S3.** Schematics of the 1-3 and 2-4 linkers of the 24-helix planar origami.

**Sequences of 1-3 linkers:**

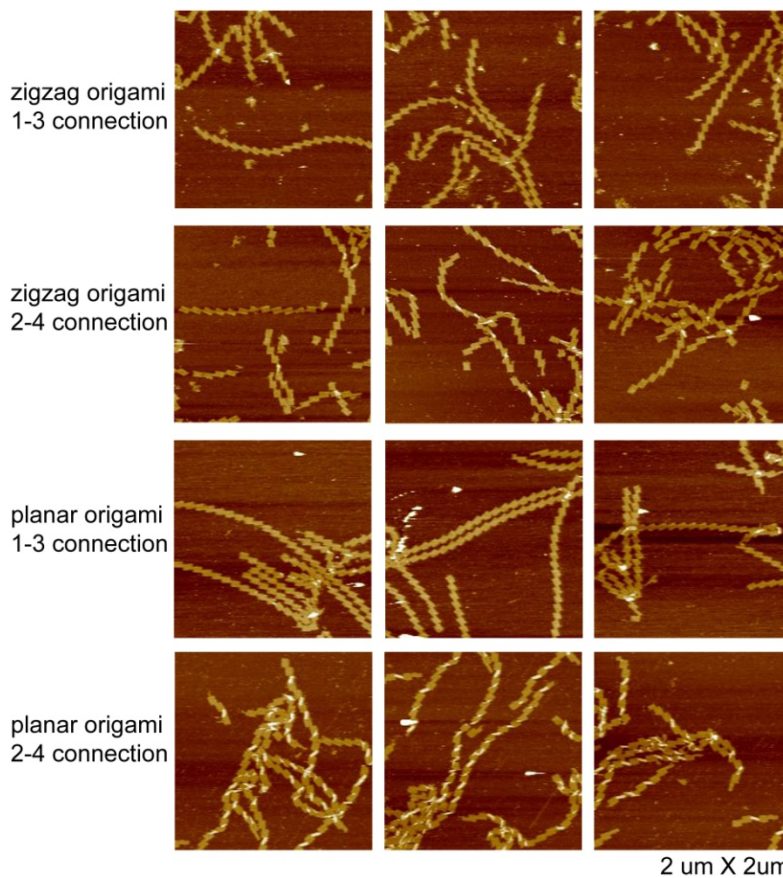
1-211: CAACATGTATTGCTGA ATATAATG ACCAGTAA  
 1-212: CCCCTCAAATCGTCA TAAATATT AATCAATA  
 1-213: AATCTACGACCAGTCA GGACGTTG TTCATCAA  
 1-214: GAACCGAAAGGCGCAG ACGGTCAA ATTAATTA  
 1-215: CGGAACGAACCCTCAG CAGCGAAA CGCGAGAA  
 1-216: ACAGTTTCTGGGATTT TGCTAAAC CGACAAA

3-106: GGTAAGTAGAGAATA TAAAGTAC AACTTTCA  
 3-107: AACTTTTATCGCAAG ACAAAGAA GACAGCAT  
 3-108: CATTAAACACATCAAG AAAACAAA TCATAAGG  
 3-109: TATAATCCTATCAGAT GATGGCAA GGAAGAAA  
 3-110: TCTGGTCACAAATATC AAACCCTC CATTGAAT  
 3-111: TAAAAGGGATTCACCA GTCACACG CTGTAGCT

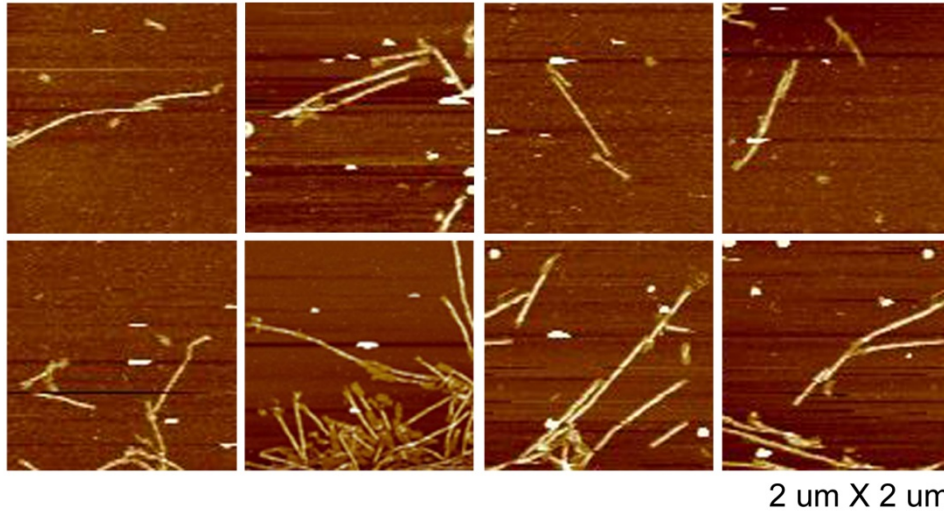
**Sequences of 2-4 linkers:**

2-100: TAGCCCGGCCGTCGAG AGGGTTGA GGTTGTAC  
2-101: TCATTAAATGATATTC ACAAACAA GATGAACG  
2-102: GCGACAGATCGATAGC AGCACCGT GTAATGGG  
2-103: GCAACATAGTAGAAAA TACATACA TGTA AAC  
2-104: AATTA ACTACAGGGAA GCGCATT A CGGTTTGC  
2-105: GGTATTCTAAATCAGA TATAGAAG CGATGGCC

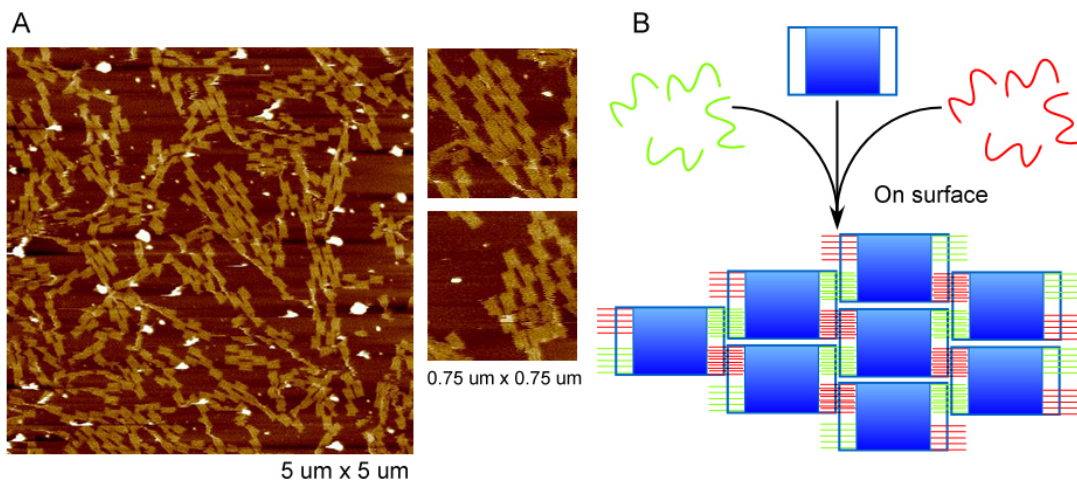
4-205: CACTACGTAAACCGTC TATCAGGG GCTTATCC  
4-206: GTATTGGGAACGCGCG GGGAGAGG GACGGGAG  
4-207: GACGGCCATTCCCAGT CACGACGT TAAAGGTG  
4-208: ATAGGTCAAAACGGCG GATTGACC AATCAGTA  
4-209: GTAATCGTAGCAAACA AGAGAATC ATAAATCC  
4-210: CAAAACAAGCATAAA GCTAAATC TATAAGTA



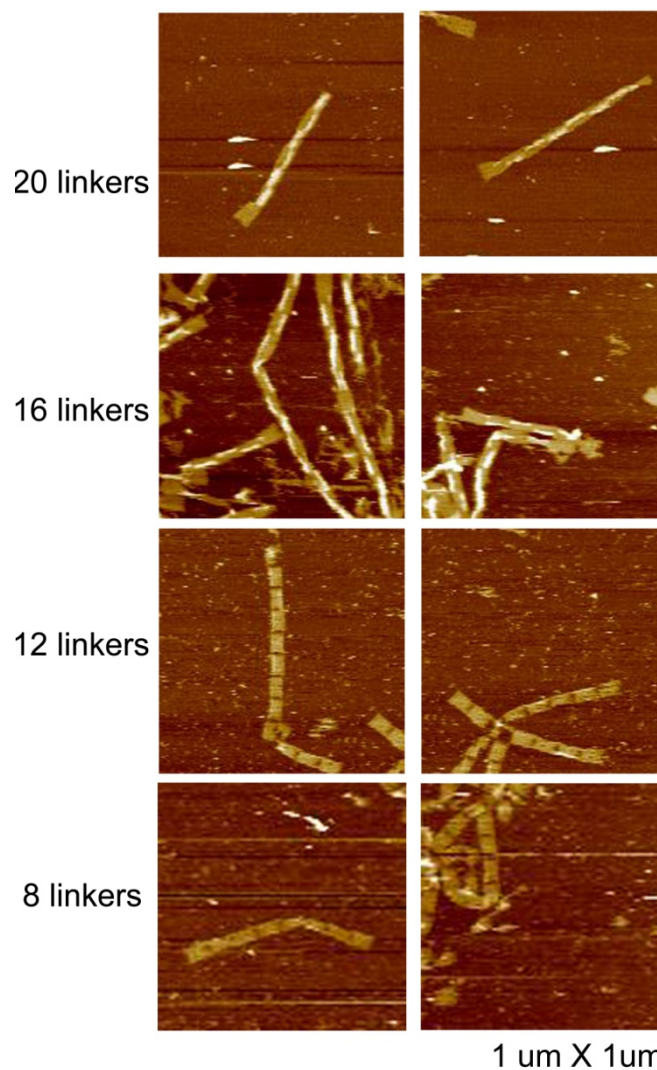
**Figure S4.** Additional AFM images of the stair-like 1D arrays formed by zigzag origami and planar origami.



**Figure S5.** Additional AFM images of the DNA origami tubes assembled from zigzag origami in solution. The linker strand connection design is the same as found in Figure 3.3 of the main text.



**Figure S6.** Surface-mediated assembly of small pieces of 2D arrays of zigzag DNA origami tiles. A: AFM images of the resulting 2D arrays. B: Schematic illustrating the inter-tile connections.



**Figure S7.** Additional AFM images of the unique structures formed from varying the numbers of linkers, as shown in Figure 3.4 of the main text.

**Sequences of 8, 12, 16, 20 linkers of zigzag origami:**

8 linkers:

8-1: TACAAAATCCAGAGCCTAATTAATGGGATAGGTCA

8-2: AAGCAGAGAAGCCCTTTTAAAGGAGCAAACAAGAG

8-11: AGTCAGAGGTCTTTACCCTGATCGGCTGTCTTTCC

8-12: ATTCTGCCCATATAACAGTTGAGCCTGTTTAGTAT

8-157:

TTATCATTCCAAGATTACGAGCATGTAGAAACCAATCAATAACTATTA

T

8-158:

CATATGCGTTATACAAACACCGGAATCATAATTACTAGAAAAATTCCC

A

8-167:  
CGTTGGTGTAGATGCCGTGGGAACAAACGGCGGATTGACCGTTGCCAG  
T

8-168:  
AATCGATGAACGGTAGGCTATCAGGTCATTGCCTGAGAGTCTGAAAAG  
T

12 linkers:

12-1: TACAAAATCCAGAGCCTAATTAGCTTGCATGCCTG

12-2: AAGCAGAGAAGCCCTTTTTAAAATGGGATAGGTCA

12-3: AATTATTGGGAAGGTAAATATGGAGCAAACAAGAG

12-10: ACTAATGGATTTAGGAATACCTCGGCTGTCTTTCC

12-11: AGTCAGAGGTCTTTACCCTGAAGCCTGTTTAGTAT

12-12: ATTCTGCCCATATAACAGTTGTTTCCCTTAGAATC

12-157:

TTATCATTCCAAGATTACGAGCATGTAGAAACCAATCAATAAACATTC  
A

12-158:

CATATGCGTTATACAAACACCGGAATCATAATTACTAGAAAACCTATTA  
T

12-159:

CTTGAAAACATAGCCTTCTGTAAATCGTCGCTATTAATTAATATTCCCA

12-166:

CAGGTGCGACTCTAGCGACGTTGTAAAACGACGGCCAGTGCCATGCCA  
GT

12-167:

CGTTGGTGTAGATGCCGTGGGAACAAACGGCGGATTGACCGTGAAAA  
GT

12-168:

AATCGATGAACGGTAGGCTATCAGGTCATTGCCTGAGAGTCTTGACGG  
A

16 linkers:

16-1: TACAAAATCCAGAGCCTAATTGTGAGACGGGCAAC

16-2: AAGCAGAGAAGCCCTTTTTAAAGCTTGCATGCCTG

16-3: AATTATTGGGAAGGTAAATATAATGGGATAGGTCA

16-4: GCCTCCCACAGAGCCACCACGGAGCAAACAAGAG

16-9: GAACCGGCATCAAGAGTAATCTCGGCTGTCTTTCC

16-10: ACTAATGGATTTAGGAATACCAGCCTGTTTAGTAT

16-11: AGTCAGAGGTCTTTACCCTGATTTCCCTTAGAATC

16-12: ATTCTGCCCATATAACAGTTGAATAAAGAAATTGC

16-165:

AGCTGATTGCCCTTGGCGCCAGGGTGGTTTTTCTTTTCACCATGCCAGT

16-166:

CAGGTGCGACTCTAGCGACGTTGTAAAACGACGGCCAGTGCCAGAAAA  
GT

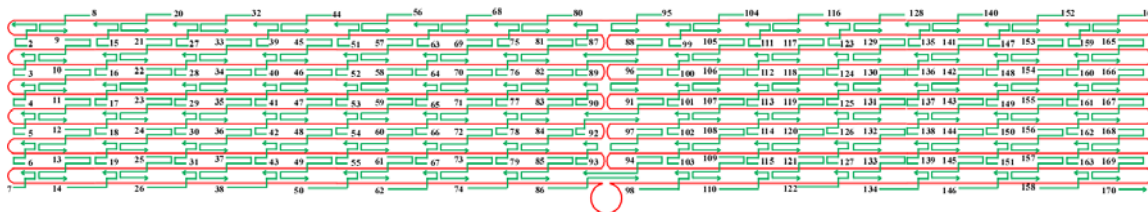
16-167:  
CGTTGGTGTAGATGCCGTGGGAACAAACGGCGGATTGACCGTTGACG  
GA  
16-168:  
AATCGATGAACGGTAGGCTATCAGGTCATTGCCTGAGAGTCTCGGAAC  
C  
16-157:  
TTATCATTCCAAGATTACGAGCATGTAGAAACCAATCAATAATTGACA  
A  
16-158:  
CATATGCGTTATACAAACACCGGAATCATAATTACTAGAAAAACATTC  
A  
16-159:  
CTTGAAAACATAGCCTTCTGTAAATCGTCGCTATTAATTAATCTATTAT  
16-160:  
GTAGATTTTCAGGTTATCAAATTATTTGCACGTAAAACAGAATTCCC  
A

20 linkers:

20-1: TACAAAATCCAGAGCCTAATT CACTAAATCGGAAC  
20-2: AAGCAGAGAAGCCC TTTTAA GTGAGACGGGCAAC  
20-3: AATTATTGGGAAGG TAAATAT AGCTTGCATGCCTG  
20-4: GCCTCCCACCAGAG CCACCAC AATGGGATAGGTCA  
20-5: GTGCCCCGGGGTCAG TGCCTTG GGAGCAAACAAGAG  
20-8: CACCAACTACGTAA TGCCACT TCGGCTGTCTTTCC  
20-9: GAACCGGCATCAAG AGTAATC AGCCTGTTTAGTAT  
20-10: ACTAATGGATTTAG GAATACC TTTCCCTTAGAATC  
20-11: AGTCAGAGGTCTTT ACCCTGA AATAAAGAAATTGC  
20-12: ATTCTGCCCATATA ACAGTTG GCACTAACAACCTAA  
20-157: TTATCATTCCAAGATTACGAGCATGTAG AAACCAATCAATAA  
ACGAAGG  
20-158: CATATGCGTTATACAAACACCGGAATCA TAATTACTAGAAAA  
TTGACAA  
20-159: CTTGAAAACATAGCCTTCTGTAAATCGT CGCTATTAATTAAT  
ACATTCA  
20-160: GTAGATTTTCAGGTTATCAAATTATTT GCACGTAAAACAGA  
CTATTAT  
20-161: TAGATTAGAGCCGTAGGAAGGTTATCTAAAATATCTTTAGGA  
ATTCCA  
20-164: CCTAAAGGGAGCCCAGTTTTTTGGGGTC GAGGTGCCGTAAAG  
TGCCAGT  
20-165: AGCTGATTGCCCTTGGCGCCAGGGTGGT TTTTCTTTTCACCA  
GAAAAGT  
20-166: CAGGTCGACTCTAGCGACGTTGTAAAAC GACGGCCAGTGCCA  
TGACGGA



20-167: CGTTGGTGTAGATGCCGTGGGAACAAAC GCGGGATTGACCGT  
CGGAACC  
20-168: AATCGATGAACGGTAGGCTATCAGGTCA TTGCCTGAGAGTCT  
AGTAACA



**Figure S8.** Schematic of the 12-helix zigzag origami structure, helper strand position and numbering assignment. Dangling loop represents unpaired sequences.

2: AACGCAAGATATAGAAGGCTTTAGCAAGCAAATCA  
 3: CATA CATAGACACCACGGAATTA AAAAGA  
 4: AGGAGCCGGCTTTTGATGATATAAGCGT  
 5: TCATTCATTTAATTGTATCGGCTCCAAA  
 6: GGAAGCAGTGAATAAGGCTTGAAGCTGC  
 7: AACTCCAACAGGTCCCAGACC  
 8: TCATCGTAGGAATCATTACCGCGCCCAAATCCGGTATTCTAA  
 9:  
 GAACGCGAGGCGTTAAAATACATACATAAAGGTGGCAACATAAAGTT  
 TATTTTGTC  
 10:  
 ACAATCAATAGAAAAGCGCAGTCTCTGAATTTACCGTTC CAGCAGGAG  
 TGTACTGG  
 11:  
 TAATAAGTTTTAACTTCACGTTGAAAATCTCCAAAAAAAAGGTTTATC  
 AGCTTGCT  
 12:  
 TTCGAGGTGAATTTGATATTCATTACCCAAATCAACGTAACACCCTGA  
 CGAGAAAC  
 13:  
 ACCAGAACGAGTAGCGGTTTTAATTCGAGCTTCAAAGCGAAAGGATT  
 AGAGAGTA  
 14: CCTTTAATTGCTCCTTTTGATAAGAGGTAAGACTT  
 15: AACGTAGTTAGCGAACCTCCAGCCGTTTTTATTT  
 16: AATGGAAATTCATATGGTTTAGTTAGCA  
 17: TAATTTTGGGGTCAGTGCCTTAAGCCAG  
 18: AGAACCGCTTAAACAGCTTGACGAATAA  
 19: CAAATATTAAATTGGGCTTGACTTGACA  
 20: CAAGTACCGCACTCATCGAGAACAAGCAGACTTGCGGGAGGT  
 21:  
 TTTGAAGCCTTAAAATGATTAAGACTCCTTATTACGCAGTATCCAGCG  
 CCAAAGAC  
 22:  
 AAAAGGGCGACATTATATTCACAAACAAATAAATCCTCATTAGAGTAA  
 CAGTGCCC

23:  
GTATAAACAGTTAAGAATAGAAAGGAACAACCTAAAGGAATTGTACCG  
ATAGTTGCG

24:  
CCGACAATGACAACAGGCTGGCTGACCTTCATCAAGAGTAATGATGGT  
TTAATTC

25:  
AACTTTAATCATTGGCATCAAAAAGATTAAGAGGAAGCCCGACATTTT  
TGCGGATG

26: GCTTAGAGCTTAATTGCTGAATATAATGAAGCAA  
27: AACTGGCTCAAGATTAGTTGCAACGGGTATTAAAC  
28: GGCCTTGCAACCGATTGAGGGCCAAAAG  
29: GGAGTGATGCCCCCTGCCTATGACGATT  
30: GGCGCATAACCATCGCCACGTTTCAGC  
31: GCGGATTTGAATTACCTTATGCAGACCA  
32: ATCGGCTGTCTTTCCTTATCATTCCAAGTATTTTGCACCCAG  
33:  
CTACAATTTTATCCCCGAGGAAACGCAATAATAACGGAATACAGGGA  
AGGTAATA

34:  
TTGACGGAAATTATAGCATTGACAGGAGGTTGAGGCAGGTCATTCGGA  
ACCTATTA

35:  
TTCTGAAACATGAATGGGATTTTGCTAAACAACCTTCAACAGCATAAC  
CGATATAT

36:  
TCGGTCGCTGAGGCCTTTGAAAGAGGACAGATGAACGGTGTACGATTT  
TAAGAACT

37:  
GGCTCATTATACCAAGGTCTTTACCCTGACTATTATAGTCAGCTGTAGC  
TCAACAT

38: GTTTTAAATATGCAACTAAAGTACGGTGATAAATC  
39: AAGGAAATGAATCTTACCAACGAAACCAATCAATA  
40: CGCCGCCTCATTAAAGGTGAATTACCAG  
41: TTCTGTAAGTATTAAGAGGCTCCAGAGC  
42: TGACCAATTGCAGGGAGTTAAATGAATT  
43: AAAAATCGTCAGGACGTTGGGACCGAAC  
44: ATATCCCATCCTAATTTACGAGCATGTAGCTAACGAGCGTCT  
45:  
TTCCAGAGCCTAATAGAAAAGTAAGCAGATAGCCGAACAAAGTTATC  
ACCGTCACC

46:  
GACTTGAGCCATTTACCCTCAGAGCCGCCACCAGAACCACCAGAGACT  
CCTCAAGA

47:  
GAAGGATTAGGATTGTTTTGTCGTCTTTCCAGACGTTAGTAAAGGCCG  
CTTTTGCG

48:  
GGATCGTCACCCTCCGAGGCGCAGACGGTCAATCATAAGGGAAAGAA  
AAATCTACG

49:  
TTAATAAAACGAACTTAAACAGTTCAGAAAACGAGAATGACCTCTGG  
AAGTTTCAT

50: TCCATATAACAGTTGATTCCCAATTCTGCCCCCTC

51: CTTTTTATTGCCAGTTACAAAGAACAAGAAAAATA

52: AGCCACCGGGAATTAGAGCCACGAAGCC

53: ATCTAAAAGCGGGGTTTTGCTCCCTCAG

54: GCCGGAAAGCAGCGAAAGACACGTAACG

55: AAATGCTTAACGGAACAACATTTACTTA

56: GCCTGTTTATCAACAATAGATAAGTCCTATAAACAGCCATAT

57:  
TATTTATCCCAATCAACAATGAAATAGCAATAGCTATCTTACGCAAAA  
TCACCAGT

58:  
AGCACCATTACCATCTCAGAGCCGCCACCCTCAGAACCGCCACAGTAC  
CAGGCGGA

59:  
TAAGTGCCGTCGAGGCATTCCACAGACAGCCCTCATAGTTAGGCATCG  
GAACGAGG

60:  
GTAGCAACGGCTACTGTGTCGAAATCCGCGACCTGCTCCATGTATTAC  
AGGTAGAA

61:  
AGATTCATCAGTTGGCGGAATCGTCATAAATATTCATTGAATCGAACG  
AGTAGATT

62: TAGTTTGACCATTAGATACATTTTCGCAATAGCGTC

63: AGCAAGACAAATAAGAAACGACTAATGCAGAACGC

64: CGCCTCCTAGCAAGGCCGGAATAATAAG

65: GCCTGTAAGGGTTGATATAAGCCGGAAC

66: GATAAATAGAGGCTTTGAGGACTACAAC

67: CAATACTAGATTTAGGAATACATCGCCT

68: AGACGACGACAATAAACAACATGTTTCAGTTTTTTGTTTAACG

69:  
TCAAAAATGAAAATTAACCCACAAGAATTGAGTTAAGCCCAAACGTC  
ACCAATGAA

70:  
ACCATCGATAGCAGATCAAAATCACCGGAACCAGAGCCACCATATAG  
CCCGGAATA

71:  
GGTGTATCACCGTATAACACTGAGTTTCGTCACCAGTACAACTAAAG  
ACTTTTTC

72:  
ATGAGGAAGTTTCCGAAACAAAGTACAACGGAGATTTGTATCCACATT  
CAACTAAT

73:  
GCAGATACATAACGGGGTAATAGTAAAATGTTTAGACTGGAATGGT  
CAATAACCT

74: GTTTAGCTATATTTTCATTTGGGGCGCGAAGTTTT

75: AGAGAGAAGCAGCCTTTACAGAAGTAATTCTGTCC

76: TTTCATACACCGTAATCAGTATAATATC

77: TGTACCGCTCAGGAGGTTTAGGCCATCT

78: CAAGCGCATTAACGGGTAAAGAACCCA

79: GCCAGAGCCAAAAGGAATTACATTATAC

80: AGAGAATATAAAGTACCGACAAAAGGTAAGAGAATAACATAA

81:  
AAACAGGGAAGCGCTGAACAAAGTCAGAGGGTAATTGAGCGCGCGAC  
AGAATCAAG

82:  
TTTGCCTTTAGCGTTTCGGTCATAGCCCCCTTATTAGCGTTTTACCGCC  
ACCCTCA

83:  
GAACCGCCACCCTCTCATTTTCAGGGATAGCAAGCCCAATAGATACGT  
AATGCCAC

84:  
TACGAAGGCACCAACTAAAACACTCATCTTTGACCCCCAGCGGAGGC  
ATAGTAAGA

85:  
GCAAACTATCATACCAAATAGCGAGAGGCTTTTGCAAAGAGCTG  
AAAAGGTGG

86: CATCAATTCTACTAATAGTAGTAGCATTGTGTAGGTAAAGA

87: AACACCCATTAGACGGGAGAATCGAGCCAGTAATA

88:  
ATTAATTACATTTACTGAGCAAAGAAGATGATGAAACAACTTAACT  
G

89: CGGCATTCAGACTGTAGCGCGTCAATATCTGGTCA

90: ACCACCCAGAACCGCCACCCTTTTTCAT

91:  
TTTTATAATCAGTGGGATTTTAGACAGGAACGGTACGCCAGACAGAGC  
C

92: GAATACACCTAAAACGAAAGATGAGAGAGTTGCAG

93: ATAAAAAACCTCGTTTACCAGGCAAAA

94:  
CGGCACCGCTTCTGGACAGTATCGGCCTCAGGAAGATCGCACGACGA  
CG

95: CCAACATGTAATTTAGGCAGAGGCATTTATCAAGAAAACAAA  
96:  
GTTGGCAAATCAACTGCTGAACCTCAAATATCAAACCCTCAAATCCTG  
AGAAGTGT  
97:  
CAAGCGGTCCACGCCAGCTGATTGCCCTTACCCGCCTGGCCCTCCAGC  
CAGCTTTC  
98: TTCAAAGGGTGAGAAAGGCCGGAGACATTTGAGG  
99: CAATTACACAATTTCAATTTGACATATTTAACAACG  
100: ATCACCTAGTTGAAAGGAATTTTCATTT  
101: ATTAAGAGGCCACCGAGTAACTAAAGC  
102: CGGGCAATGGTTTGCCCCAGCGAGGCCG  
103: GGACGACGTGCCGGAACCAGAGTGAGA  
104: TCAACAGTAGGGCTTAATTGAGAATCGCATTACCTTTTTTAA  
105:  
TGGAACAGTACATAGTTACAAAATCGCGCAGAGGCCGAATTAGAGGA  
AGGTTATCT  
106:  
AAAATATCTTTAGGCGCTGAGAGCCAGCAGCAAATGAAAATAAGAG  
TCTGTCCAT  
107:  
CACGCAAATTAACCCGTTAGAATCAGAGCGGGAGCTAAACAGAGGCCG  
AAAATCCTG  
108:  
TTTGATGGTGGTTCGGGCGCCAGGGTGGTTTTTCTTTTCACCGCAAAGC  
GCCATTC  
109:  
GCCATTCAGGCTGCGGGCGCATCGTAACCGTGCATCTGCCAGGTCAAA  
TCACCATC  
110: AATATGATATTCAACCGTTCTAGCTGATACGTTGG  
111: AATACCAAATCAATATATGTTATAAAGCCAACGC  
112: AGTGCCAAGCACTAACAACACTATGCTTTG  
113: CTTTCCTGTTGTAGCAATACTCTGCAAC  
114: GCGTATTCGAAATCGGCAAATAACGTG  
115: TGTAGATGCAACTGTTGGGAAGCGGTTT  
116: TCATATGCGTTATACAAATTCTTACCAGGAGTGAATAACCTT  
117:  
GCTTCTGTAAATCGGGGAGAAACAATAACGGATTTCGCCTGATATAGAT  
TAGAGCCG  
118:  
TCAATAGATAATACGAGGTGAGGCGGTCAGTATTAACACCGCTCTTTG  
ATTAGTAA  
119:  
TAACATCACTTGCCGTACTATGGTTGCTTTGACGAGCACGTATCCCTTA  
TAAATCA

120:  
AAAGAATAGCCCGATAATGAATCGGCCAACGCGCGGGGAGAGGGGCG  
ATCGGTGCG

121:  
GGCCTCTTCGCTATCGGCGGATTGACCGTAATGGGATAGGTCAAATTA  
ATGCCGGA

122: GAGGGTAGCTATTTTTGAGAGATCTACATCCGTGG

123: TTACATCTCGCTATTAATTAAGCCTGTTTAGTA

124: TAAACAATTTGAGGATTTAGGTACCTT

125: AGGGCGCTGAGTAGAAGAACTCAGAAGA

126: GCTGCATGATAGGGTTGAGTGCCGCTAC

127: GAACAAATACGCCAGCTGGCGCGTGCCA

128: TAAACACCGGAATCATAATTACTAGAAATTTCCCTTAGAAT

129:  
CCTTGAAAACATAGTTTAAACGTCAGATGAATATACAGTAACAAAGTAT  
TAGACTTT

130:  
ACAAACAATTCGACCCATTAATAATACCGAACGAACCACCAGCAAAC  
TATCGGCCT

131:  
TGCTGGTAATATCCAACCACCACACCCGCCGCGCTTAATGCGTTGTTC  
CAGTTTGG

132:  
AACAAGAGTCCACTCTGCCCGCTTCCAGTCGGGAAACCTGTAAAGGG  
GGATGTGC

133:  
TGCAAGGCGATTAATGTGAGCGAGTAACAACCCGTCGGATTCAAGGCT  
ATCAGGTC

134: ATTGCCTGAGAGTCTGGAGCAAACAAGATCATCAA

135: TTCAGGCGATAGCTTAGATTGCGTTAAATAAGAA

136: AACATCGAACTCGTATTAAATCGTAGAT

137: TGCGCGTAGAACAATATTACCGCCCTAA

138: GCGCTCAATTAAGAACGTGGGTCACGC

139: CATTAAAGTTGGGTAACGCCATTGCGTT

140: TTGAAATACCGACCGTGTGATAAATAAGAAGACGCTGAGAAG

141:  
AGTCAATAGTGAATTGCACGTAAAACAGAAATAAAGAAATTGCCTTTG  
CCCGAACG

142:  
TTATTAATTTTAAACTATTAGTCTTTAATGCGCGAACTGATAGCCAGCC  
ATTGCAA

143:  
CAGGAAAACGCTCGGGCGCTAGGGCGCTGGCAAGTGTAGCGACTCC  
AACGTCAAA

144:  
GGGCGAAAAACCGTGCCTAATGAGTGAGCTAACTCACATTAAGGGTTT  
TCCCAGTC  
145:  
ACGACGTTGTAAAATCGCGTCTGGCCTTCCTGTAGCCAGCTTGAATCG  
ATGAACGG  
146: TAATCGTAAAACCTAGCATGTCAATCATACCATCAA  
147: AATTATTTTATCAAATCATACTAAATTTAATGGT  
148: TGAATGGAGTTTGAGTAACATATATCAA  
149: AAGGAGCATGGAAATACCTACATATTTT  
150: CTGGGGTCTATCAGGGCGATGAAAGCGA  
151: AAATAATCGACGGCCAGTGCCGTAAAGC  
152: TATATTTTAGTTAATTTTCATCTTCTGACGGTCTGAGAGACTA  
153:  
CCTTTTTAACCTCCCTGAATAATGGAAGGGTTAGAACCTACCTATCATT  
TTGCGGA  
154:  
ACAAAGAAACCACCGAAAGCGTAAGAATACGTGGCACAGACAATTTT  
GACGCTCAA  
155:  
TCGTCTGAAATGGAGGCGAACGTGGCGAGAAAGGAAGGGAAGGCCCA  
CTACGTGAA  
156:  
CCATCACCCAAATCCACAACATACGAGCCGGAAGCATAAAGTAAGCT  
TGCATGCCT  
157:  
GCAGGTCGACTCTATCAGCTCATTTTTTTAACCAATAGGAACGTGTACC  
CCGGTTGA  
158: TAATCAGAAAAGCCCCAAAAACAGGAAGAAATTTT  
159: TATACTTGGCTTAGGTTGGGTAAAACCTTTTTCAA  
160: CTGACCTAGAAGGAGCGGAATTTTGGAT  
161: GAAAGCCTTATTTACATTGGCAACCCTT  
162: AATTCAAAGTTTTTTGGGGTTGACGGG  
163: TGTTAAAGAGGATCCCCGGGTCGCTCAC  
164: AATCCAATCGCAAGACAAAGAACGCGAGTATATAACTATATG  
165:  
TAAATGCTGATGCATGGCAATTCATCAATATAATCCTGATTGTATCATC  
ATATTCC  
166:  
TGATTATCAGATGAAAAGGGACATTCTGGCCAACAGAGATAGAGATT  
CACCAGTCA  
167:  
CACGACCAGTAATACCCTAAAGGGAGCCCCCGATTTAGAGCTCGAGG  
TGCCGTAAA



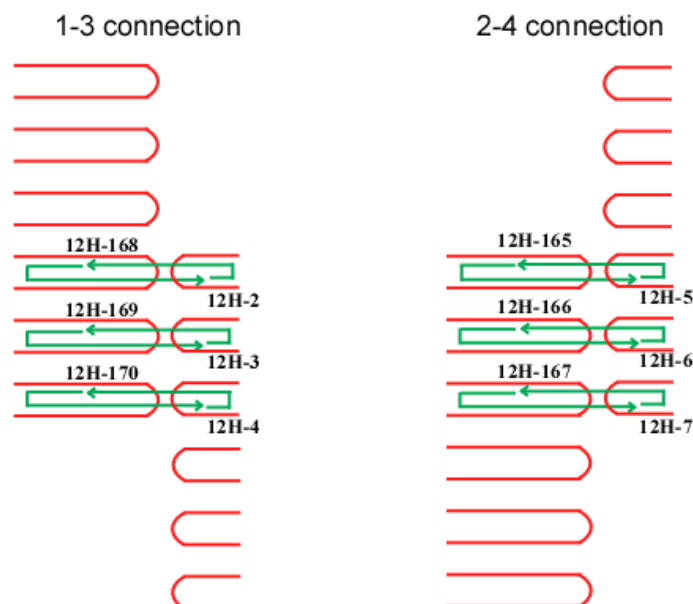
168:

GCACTAAATCGGAATAGCTGTTTCCTGTGTGAAATTGTTATCACCGAG  
CTCGAATT

169:

CGTAATCATGGTCAACGTTAATATTTTGTAAAATTTCGCATTATTGTAT  
AAGCAA

170: TATTTAAATTGTAA



**Figure S9.** Schematics of the 1-3 and 2-4 linkers of the 12-helix zigzag origami tile.

**Sequences of linkers:**

12H-2: AAGGCTTTAGCAAGCAAATCACCTAAAGGGAGCC

12H-3: ACGGAATTAAGAAACGCAATAGCTGTTTCCTGT

12H-4: GATGATATAAGCGTCATACATACGTTAATATTTTG

12H-5: GTATCGGCTCCAAAAGGAGCCAATCCAATCGCAAG

12H-6: AGGCTTGAAGCTGCTCATTCATGGCAATTCATCAA

12H-7: ACAGGTCCCAGACCGGAAGCAAAAAGGGACATTCTG

12H-165:

ACAAAGAACGCGAGTATATAACTATATGTAAATGCTGATGCATTTAAT  
T

12H-166:

TATAATCCTGATTGTATCATCATATTCCTGATTATCAGATGAGTGAATA

12H-167:

GCCAACAGAGATAGAGATTCACCAGTCACACGACCAGTAATAAACTC  
CA

12H-168:

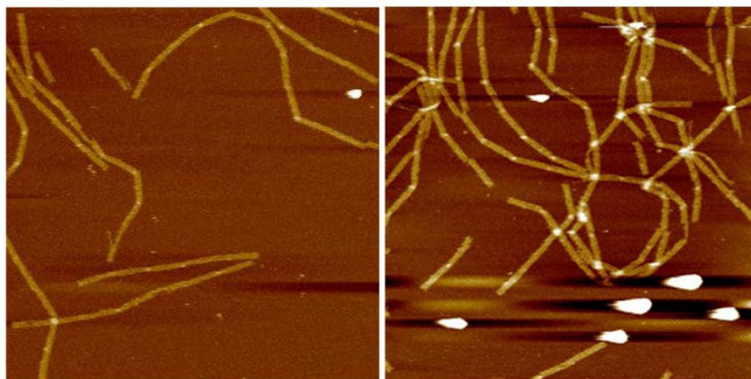
CCCGATTTAGAGCTCGAGGTGCCGTAAAGCACTAAATCGGAAGATATA  
G

12H-169:

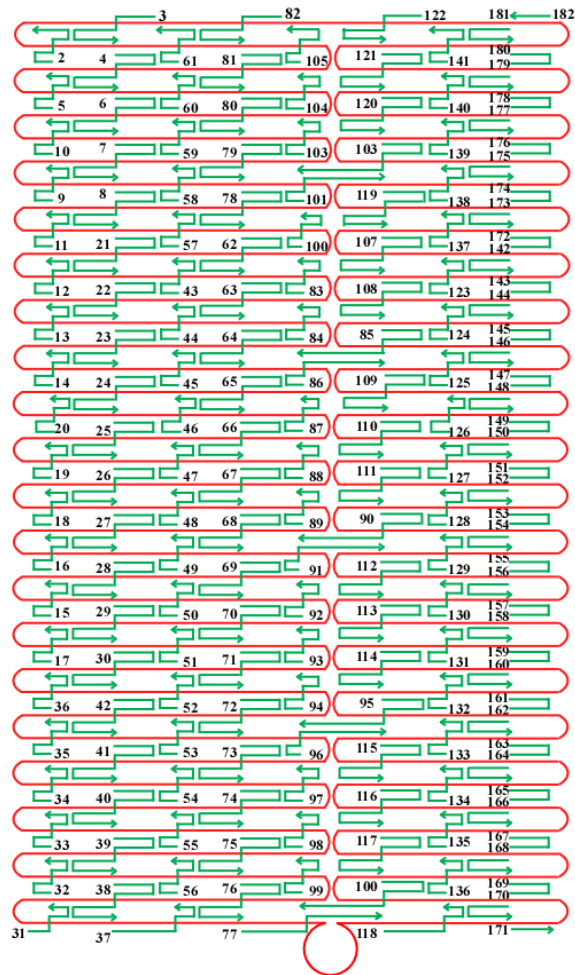
GTGAAATTGTTATCACCGAGCTCGAATTCGTAATCATGGTCAAGACAC  
C

12H-170:

TTAAAATTCGCATTATTGTATAAGCAAATATTTAAATTGTAAGGCTTTT



**Figure S10.** Additional AFM images of the 1D chains formed from 12-helix zigzag origami tiles with the linker strand connection design illustrated in Figure 3.5 of the main text.



**Figure S11.** Schematic of the 40-helix zigzag origami structure, helper strand position and numbering assignment. Dangling loop represents unpaired sequences.

2: GACAATAAAGCCTGTTTAGTAATAATTACTAGAAA

3: GCGTTAAATAAGAATAAACACCGGAATCTCATATGCGTTATA

4:

CAAATTCTTACCAGACCGACAAAAGGTAAAGTAATTCTGTCCCTAATG  
CAGAACGC

5: TTTATTTAACAACATGTTTCAGAGACGAC

6:

GCCTGTTTATCAACCAAGTACCGCACTCATCGAGAACAAGCAATTACC  
GCGCCCAA

7:

TAGCAAGCAAATCACTACAATTTTATCCTGAATCTTACCAACTTGCCA  
GTTACAAA

8:

ATAAACAGCCATATTTAACTGAACACCCTGAACAAAGTCAGATAACCC  
ACAAGAAT

9: TGAGCGCTTCCAGAGCCTAATGCTAACG

10: AGCGTCTTCATCGTAGGAATCAGCCGTT  
11: AGACTCCTAATATCAGAGAGAGGGTAAT  
12: AAATTATTTATTACGCAGTATATGATTA  
13: CGGCATTTTCATTAAAGGTGAATTGACGG  
14: CAGGTCATTTCGGTCATAGCCCTTTTCAT  
15: GGGTAAACCGACAATGACAACCTACCGAT  
16: AGTTGCGTGGGATTTTGCTAAATGAATT  
17: CAGACGGATACGTAATGCCACATTAAAC  
18: TTCTGTAAGAACCGCCACCCTGAACCGC  
19: CACCCTCTTCGGAACCTATTATGCCCCC  
20: TGCCTATGACGATTGGCCTTGGTTGAGG  
21:  
TGAGTTAAGCCCAATAATAACGGAATACCCAAAAGAACTGGCGTTAG  
CAAACGTAG  
22:  
AAAATACATACATAACAACCGATTGAGGGAGGGAAGGTAAATATTATC  
ACCGTCACC  
23:  
GACTTGAGCCATTTTTTGCCTTTAGCGTCAGACTGTAGCGCGCCTTATT  
AGCGTTT  
24:  
GCCATCTTTTCATACCAGAGCCGCCGCCAGCATTGACAGGAGATATTC  
ACAAACAA  
25:  
ATAAATCCTCATTAGAGTAACAGTGCCCGTATAAACAGTTAATTCTGA  
AACATGAA  
26:  
AGTATTAAGAGGCTCTCAGGAGGTTTAGTACCGCCACCCTCACAGAGC  
CACCACCC  
27:  
TCATTTTCAGGGATGTTTTGTCGTCTTCCAGACGTTAGTAAACAACCTT  
TCAACAG  
28:  
TTTCAGCGGAGTGATTTCGAGGTGAATTTCTTAAACAGCTTGAAACCAT  
CGCCCACG  
29:  
CATAACCGATATATCTAAAGACTTTTTTCATGAGGAAGTTTCCTACGAA  
GGCACCAA  
30:  
CCTAAAACGAAAGACGACCTGCTCCATGTTACTTAGCCGGAAACCGA  
ACTGACCAA  
31: GATACATTTTCGCAATAGTTTG  
32: ACCATTAAGGATTAGAGAGTAAACTCCA  
33: ACAGGTCCCCCTCAAATGCTAATATTC  
34: ATTGAATGCAGATACATAACGCACATTC  
35: AACTAATTAATTGGGCTTGAACCAGAA

36: CGAGTAGTCAATCATAAGGGACGAGGCG  
37: GTTTAGCTATATTTTCATTTGGGGCGCGTCCATAT  
38:  
TTTTGATAAGAGGTGATTCCCAATTCTGCGAACGAGTAGATTATGGTC  
ATAACCT  
39:  
AAACGAGAATGACCAGCTTCAAAGCGAACCGACCGGAAGCACCTTT  
AATTGCTCC  
40:  
GAGGCATAGTAAGATAGCGTCCAATACTGCGGAATCGTCATATTAAC  
AGTTCAGA  
41:  
AACTTTAATCATTGAGATTCATCAGTTGAGATTTAGGAATACCCAAA  
GGAATTAC  
42:  
CTTTGAAAGAGGACGTGAATAAGGCTTGCCCTGACGAGAAACGATGG  
TTAATTTTC  
43: CGACATTAAGGTGGCAACATACCGAGGA  
44: AATCAAGGGGAATTAGAGCCAAAAGGG  
45: ACCACCAATCAAATCACCGGGCGACAG  
46: GTGCCTTAAGCCAGAATGGAACACCAGA  
47: CACCGTAGAGACTCCTCAAGAGGGGTCA  
48: ATCTAAAAGCAAGCCCAATAGGGTGTAT  
49: GCTTGCTGAATAGAAAGGAACCGTAACG  
50: TTGAGGATCGGTCGCTGAGGCTTTATCA  
51: AAATCCGGGCAAAGAATACAAGAGGCT  
52: TCATTCAAGATGAACGGTGTATGTGTCG  
53: GGTAGAATGAATTACCTTATGAAGCTGC  
54: GACTGGAGCAACACTATCATATATTACA  
55: TAATTCGATAAATCAAAAATCATGTTTA  
56: AACAGTTCATTTTTGCGGATGCGCGTTT  
57: AACGCAATAATAAGAGCAAGAATTAGAC  
58: GGGAGAATATTTATCCCAATCTATTTTG  
59: CACCCAGGATATAGAAGGCTTAACGGGT  
60: ATTAACAATAGATAAGTCCTAGAGAAT  
61: ATAAAGTTATAAAGCCAACGCGTGTGATAAATAAG  
62:  
AATAGCTATCTTACATAGCCGAACAAAGTTACCAGAAGGAAATAAAA  
GAAACGCAA  
63:  
AGACACCACGGAATATTCATATGGTTTACCAGCGCCAAAGACGCAA  
ATCACCAGT  
64:  
AGCACCATTACCATACCATCGATAGCAGCACCGTAATCAGTAAACCAG  
AGCCACCA

65:  
CCGGAACCGCCTCCCCCTCAGAGCCACCACCCTCAGAGCCGCAGCGCA  
GTCTCTGA

66:  
ATTTACCGTTCCAGCAGGAGTGTACTGGTAATAAGTTTTAACGAAGGA  
TTAGGATT

67:  
AGCGGGGTTTTGCTAGGGTTGATATAAGTATAGCCCGGAATAGAACCC  
ATGTACCG

68:  
TAACACTGAGTTTCGCATTCCACAGACAGCCCTCATAGTTAGAACTAA  
AGGAATTG

69:  
CGAATAATAATTTTCTCCAAAAGGAGCCTTTAATTGTATCGGTTGCAG  
GGAGTTAA

70:  
AGGCCGCTTTTGCGGCATCGGAACGAGGGTAGCAACGGCTACCTAAA  
ACACTCATC

71:  
TTTGACCCCCAGCGCGGAGATTTGTATCATCGCCTGATAAATCAGACC  
AGGCGCAT

72:  
AGGCTGGCTGACCTGATATTCATTACCCAAATCAACGTAACACGATTT  
TAAGAACT

73:  
GGCTCATTATAACCATTAATAAAAACGAACTAACGGAACAACATACCCTC  
GTTTACCA

74:  
GACGACGATAAAAAAAGTTTTGCCAGAGGGGGTAATAGTAAAAGGTC  
TTTACCCTG

75:  
ACTATTATAGTCAGAAGAGGAAGCCCGAAAGACTTCAAATATGCTTAG  
AGCTTAAT

76:  
TGCTGAATATAATGACTAAAGTACGGTGTCTGGAAGTTTCATAGCTGA  
AAAGGTGG

77: CATCAATTCTACTAATAGTAGTAGCATTAAACCAATAGGAACG

78:  
TTTTTTGTTTAACGAGAGAATAACATAAAAACAGGGAAGCGCAACAAT  
GAAATAGC

79:  
GAACGCGAGGGCGTTTTTTGAAGCCTTAAATCAAGATTAGTTGCCAAATA  
AGAAACGA

80:  
ATATCCCATCCTAAATCGGCTGTCTTTCCCTTATCATTCCAAGATCCGGT  
ATTCTAA

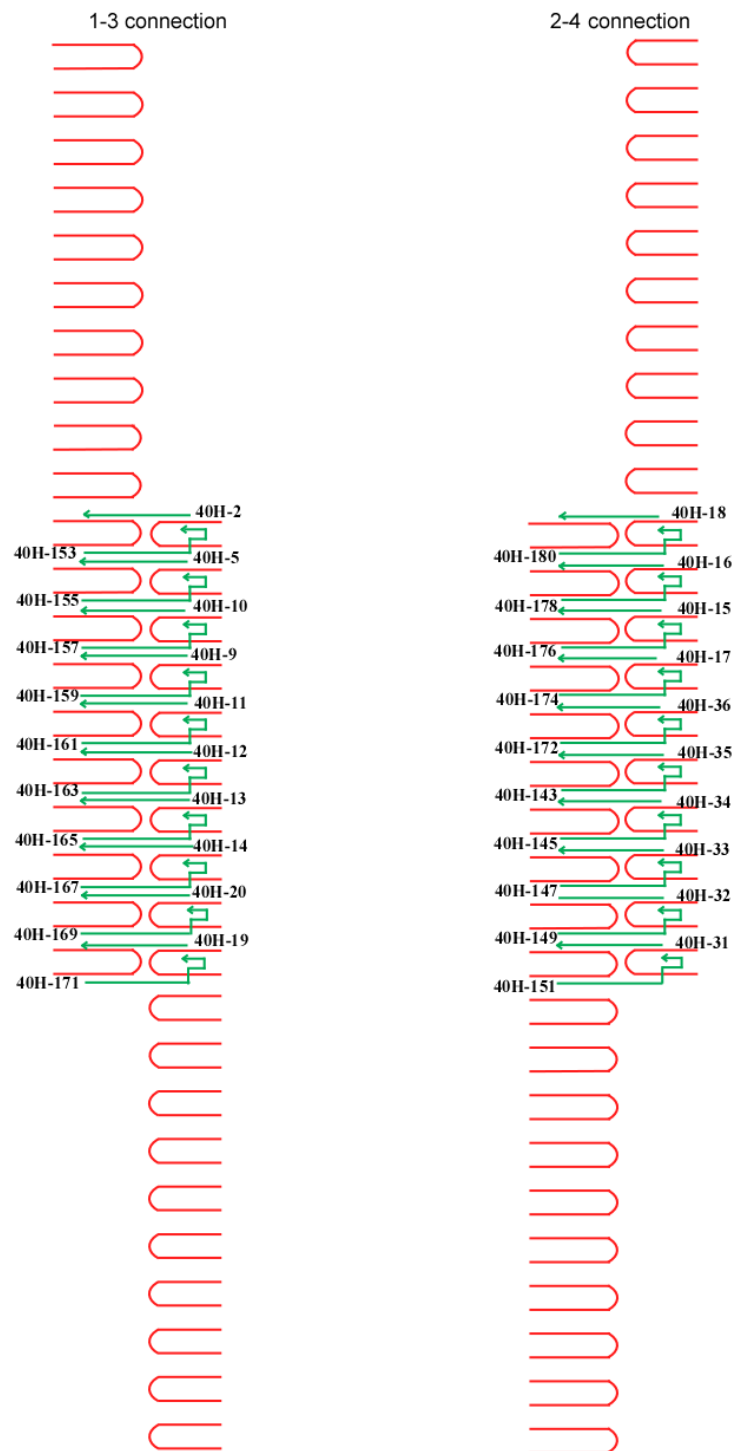
81:  
TAATTGAGAATCGCAGGCAGAGGCATTTTCGAGCCAGTAATAGAACA  
AGAAAAATA  
82: CTAATTTAATGGTTTGAAATACCGACCTCAACAGTAGGGCT  
83: ATAGAAAAAGTTTATTTTGTGAGAAAAG  
84: CAATGAATAGCAAGGCCGAAACAATCA  
85:  
CGCTGAGAGCCAGCGAGGTGAGGCGGTCAGTATTAACACCGCACGTC  
AC  
86: ACCGCCACTCAGAGCCGCCACACGTGGCACAGACA  
87: GATGATATAAGCGTCATACATCCTCAGA  
88: CGTCGAGCAGTACCAGGCGGAGGCTTTT  
89: GCCTGTAGTCACCAGTACAAATAAGTGC  
90:  
CGTTAGAATCAGAGGTACTATGGTTGCTTTGACGAGCACGTACTACAA  
C  
91: AAAAAGGTTACGTTGAAAATGAAAGGAAGGGAAG  
92: AAAGACAGGATCGTCACCCTCCTCCAAA  
93: AGTACAAATTATACCAAGCGCAGCAGCG  
94: AGAACCGTCATCAAGAGTAATGAAACAA  
95:  
GGGCGCCAGGGTGGTAATGAATCGGCCAACGCGCGGGGAGAGCTTGA  
CA  
96: ATCTACGGTCAGGACGTTGGGCGGAAGCATAAAGT  
97: GCAAAGCCAAAATAGCGAGAAAGAAAA  
98: AAAGATTAAGCAAAGCGGATTGGCTTTT  
99: ATATGCACTGTAGCTCAACATGCATCAA  
100:  
GGGCGCATCGTAACCGGCGGATTGACCGTAATGGGATAGGTCGTTTAA  
A  
101: TAAGCAGCGAAGCCCTTTTAAAGCAGCC  
102: TTTACAGTCAAAAATGAAAATGGTTAGAACCTACC  
103:  
AGTTACAAAATCGCGGGAGAAACAATAACGGATTGCGCTGATGACTT  
GC  
104: GGGAGGTTTAGCGAACCTCCCGAAACCA  
105: ATCAATATTTACGAGCATGTACCAACAT  
106: GTAATTTTCATATTTAACAACGTTTCATCTTCTGAC  
107:  
TATCATTTTGCAGGACCTTTGCCCGAACGTTATTAATTTTAAAAAATAT  
CTTTAGG  
108:  
AGCACTAACAATAAGTTGAAAGGAATTGAGGAAGGTTATCTCTGCA  
ACAGTGCCA



109: ATATTTTTGAATGGAACCCTTCTGACCTGAAAGCGTAAGAATATGGAA  
 ATACCTAC  
 110: ATTTTGACGCTCAAGCCAGCCATTGCAACAGGAAAAACGCTCCACGCA  
 AATTAACC  
 111: GTTGTAGCAATACTAGGCCACCGAGTAAAAGAGTCTGTCCATTAACGT  
 GCTTTCCT  
 112: AAAGCGAAAGGAGCTGACGGGGAAAGCCGGCGAACGTGGCGACTATC  
 AGGGCGATG  
 113: GCCCACTACGTGAAACTCCAACGTCAAAGGGCGAAAAACCGTTTTGAT  
 GGTGGTTC  
 114: CGAAATCGGCAAAATGGTTTGCCCCAGCAGGCGAAAATCCTGGCGGTT  
 TCGTATT  
 115: GTAAAGCCTGGGGTCGCTCACAATTCCACACAACATACGAGCCGACG  
 GCCAGTGCC  
 116: AAGCTTGCATGCCTGGGTTTTCCAGTCACGACGTTGTAAAAGCCATT  
 CAGGCTGC  
 117: GCAACTGTTGGGAAGTGCCGGAAACCAGGCAAAGCGCCATTCACGTT  
 GGTGTAGAT  
 118: CCATCAAAAATAATTCGCGTCTGGCCTTTCCGTGG  
 119: ATATCAAAATTATTTTTGGATTATACTTCTGAATAATGGAAGAGTTTGA  
 GTAACAT  
 120: AAATCAATATATGTACAATTTCAATTTGAATTACCTTTTTTAATGCTTTG  
 AATACCA  
 121: GGTCTGAGAGACTAAAGACGCTGAGAAGAGTCAATAGTGAATTGGAA  
 ACAGTACAT  
 122: AAAACTTTTTCAAATATATTTTAGTTAATTATCAAAATCATA  
 123: AATCAACATAGATTAGAGCCGAACTCGT  
 124: TAAAACAAGCAAATGAAAAATGTTGGCA  
 125: GAGATAGCTATTAGTCTTTAACAGAAGA  
 126: TATTACCTCGTCTGAAATGGAGCCAACA  
 127: ATCAGTGTCTTTGATTAGTAAAGAACAA  
 128: AGGGCGCCGGGAGCTAAACAGTTTTATA  
 129: TAGAGCTGGGCGCTAGGGCGCCCGCTAC  
 130: AACGTGGCCATCACCCAAATCCCCGATT

131: TCCACGCTCCCTTATAAATCAATTAAAG  
132: GCTGCATTTTTTCTTTTCACCCAAGCGG  
133: TGTTATCGCCTAATGAGTGAGCGTGCCA  
134: AACGCCAGCAGGTCGACTCTAGTGAAAT  
135: GCTTCTGGGGCGATCGGTGCGGTTGGGT  
136: GAACAAACGTGCATCTGCCAGCGGCACC  
137: ATTAAATACAAAGAAACCACCTATAATC  
138: CTGATTGTGCACGTAAAACAGGTACCTT  
139: TTACATCGCAGAGGGCGAATTAATTAATT  
140: ACATTTAGAGTGAATAACCTTCGATAGC  
141: TTAGATTCCTTTTTAACCTCCACAAAGAACGCGAG  
142: ACAACAATTCGACTCAATAGATAATAC  
143: ATTTGAGGATTTAGTATCAAACCCTCAA  
144: TCAATATCTGGTCACTAAAGCATCACCT  
145: TGCTGAACCTCAAACCATTA AAAATACC  
146: GAACGAACCACCAGTGCGCGAACTGATA  
147: GCCCTAAAACATCGCACGACCAGTAATA  
148: AAAGGGACATTCTGTTATTTACATTGGC  
149: AGATTCACCAGTCACAAACTATCGGCCT  
150: TGCTGGTAATATCCTAACATCACTTGCC  
151: TGAGTAGAAGA ACTAACGGTACGCCAGA  
152: ATCCTGAGAAGTGTGAGGCCGATTAAAG  
153: GGATTTTAGACAGGAACCACCACACCCG  
154: CCGCGCTTAATGCGTGGCAAGTGTAGCG  
155: GTCACGCTGCGCGTGCCTAAATCGGAA  
156: CCCTAAAGGGAGCCAAGTTTTTTGGGGT  
157: CGAGGTGCCGTA AATTGTTCCAGTTTGG  
158: AACAAGAGTCCACTAAAGAATAGCCCGA  
159: GATAGGGTTGAGTGTACCCGCCTGGCCC  
160: TGAGAGAGTTGCAGAGTGAGACGGGCAA  
161: CAGCTGATTGCCCTCTGCCCGCTTTCCA  
162: GTCGGGAAACCTGTCTAACTCACATTAA  
163: TTGCGTTGCGCTCACGTAATCATGGTCA  
164: TAGCTGTTTCCTGTGAGGATCCCCGGGT  
165: ACCGAGCTCGAATTAAGGGGGGATGTGC  
166: TGCAAGGCGATTAAGGCCTCTTCGCTAT  
167: TACGCCAGCTGGCGCAGGAAGATCGCAC  
168: TCCAGCCAGCTTTCTTTGAGGGGACGAC  
169: GACAGTATCGGCCTTGTGAGCGAGTAAC  
170: AACCCGTCGGATTCCTGTAGCCAGCTT  
171: TCATCAACATTAAA  
172: TATCATCATATTCCAAGTATTAGACTTT  
173: TGGCAATTCATCAAAGAAGGAGCGGAAT  
174: CGTAGATTTTCAGGTGATTATCAGATGA  
175: AATATACAGTAACAAAATAAAGAAATTG  
176: CTGAGCAAAGAAGTTTAACGTCAGATG

177: ATCAAGAAAACAAATTCATTTCAATTAC  
178: TCGCTATTAATTAAATGATGAAACAAAC  
179: CCTTGAAAACATAGGCTTCTGTAAATCG  
180: TATATAACTATATGTTTTCCCTTAGAAT  
181: AATCCAATCGCAAGGGCTTAGGTTGGGT  
182: TAAATGCTGATGCA



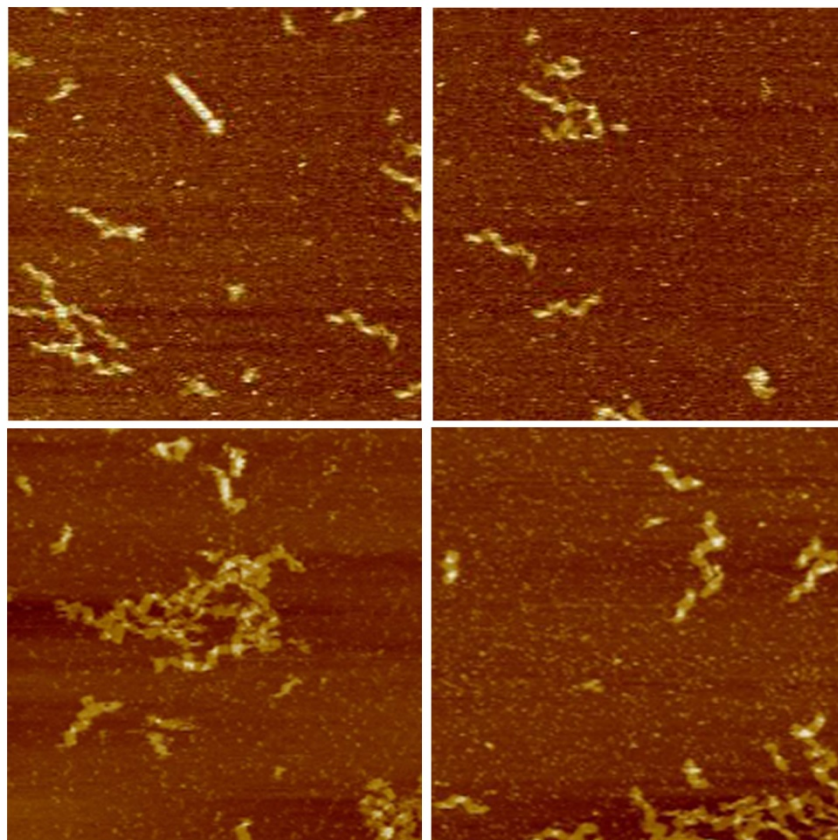
**Figure S12.** Schematics of the 1-3 and 2-4 linkers of the 40-helix zigzag origami tile.

**Sequences of linkers:**

40H-2: CTAGAAAAACGGTACGCCAGA

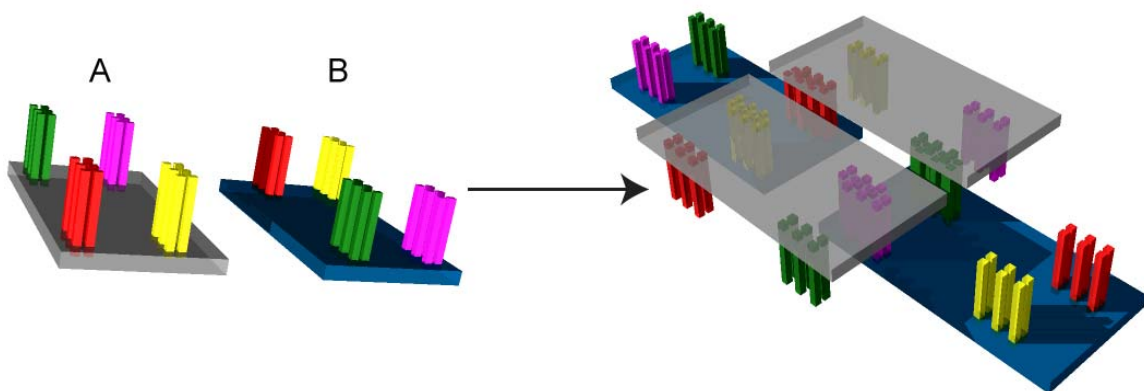
40H-5: GACAATAAACCACCACACCCG

40H-9: AGCGTCTTTGTTCCAGTTTGG  
40H-10: TTTATTTGCACTAAATCGGAA  
40H-11: TGAGCGCTCACCGCCTGGCCC  
40H-12: AGACTCCCTGCCCGCTTTCCA  
40H-13: AAATTATCGTAATCATGGTCA  
40H-14: CGGCATTAAAGGGGGATGTGC  
40H-15: AGTTGCGATGATGAAACAAAC  
40H-16: TTCTGTATTTTCCCTTAGAAT  
40H-17: GGGTAAATTTAACGTCAGATG  
40H-18: CACCCTCTAAATGCTGATGCA  
40H-19: TGCCTATTGTGAGCGAGTAAC  
40H-20: CAGGTCACAGGAAGATCGCAC  
40H-31: ACCATTACAAACTATCGGCCT  
40H-32: ACAGGTCCACGACCAGTAATA  
40H-33: ATTGAATCCATTA AAAAATACC  
40H-34: AACTAATTATCAAACCCTCAA  
40H-35: CGAGTAGAAGTATTAGACTTT  
40H-36: CAGACGGTGATTATCAGATGA  
40H-143: ATTTGAGGATTTAGTAAATTGGGCTTGAACCAGAA  
40H-145: TGCTGAACCTCAAAGCAGATACATAACGCACATTC  
40H-147: GCCCTAAAACATCGCCCCCTCAAATGCTAATATTC  
40H -149: AGATTCACCAGTCAAGGATTAGAGAGTAAACTCCA  
40H -151: TGAGTAGAAGA AACTGATACATTTTCGCAATAGTTTG  
40H -153: GGATTTTAGACAGGAAGCCTGTTTAGTAATAATTA  
40H-155: GTCACGCTGCGCGTAACAACATGTTTCAGAGACGAC  
40H-157: CGAGGTGCCGTA AATCATCGTAGGAATCAGCCGTT  
40H-159: GATAGGGTTGAGTGTTCCAGAGCCTAATGCTAACG  
40H-161: CAGCTGATTGCCCTTAATATCAGAGAGAGGGTAAT  
40H-163: TTGCGTTGCGCTCATTATTACGCAGTATATGATTA  
40H-165: ACCGAGCTCGAATTTTATTAAAGGTGAATTGACGG  
40H-167: TACGCCAGCTGGCGTTCGGTCATAGCCCTTTTCAT  
40H-169: GACAGTATCGGCCTGACGATTGGCCTTGGTTGAGG  
40H-171: TCATCAACATTA AATTCGGAACCTATTATGCCCCC  
40H-172: TATCATCATATTCCTCAATCATAAGGGACGAGGCG  
40H-174: CGTAGATTTTCAGGATACGTAATGCCACATTA AAC  
40H-176: CTGAGCAAAGAAGCCGACAATGACA ACTACCGAT  
40H-178: TCGCTATTAATTAATGGGATTTTGCTAAATGAATT  
40H-180: TATATACTATATGAGAACCGCCACCCTGAACCGC

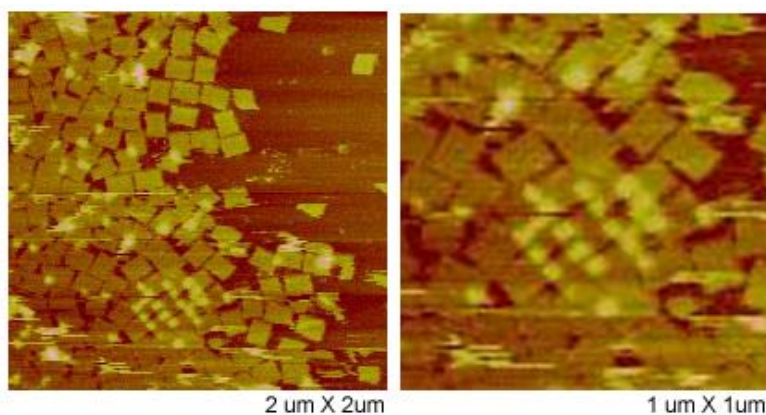


2 um X 2um

**Figure S13.** Additional AFM images of the zigzag ribbons or linear, double-layer ribbons formed from the 40-helix zigzag origami tiles with the linker strand connection design illustrated in Figure 3.6 of the main text.



**Figure S14.** Schematic drawing shows the assembly of 2D arrays using the original planar origami. An AB-tile system in which each tile carries 6 x 4 complementary sticky ends was used.



**Figure S15.** AFM images of the small pieces of 2D arrays formed by the original planar origami.

APPENDIX C

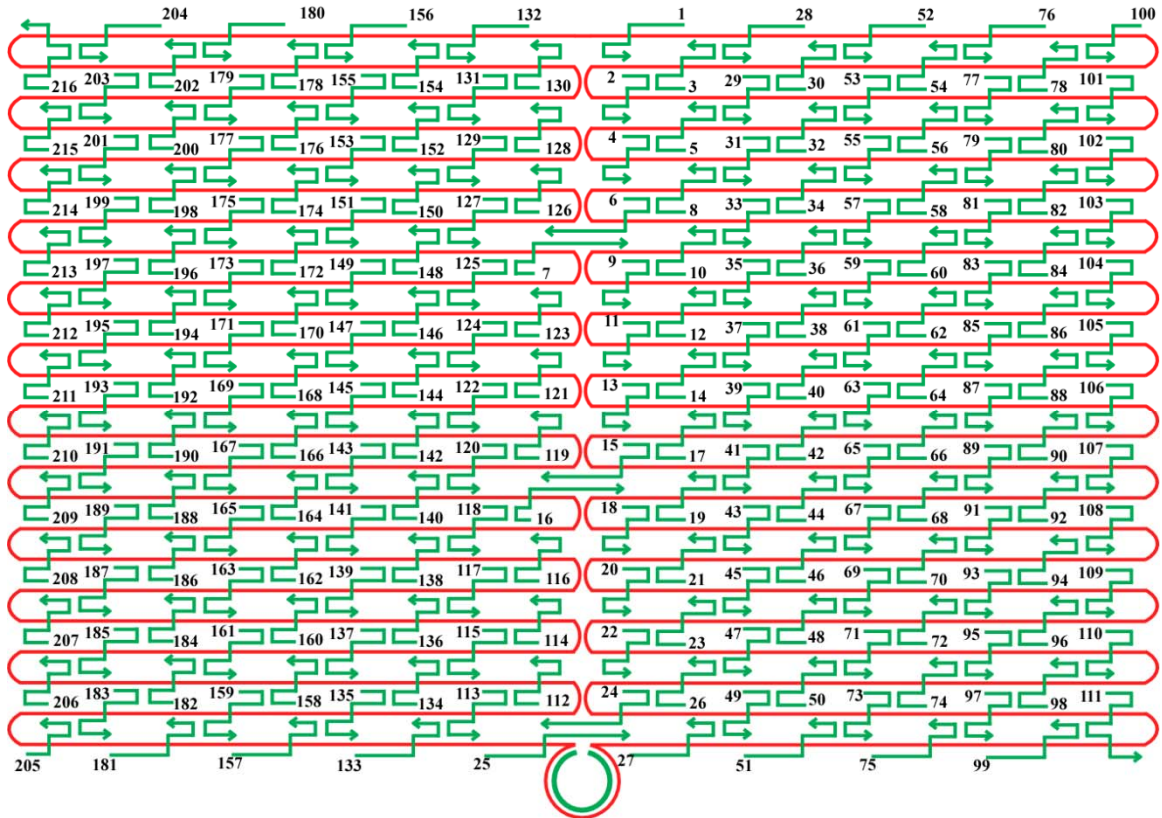
SUPPLEMENTAL INFORMATION FOR CHAPTER 4



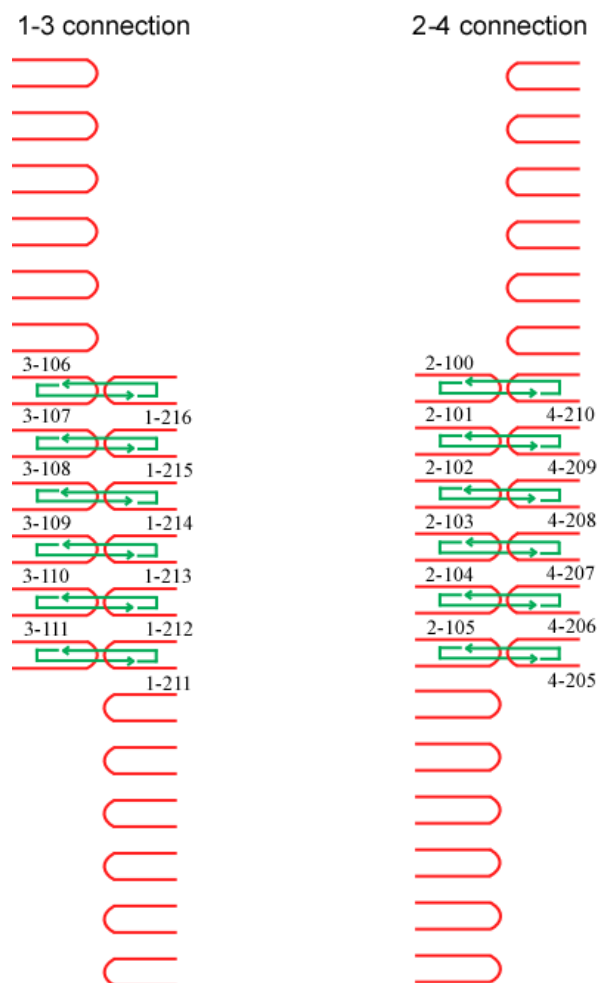
## Supplemental Information

### Effect of DNA Hairpin Loops on the Twist of Planar DNA Origami Tiles

Zhe Li, Lei Wang, Hao Yan, Yan Liu



**Figure S1.** Schematic of the rectangular origami structure, helper strand position and numbering assignment. The continuous red strand corresponds to the circular M13 viral genome with all helper strands shown in green. The arrows indicate the 3'- ends of the oligonucleotides. Dangling loop represents unpaired sequences. Sequences of helper strands used in these experiments are given below.



**Figure S2.** Schematics of the 1'-3' and 2'-4' linkers.

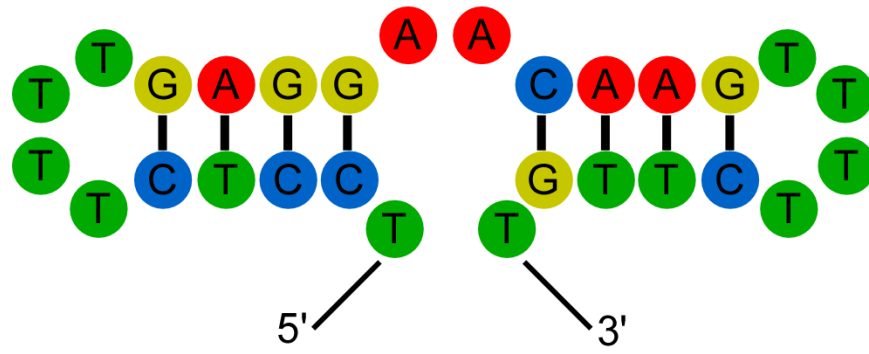
**Sequences of 1-3 linkers:**

1-211: CAACATGTATTGCTGA ATATAATG ACCAGTAA  
 1-212: CCCCTCAAATCGTCA TAAATATT AATCAATA  
 1-213: AATCTACGACCAGTCA GGACGTTG TTCATCAA  
 1-214: GAACCGAAAGGCGCAG ACGGTCAA ATTAATTA  
 1-215: CGGAACGAACCCTCAG CAGCGAAA CGCGAGAA  
 1-216: ACAGTTTCTGGGATTT TGCTAAAC CGACAAA  
 3-106: GGTAAGTAGAGAATA TAAAGTAC AACTTTCA  
 3-107: AACTTTTTATCGCAAG ACAAAGAA GACAGCAT  
 3-108: CATTAAACACATCAAG AAAACAAA TCATAAGG  
 3-109: TATAATCCTATCAGAT GATGGCAA GGAAGAAA  
 3-110: TCTGGTCACAAATATC AAACCCTC CATTGAAT  
 3-111: TAAAAGGGATTCACCA GTCACACG CTGTAGCT

**Sequences of 2-4 linkers:**

2-100: TAGCCCGGCCGTCGAG AGGGTTGA GGTTGTAC  
 2-101: TCATTAAATGATATTC ACAAACAA GATGAACG  
 2-102: GCGACAGATCGATAGC AGCACCGT GTAATGGG

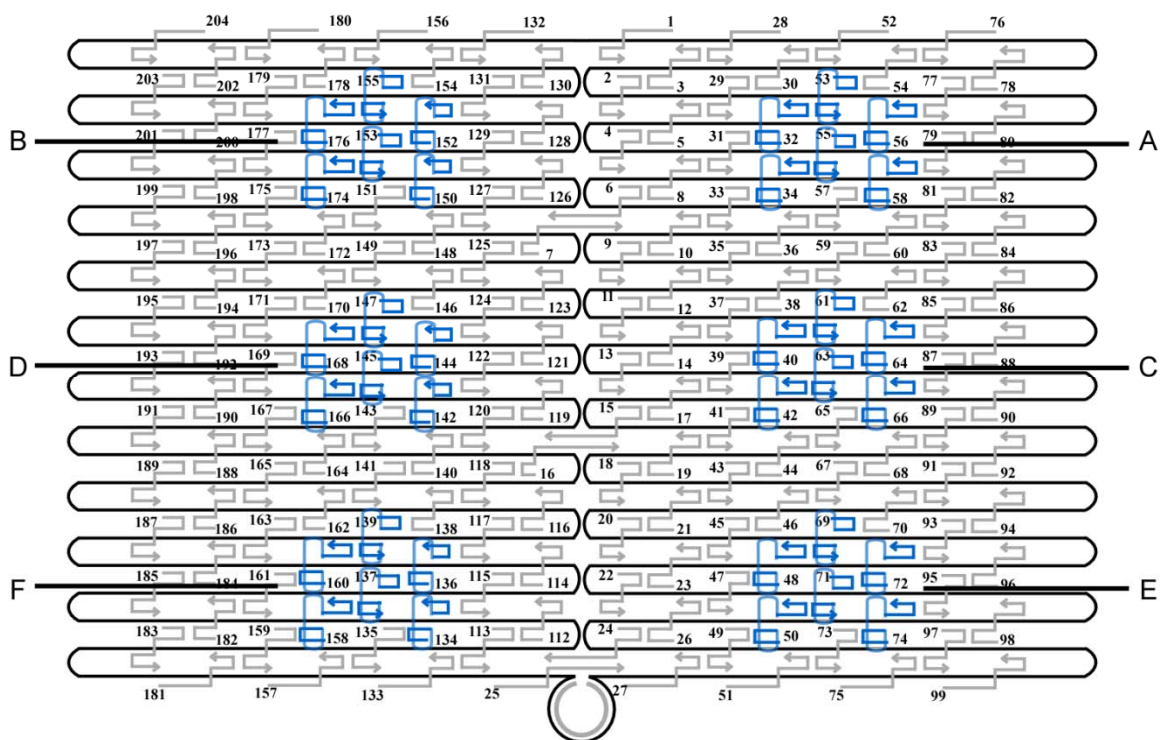
2-103: GCAACATAGTAGAAAA TACATACA TGTA AAAAC  
2-104: AATTA ACTACAGGGAA GCGC ATTA CGGTTTGC  
2-105: GGTATTCTAAATCAGA TATAGAAG CGATGGCC  
4-205: CACTACGTAAACCGTC TATCAGGG GCTTATCC  
4-206: GTATTGGGAACGCGCG GGGAGAGG GACGGGAG  
4-207: GACGGCCATTCCCAGT CACGACGT TAAAGGTG  
4-208: ATAGGTCAAAACGGCG GATTGACC AATCAGTA  
4-209: GTAATCGTAGCAAACA AGAGAATC ATAAATCC  
4-210: CAAAACAAGCATAAA GCTAAATC TATAAGTA



*Figure S3.* Schematic of the secondary structure of a dumbbell DNA loop.

**Sequence of the dumbbell loop:**

TCCTCTTTGAGGAACAAGTTTCTTGT



**Figure S4.** Schematic of the positions of the 6 groups of dumbbell DNA loops on the top surface of origami tiles. Helper strands with dumbbell loops are highlighted in blue. In this design, the sequence of the dumbbell loop is inserted between two fragments of a helper strand.

**Sequences of group A loops:**

|   |                              |
|---|------------------------------|
| 32: GTTTGCCACCTCAGAG<br>CCGCCACCGATAACAGG | TCCTCTTTTGAGGAACAAGTTTTCTTGT |
| 34: AGCGCCAACCATTTGG<br>GAATTAGATTATTAGC  | TCCTCTTTTGAGGAACAAGTTTTCTTGT |
| 53: CCTCAAGAATACATGG<br>CTTTTGATAGAACCAC  | TCCTCTTTTGAGGAACAAGTTTTCTTGT |
| 55: CACCAGAGTTCGGTCA<br>TAGCCCCCGCCAGCAA  | TCCTCTTTTGAGGAACAAGTTTTCTTGT |
| 56: TCGGCATTCCGCCGCC<br>AGCATTGACGTTCCAG  | TCCTCTTTTGAGGAACAAGTTTTCTTGT |
| 58: TCACAATCGTAGCACC<br>ATTACCATCGTTTTCA  | TCCTCTTTTGAGGAACAAGTTTTCTTGT |

**Sequences of group B loops:**

|   |                              |
|---|------------------------------|
| 150: ACGAGTAGTGACAAGA<br>ACCGGATATACCAAGC | TCCTCTTTTGAGGAACAAGTTTTCTTGT |
| 152: GCGAAACATGCCACTA<br>CGAAGGCATGCGCCGA | TCCTCTTTTGAGGAACAAGTTTTCTTGT |
| 153: ATACGTAAGTACAA<br>CGGAGATTCATCAAG    | TCCTCTTTTGAGGAACAAGTTTTCTTGT |

155: AAAAAAGGACAACCAT TCCTCTTTTGAGGAACAAGTTTTCTTGT  
 CGCCACGCGGGTAAA  
 174: TTCAACTATAGGCTG TCCTCTTTTGAGGAACAAGTTTTCTTGT  
 GCTGACCTTGTATCAT  
 176: CGCCTGATGGAAGTTT TCCTCTTTTGAGGAACAAGTTTTCTTGT  
 CCATTAACATAACCG

**Sequences of group C loops:**

40: TAAGTCTACCAAGTA TCCTCTTTTGAGGAACAAGTTTTCTTGT  
 CCGCACTCTTAGTTGC  
 42: AGGCGTTACAGTAGGG TCCTCTTTTGAGGAACAAGTTTTCTTGT  
 CTTAATTGACAATAGA  
 61: TTTTGTTTAAGCCTTA TCCTCTTTTGAGGAACAAGTTTTCTTGT  
 AATCAAGAATCGAGAA  
 63: CAAGCAAGACGCGCCT TCCTCTTTTGAGGAACAAGTTTTCTTGT  
 GTTATCAAGAATCGC  
 64: AATGCAGACCGTTTTT TCCTCTTTTGAGGAACAAGTTTTCTTGT  
 ATTTTCATCTTGCGGG  
 66: AATGGTTTACAACGCC TCCTCTTTTGAGGAACAAGTTTTCTTGT  
 AACATGTAGTTCAGCT

**Sequences of group D loops:**

142: ACCGTTCTAAATGCAA TCCTCTTTTGAGGAACAAGTTTTCTTGT  
 TGCCCTGAGAGGTGGCA  
 144: TCAATCTTTTAGTTT TCCTCTTTTGAGGAACAAGTTTTCTTGT  
 GACCATTACCAGACCG  
 145: CGAGTAGAACTAATAG TCCTCTTTTGAGGAACAAGTTTTCTTGT  
 TAGTAGCAAACCCTCA  
 147: TCAGAAGCCTCCAACA TCCTCTTTTGAGGAACAAGTTTTCTTGT  
 GGTCAGGATCTGCGAA  
 166: GGTAGCTAGGATAAAA TCCTCTTTTGAGGAACAAGTTTTCTTGT  
 ATTTTLAGTTAACATC  
 168: CAATAAATACAGTTGA TCCTCTTTTGAGGAACAAGTTTTCTTGT  
 TTCCAATTTAGAGAG

**Sequences of group E loops:**

48: AGATTAGATTTAAAAG TCCTCTTTTGAGGAACAAGTTTTCTTGT  
 TTTGAGTACACGTA  
 50: GAATGGCTAGTATTAA TCCTCTTTTGAGGAACAAGTTTTCTTGT  
 CACCGCCTCAACTAAT  
 69: GCGCAGAGATATCAA TCCTCTTTTGAGGAACAAGTTTTCTTGT  
 ATTATTTGACATTATC  
 71: ATTTTGCGTCTTTAGG TCCTCTTTTGAGGAACAAGTTTTCTTGT  
 AGCACTAAGCAACAGT  
 72: CTAATAAGAAACAAG TCCTCTTTTGAGGAACAAGTTTTCTTGT  
 AAACCACCAGGGTTAG

74: GCGTAAGAGAGAGCCA TCCTCTTTTGAGGAACAAGTTTTCTTGT  
GCAGCAAAAAGGTTAT

**Sequences of group F loops:**

134: GAATAGCCGCAAGCGG TCCTCTTTTGAGGAACAAGTTTTCTTGT  
TCCACGCTCCTAATGA

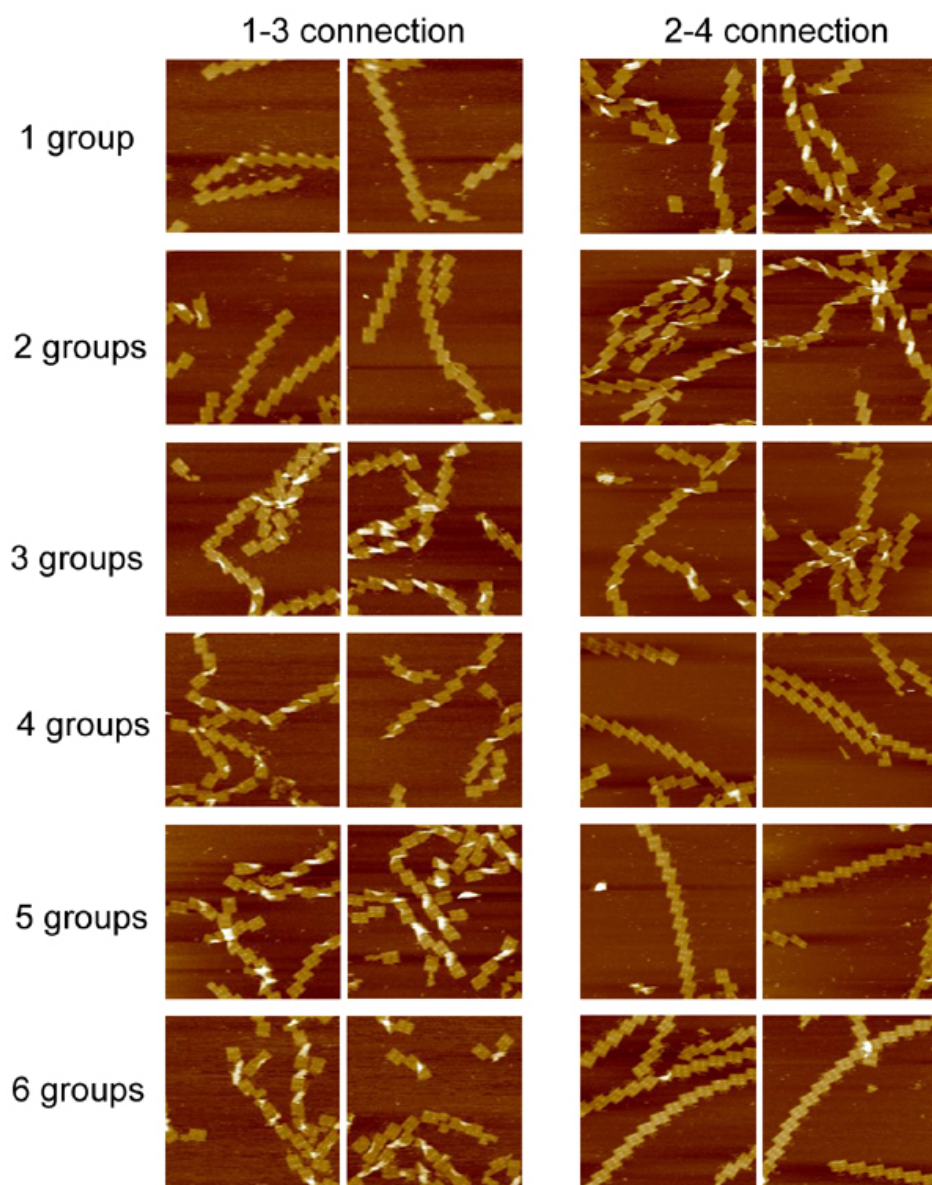
136: GTGAGCTAGTTTCCTG TCCTCTTTTGAGGAACAAGTTTTCTTGT  
TGTGAAATTTGGGAAG

137: TCATAGCTACTCACAT TCCTCTTTTGAGGAACAAGTTTTCTTGT  
TAATTGCGCCCTGAGA

139: GAAGATCGGTGCGGGC TCCTCTTTTGAGGAACAAGTTTTCTTGT  
CTCTTCGCAATCATGG

158: AGTTTGGAGCCCTTCA TCCTCTTTTGAGGAACAAGTTTTCTTGT  
CCGCCTGGTTGCGCTC

160: ACTGCCCGCCGAGCTC TCCTCTTTTGAGGAACAAGTTTTCTTGT  
GAATTCGTTATTACGC

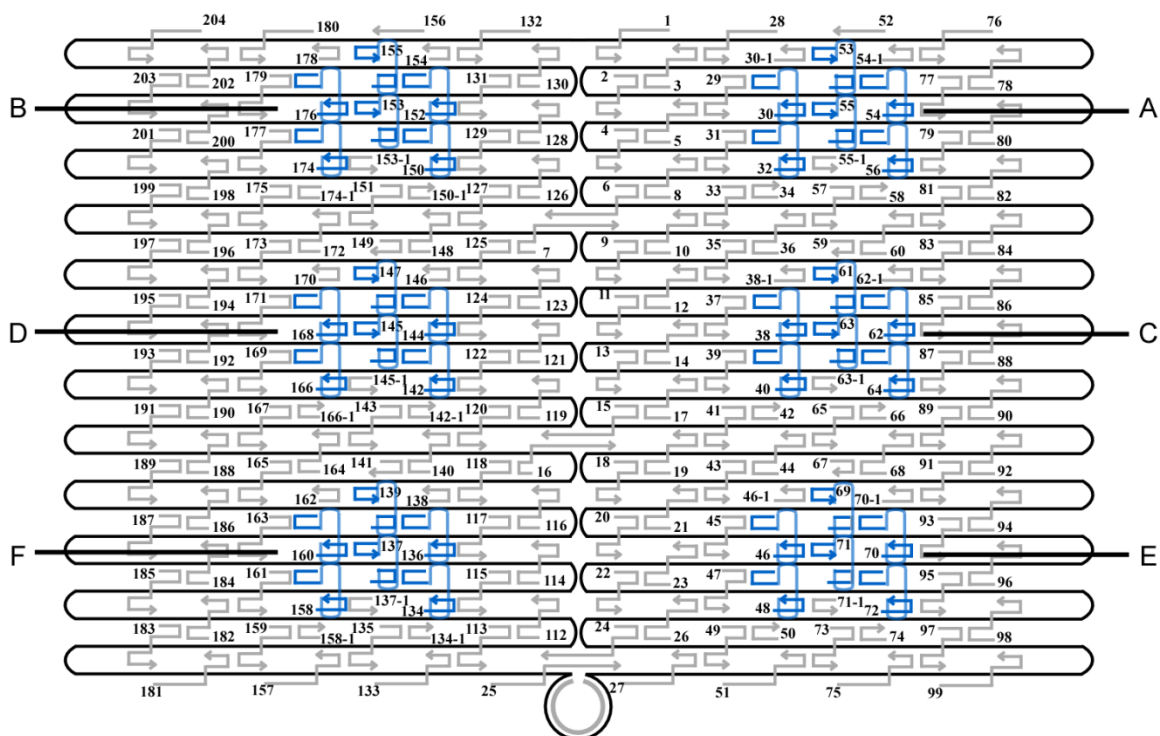


**Figure S5.** Additional AFM images of 1D DNA ribbons assembled from the rectangular origami tiles with different numbers of dumbbell loops on the top surface. Images are 1  $\mu\text{m}$  X 1  $\mu\text{m}$ .



| Number of loops | Ribbons in 1-3 connection      |  | Ribbons in 2-4 connection      |  |
|-----------------|--------------------------------|--|--------------------------------|--|
|                 | Average length (in tile units) | Average period between full twists (in tile units) | Average length (in tile units) | Average period between full twists (in tile units) |
| 1 group         | 7.6                            | N/A  | 7.1                            | 2.9  |
| 2 groups        | 7.9                            | N/A  | 8.2                            | 4.6  |
| 3 groups        | 7.4                            | 4.2  | 7.2                            | 6.2  |
| 4 groups        | 5.9                            | 3.1  | 8.9                            | 22.7   |
| 5 groups        | 4.7                            | 3.0  | 8.0                            | N/A  |
| 6 groups        | 4.2                            | 2.6  | 7.8                            | N/A  |

**Table S1.** Summary of observations of DNA ribbons assembled from the rectangular origami tiles with different numbers of dumbbell loops on the top surface, as shown in Figure 4.2 of the main text. 200~300 origami tiles were counted for each group.



**Figure S6.** Schematic of the positions of the 6 groups of dumbbell DNA loops on the bottom surface of origami tiles. Helper strands with dumbbell loops are highlighted in blue. In this design, besides the insertion of the dumbbell sequence, many other helper strands need to be chopped or connected with other fragments. All the helper strands whose sequences have been varied are listed as follows.

**Sequences of group A loops:**

30-1: TTAAGAGGCCGCCACC  
 30: CCGCCACCGATACAGG TCCTCTTTTGAGGAACAAGTTTTCTTGT  
 AGTGTACTTGAAAGTA  
 32: GAATTAGATTATTAGC TCCTCTTTTGAGGAACAAGTTTTCTTGT  
 GTTGCCACCTCAGAG  
 34: AGCGCCAACCATTTGG  
 52: CCCTCAGAACCGCCAC  
 53: CCTCAGAACTGAGACT TCCTCTTTTGAGGAACAAGTTTTCTTGT  
 CCTCAAGAATACATGG  
 55: CTTTTGATAGAACCAC TCCTCTTTTGAGGAACAAGTTTTCTTGT  
 CACCAGAGTTCGGTCA  
 55-1: TAGCCCCCGCCAGCAA  
 54-1: AGGATTAGTACCGCCA  
 54: TAAGCGTCGAAGGATT TCCTCTTTTGAGGAACAAGTTTTCTTGT  
 AGCATTGACGTTCCAG  
 56: ATTACCATCGTTTTCA TCCTCTTTTGAGGAACAAGTTTTCTTGT  
 TCGGCATTCCGCCGCC  
 58: TCACAATCGTAGCACC

**Sequences of group B loops:**

150-1: ACGAGTAGTGACAAGA

150: ACCGGATATACCAAGC TCCTCTTTTGAGGAACAAGTTTTCTTGT  
 GCGAAACATGCCACTA  
 152: CGAAGGCATGCGCCGA TCCTCTTTTGAGGAACAAGTTTTCTTGT  
 CAATGACACTCCAAAA  
 154: GGAGCCTTACAACGCC  
 153-1: CGGAGATTTCATCAAG  
 153: CGCCACGCGGGTAAA TCCTCTTTTGAGGAACAAGTTTTCTTGT  
 ATACGTAAAAGTACAA  
 155: CAGCCCTCATCTCCAA TCCTCTTTTGAGGAACAAGTTTTCTTGT  
 AAAAAAGGACAACCAT  
 156: TGTAGCATTCCACAGA  
 174-1: TTCAACTATAGGCTG  
 174: GCTGACCTTGATCAT TCCTCTTTTGAGGAACAAGTTTTCTTGT  
 CGCCTGATGGAAGTTT  
 176: CCATTAACATAACCG TCCTCTTTTGAGGAACAAGTTTTCTTGT  
 ATATATTCTTTTTTCA  
 178: CGTTGAAAATAGTTAG

**Sequences of group C loops:**

38-1: CAAATAAGTGAGTTAA  
 38: CCGCACTCTTAGTTGC TCCTCTTTTGAGGAACAAGTTTTCTTGT  
 TATTTTGCTCCCAATC  
 40: CTTAATTGACAATAGA TCCTCTTTTGAGGAACAAGTTTTCTTGT  
 TAAGTCCTACCAAGTA  
 42: AGGCGTTACAGTAGGG  
 59: ATACCCAAGATAACCC  
 61: ACAAGAATAAACGATT TCCTCTTTTGAGGAACAAGTTTTCTTGT  
 TTTTGTTTAAGCCTTA  
 63: AATCAAGAATCGAGAA TCCTCTTTTGAGGAACAAGTTTTCTTGT  
 CAAGCAAGACGCGCCT  
 63-1: GTTTATCAAGAATCGC  
 62-1: AAATGAAAGCGCTAAT  
 62: ATTTTCATCTTGCGGG TCCTCTTTTGAGGAACAAGTTTTCTTGT  
 AGGTTTTGAACGTCAA  
 64: AACATGTAGTTCAGCT TCCTCTTTTGAGGAACAAGTTTTCTTGT  
 AATGCAGACCGTTTTT  
 66: AATGGTTTACAACGCC

**Sequences of group D loops:**

142-1: ACCGTTCTAAATGCAA  
 142: TGCCTGAGAGGTGGCA TCCTCTTTTGAGGAACAAGTTTTCTTGT  
 TCAATTCTTTTAGTTT  
 144: GACCATTACCAGACCG TCCTCTTTTGAGGAACAAGTTTTCTTGT  
 GAAGCAAAAAGCGGA  
 146: TTGCATCAGATAAAAA  
 145-1: TAGTAGCAAACCTCA

145: GGTCAGGATCTGCGAA TCCTCTTTTGAGGAACAAGTTTTCTTGT  
 CGAGTAGAACTAATAG  
 147: CTTTTCATATTATAG TCCTCTTTTGAGGAACAAGTTTTCTTGT  
 TCAGAAGCCTCCAACA  
 149: CATTCAACGCGAGAGG  
 166-1: GGTAGCTAGGATAAAA  
 166: ATTTTGTAGTTAACATC TCCTCTTTTGAGGAACAAGTTTTCTTGT  
 CAATAAATACAGTTGA  
 168: TTCCCAATTTAGAGAG TCCTCTTTTGAGGAACAAGTTTTCTTGT  
 TACCTTTAAGGTCTTT  
 170: ACCCTGACAAAGAAGT

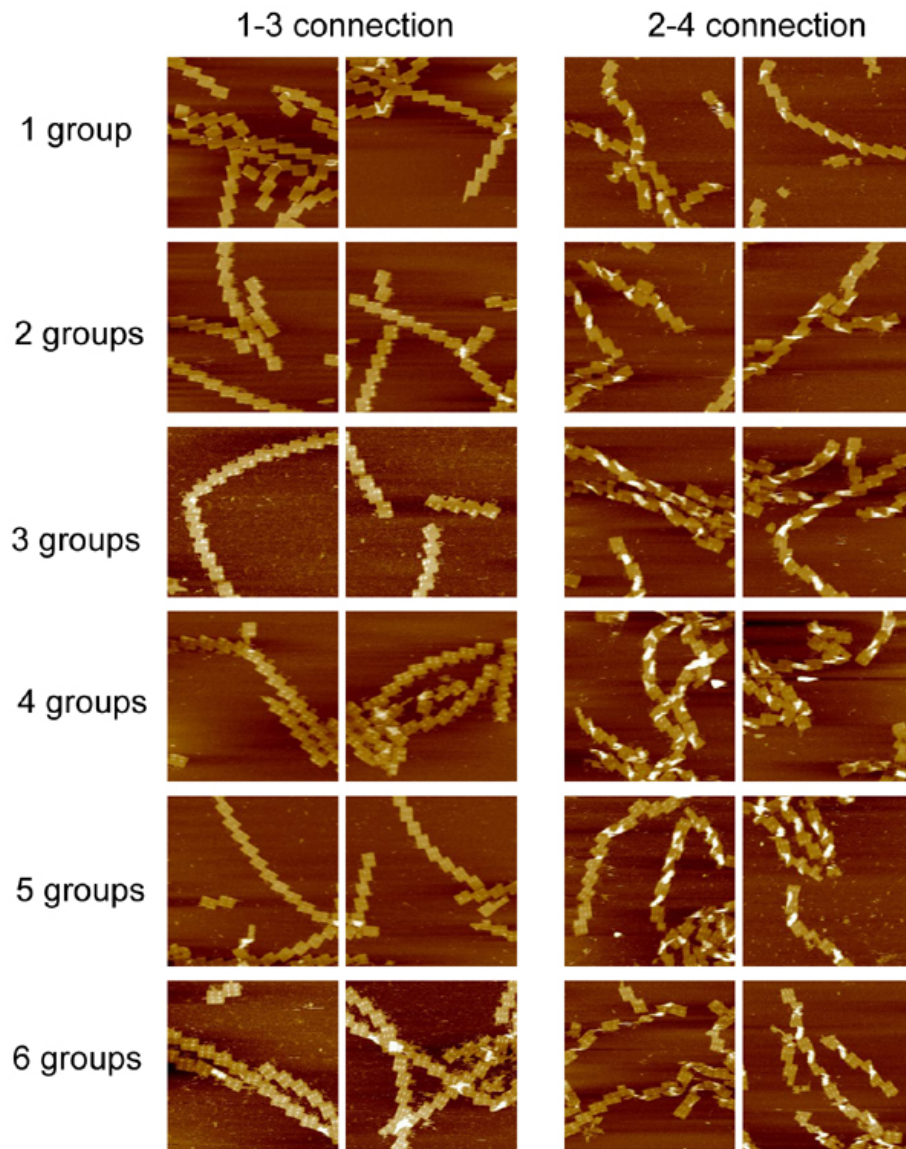
**Sequences of group E loops:**

46-1: ACCAAGTTCCTTGCTT  
 46: TTTGAGTACACGTAAA TCCTCTTTTGAGGAACAAGTTTTCTTGT  
 ACAGAAATCTTTGAAT  
 48: CACCGCTCAACTAAT TCCTCTTTTGAGGAACAAGTTTTCTTGT  
 AGATTAGATTTAAAAG  
 50: GAATGGCTAGTATTAA  
 67: TAACCTCCATATGTGA  
 69: GTGAATAAACAAAATC TCCTCTTTTGAGGAACAAGTTTTCTTGT  
 GCGCAGAGATATCAAA  
 71: ATTATTTGACATTATC TCCTCTTTTGAGGAACAAGTTTTCTTGT  
 ATTTTGCCTCTTTAGG  
 71-1: AGCACTAAGCAACAGT  
 70-1: TTCATTTCCAGTACAT  
 70: AAACCACCAGGGTTAG TCCTCTTTTGAGGAACAAGTTTTCTTGT  
 AACCTACCGCAATTA  
 72: GCAGCAAAAAGGTTAT TCCTCTTTTGAGGAACAAGTTTTCTTGT  
 CTAATAATAGAACAAAG  
 74: GCGTAAGAGAGAGCCA

**Sequences of group F loops:**

134-1: GAATAGCCGCAAGCGG  
 134: TCCACGCTCCTAATGA TCCTCTTTTGAGGAACAAGTTTTCTTGT  
 GTGAGCTAGTTTCCTG  
 136: TGTGAAATTTGGGAAG TCCTCTTTTGAGGAACAAGTTTTCTTGT  
 GGCGATCGCACTCCAG  
 138: CCAGCTTTGCCATCAA  
 137-1: TAATTGCGCCCTGAGA  
 137: CTCTTCGCAATCATGG TCCTCTTTTGAGGAACAAGTTTTCTTGT  
 TCATAGCTACTCACAT  
 139: GCCTTCCTGGCCTCAG TCCTCTTTTGAGGAACAAGTTTTCTTGT  
 GAAGATCGGTGCGGGC  
 141: GCAAATATCGCGTCTG  
 158-1: AGTTTGGAGCCCTTCA

158: CCGCCTGGTTGCGCTC TCCTCTTTTGAGGAACAAGTTTTCTTGT  
ACTGCCCCGCCGAGCTC  
160: GAATTCGTTATTACGC TCCTCTTTTGAGGAACAAGTTTTCTTGT  
CAGCTGGCGGACGACG  
162: ACAGTATCGTAGCCAG



**Figure S7.** Additional AFM images of 1D DNA ribbons assembled from the rectangular origami tiles with different numbers of dumbbell loops on the bottom surface. Images are 1  $\mu\text{m}$  X 1  $\mu\text{m}$ .

| Number of loops | Ribbons in 1-3 connection      |  | Ribbons in 2-4 connection      |  |
|-----------------|--------------------------------|--|--------------------------------|--|
|                 | Average length (in tile units) | Average period between full twists (in tile units) | Average length (in tile units) | Average period between full twists (in tile units) |
| 1 group         | 7.6                            | N/A  | 8.9                            | 3.1  |
| 2 groups        | 7.3                            | N/A  | 6.3                            | 2.8  |
| 3 groups        | 8.3                            | N/A  | 7.8                            | 2.2  |
| 4 groups        | 10.3                           | N/A  | 7.9                            | 2.1  |
| 5 groups        | 9.4                            | N/A  | 7.1                            | 2.3  |
| 6 groups        | 9.7                            | N/A  | 5.8                            | 2.1  |

**Table S2.** Summary of observations of DNA ribbons assembled from the rectangular origami tiles with different numbers of dumbbell loops on the bottom surface, as shown in Figure 4.3 of the main text. 200~300 origami tiles were counted for each group.

| Number and position of loops           | Ribbons in 1-3 connection      |  | Ribbons in 2-4 connection      |  |
|--|--------------------------------|--|--------------------------------|--|
|  | Average length (in tile units) | Average period between full twists (in tile units) | Average length (in tile units) | Average period between full twists (in tile units) |
| A and F on top                         | 11.3                           | N/A  | 7.3                            | 3.6  |
| A, C, D, F on top                      | 9.7                            | 5.8  | 8.4                            | N/A  |
| A, C, D, F on top<br>B and E on bottom | 4.7                            | 11.0   | 5.3                            | 10.6   |

**Table S3.** Summary of observations of DNA ribbons assembled from the rectangular origami tiles with different numbers and positions of dumbbell loops, as shown in Figure 4.5 of the main text. 200~300 origami tiles were counted for each group.



APPENDIX D  
CO-AUTHOR APPROVAL

I verify that the following co-authors have approved of my use of our publications  
in my dissertation.

Hao Yan (Arizona State University)

Yan Liu (Arizona State University)

Chenxiang Lin (Arizona State University)

Jeanette Nangreave (Arizona State University)

Minghui Liu (Arizona State University)

Bryan Wei (Hong Kong University of Science and Technology)

Yongli Mi (Hong Kong University of Science and Technology)

Lei Wang (Shandong University)